NANOPARTICLES FOR GENE THERAPY AND PROTEIN DELIVERY TO INDUCE ANGIOGENESIS AS AN ALTERNATIVE TREATMENT FOR PERIPHERAL ARTERIAL DISEASE

by

LINDA CHRISTELLIA NOUKEU

Presented to the Faculty of the Graduate School of

The University of Texas at Arlington in Partial Fulfillment

of the Requirements

for the Degree of

DOCTOR OF PHILOSOPHY

THE UNIVERSITY OF TEXAS AT ARLINGTON

August 2018

Acknowledgements

It has been a long journey, but I am honored to present to you my completed PhD dissertation in the following pages. This journey would not have been complete without the support and encouragement of some very prominent people. I would like to seize this opportunity to acknowledge and extend my humble and sincere gratitude to them all.

First, I would like to express my gratitude to Dr. Kytai T. Nguyen – my mentor, advisor and "fighter for all students." Thank you for accepting me and never giving up on me. You gave me the opportunity to gain invaluable research and life experience with a group of special individuals. Your patience, kindness, wisdom and commitment to your team has been a constant source of inspiration and motivation in molding me into a well-rounded scientist. Her selflessness and faith in my abilities has helped me grow both as a person and as an independent researcher. I am also extremely grateful to Dr. Xu, Dr. Chuong and Dr. Cho for taking time out of their busy schedules throughout these years with indispensable support and assistance in my search for various funding opportunities for my research and with their guidance and help as my thesis committee members. To Dr. Dong, I am grateful and humbled to have you on my committee. I would also like to take this opportunity to acknowledge Dr. Hsia at the University of Texas Southwestern Medical Center at Dallas (UTSW) for providing us with DNA plasmids.

In addition, I would like to thank members of the Nanomedicine and Drug Delivery Lab at UTA for maintaining a healthy and motivating research environment. In particular, I would like to thank my mentees Priyanka Iyer and Natalie Bonaventura for their dedication and involvement in my work. I am also extremely grateful to Dr. Tang, Amir Hakamivala, Dr. Tam Nguyen, and Duong Le for their help with animal studies. I would also like to appreciate other members of the nanomedicine and drug delivery lab and other BE graduate students for their friendship, encouragement and advice throughout my Ph.D study at UTA. My special

thanks are also due to Ms. Julie Rockow for always being a trooper. Your jokes and dedication to students was always a breath of fresh air.

Most importantly, I would like to thank my family for being the incredible support system that they are. I am deeply grateful to my siblings and best friend, Nzinga Tchameni, for the constant motivation calls. Your encouragement over the course of my Ph.D has been priceless. To my in-laws, I cannot thank you enough for all the help and inspiration you sent my way. I am forever indebted to my husband for his unconditional love and support in all my endeavors. Without his persuasions and blessings, this completed program would not have been possible. To him, I dedicate this thesis.

Lastly, I am thankful to God for all his blessings, steadfastness and love over the course of these years. He provided me with perseverance, strength and intellect to achieve this diploma and I can only wish to continue to be blessed and be a blessing to others.

August 10th, 2018

Abstract

NANOPARTICLES FOR GENE THERAPY AND PROTEIN DELIVERY TO INDUCE ANGIOGENESIS AS AN ALTERNATIVE TREATMENT FOR PERIPHERAL ARTERIAL DISEASE

Linda Noukeu, Ph.D

The University of Texas at Arlington, 2018

Supervising professor: Kytai T. Nguyen

Peripheral arterial disease (PAD) is defined as a slow, progressive disorder of the lower extremity arterial vessels characterized by chronic narrowing that often results in occlusion and is associated with loss of functional capacity. Although the PAD occurrence rate is increasing in the elderly population, outcomes with current treatment strategies are suboptimal. Hence, there is an urgent need to develop new technologies that overcome limitations of traditional modalities for PAD detection and therapy. In this research, nanoparticles have been developed and used as carriers for various therapeutic agents to treat PAD.

In particular, via protein/gene delivery, we developed and formulated nanoparticles (NPs) loaded with Erythropoietin (Epo) protein and/or complimentary deoxyribonucleic acid (cDNA) plasmids of the Epo receptor (EpoR) to enhance angiogenesis and/or restore vessel functions for use as an alternative PAD treatment. Epo and EpoR signaling pathways are selected for this research as they have been shown to play an important role in angiogenesis, cellular protection and proliferation of endothelial cells under the oxidative stress and hypoxic conditions, especially that of the ischemia. We observed that the fabricated NPs showed positive surface charges with average diameters of around 200 nm, demonstrated a sustained release of the payloads (e.g. Epo and EpoR cDNA), and maintained their stability in different

aqueous solutions. In addition, these NPs were hemocompatible with very low levels of hemolysis and produced a blood clotting time similar to that of the normal control. Moreover, these NPs were cyto-compatible with HUVECs, and the cellular uptake was dose-dependent. Despite no synergism observed in EpoR/Epo NPs compared to that of either Epo NPs or EpoR NPs, all three NPs (e.g. Epo NPs, EpoR NPs, and EpoR/Epo NPs) demonstrated to have potential angiogenic properties in HUVECs via enhanced cell proliferation, a boost in cell migration, provided cell protection in the stressed condition, and promoted tube formation under hypoxia compared to those of control (blank) NPs, free reagents, and no treatment.

Lastly, we focused on applying gene therapy as a therapeutic approach in inducing angiogenesis in the ischemic hindlimb mice. We formulate and characterized NPs loaded with either single or a combination of sense and antisense cDNA plasmids to enhance angiogenesis and restore vessel functions in the ischemic tissues. The investigated nanoparticles are EpoR NPs, RopE NPs (or anti-sense erythropoietin receptor cDNA) and EpoR/RopE NPs. For this study, we investigated how these NPs effectively improved angiogenesis *in vitro* and *in vivo* and whether a combination used is better than that of a single one. EpoR is selected for this research for its important role in inducing angiogenesis, maintaining cell protection, and facilitating proliferation of endothelial cells under oxidative stress and hypoxic conditions, especially those exposed to ischemia, while Rope has been reported for increasing EpoR protein expression. From this work, we can conclude that the fabricated positive surface charge NPs had an average diameter of around 200 nm and demonstrated a biphasic release (burst and sustained) of the payloads, EpoR, RopE, and/or EpoR/RopE cDNA plasmids. They also facilitated cell proliferation, provided cell protection, and induced cell migration properties *in vitro*. In the ischemic tissue, via angiogenesis, these NPs restored limb functions by its rapid, improved secretion of angiogenic proteins, capillary density, blood flow reperfusion and stronger muscle strength properties.

Table of Contents

List of Figures

List of Tables

CHAPTER 1

INTRODUCTION

1.1. Background

Peripheral arterial disease (PAD) is portrayed by chronic narrowing of the arteries in the lower extremities and often results in the occlusion and/or loss of functionality.[1] Damage to the endothelial wall lining often alters its native extracellular matrix (ECM) architecture,[2, 3] leading to a narrowed vessel and impaired delivery of oxygen-rich blood to organs, and this is one of the common problems associated with PAD development. PAD affects around 12 million people in the United States, especially elderly males 65 years and older, and it is linked to high morbidity and mortality rates.[4] Conventional modes of detection (Ankle Brachial Index or ABI, Toe Brachial Index or TBI, and angiography) and treatment (medicine, surgical bypass, endovascular techniques, and cell-based therapies) of PAD are limited by expensive associated costs, inability for early detection,[5] fibrotic complications,[6] adverse drug side effects,[7] and insignificant changes in ABI reading and/or total oxygen pressure after cell-based therapies.[8-10]

Conventional PAD detection is often performed using an Ankle-Brachial Index (ABI). As the most frequently used test, ABI measures the ratio of pressure in the brachium to that in the ankle, while the patient is at rest using a handheld Doppler ultrasound device.[11] With a 95% sensitivity,[12, 13] readings of ≥1.30, 0.91-1.29, 0.41-0.90, and ≤0.40 are interpreted as non-compressible, normal, mild-moderate and severe PAD, respectively.[14-16] ABI has many limitations, including lacking the ability to assess the exact severity of the disease, especially in individuals with calcified vessels, patients with poor blood flow, obesity, or non-compliant behaviors. The Toe Brachial Index (TBI) is often carried out on individuals with non-

compressible, calcified arteries to detect the presence of PAD via measuring the systolic pressure of either the big toe or the second toe and comparing it to the higher systolic pressure in both arms. With TBI, PAD can be detected in patients with measurements as high as 0.70 (abnormal arteries) using a plethysmography.[17] However, limitations of TBI include its expensive cost, its failure to detect early stages of atherosclerosis and its almost exclusively used on patients with suspected or unknown arterial injuries.[5] Additionally, suggestions on a positive/negative correlation between the severity of PAD and the biomarker levels such as serum bilirubin,[18] N-terminal pro-B-type natriuretic peptide,[19] plasma C-reactive protein (CRP), von Willebrand factor (vWF), interleukin 6 (IL-6), red cell folate, vitamin B12, total homocysteine[20] miR-16, miR-363, and miR-15b[21] are used to detect the presence of PAD. However, detection of PAD via biomarkers is still in its early stages and has only been applied to a small number of cohorts. Lastly, images produced by angiography have also been reported, but they are limited with the risks of renal toxicity and catheter trauma, and systemic complications from the use of contrast agents.[22] Lastly, elastography and dynamic contrast-enhanced (DCE) MRI[23] are deemed very beneficial for detailed information,[24] however, this tool often causes system fibrosis in patients with kidney diseases due to its use of exogenous gadolinium based contrast agents.[6]

For treatment of PAD, conventional PAD therapy could be categorized as non-invasive and invasive therapy. Non-invasive therapy towards treatment of PAD includes, but is not limited to, preventive management of the associated risk factors [25, 26] (e.g. hypercholesterolemia, hypertension, and smoking) with physical rehabilitation,[27] medicinal approaches such as statin therapy[28, 29] lipid inhibitors,[30] beta-blockers and diuretics,[31] Ramipril administration[32], and cell based therapy.[33-37] However, these therapeutic approaches have shortcomings. For instance, preventive treatments are only effective for patients who are motivated and committed to completing the program, and most of these

programs are not covered by health insurance.[38] Despite its common use, medicinal approach could have negative impacts. For instance, when administered as single or combination drugs to PAD patients, complications such as life threatening bleeding, cardiac complications, and liver problems can occur.[7] On the other hand, invasive PAD therapies such as surgical bypass, endovascular intervention,[39] angioplasty balloon catheters,[40] and bare metal stents[41, 42] have been reported for PAD treatment. Despite improving blood flow to tissues and organs, these therapeutic approaches are limited by availability of venous vessels, evasion of treating diseased vessels, impaired blood flow at the donor site, limited applications in cases of extremely diseased arteries,[43] excessive blood loss, bleeding issues post operation, and compressing lipid plaques onto the endothelial wall; hence evading their eradication from the disease arterial vessels.[44] Stent implantation has been reported to cause stent fractures[45] and progressive problems, which require repeated insertion and revascularization.[46] Other limitations include vascular trauma and endothelium denudation from balloon angioplasty and/or stents. Furthermore, due to the anatomical location of arteries such as the femoral and popliteal, forces of bending, stretching, and crushing exerted on the muscles promote complications post stent implantation such as stent fractures and/or dislocation.[47]

Thus, there is a crucial need for development of reliable detection tools and effective treatment options for PAD to improve the patients' quality of life and to reduce morbidity and mortality rates. Today, despite being in its early stages, nanotechnology stands out as a promising alternative path towards diagnostic, therapeutic and theranostic approaches to detect and treat PAD (**Figure 1.1**). Nanoparticles for use in PAD detection and therapy are reviewed in detail in addition to a brief discussion about current diagnosis and treatment modalities.

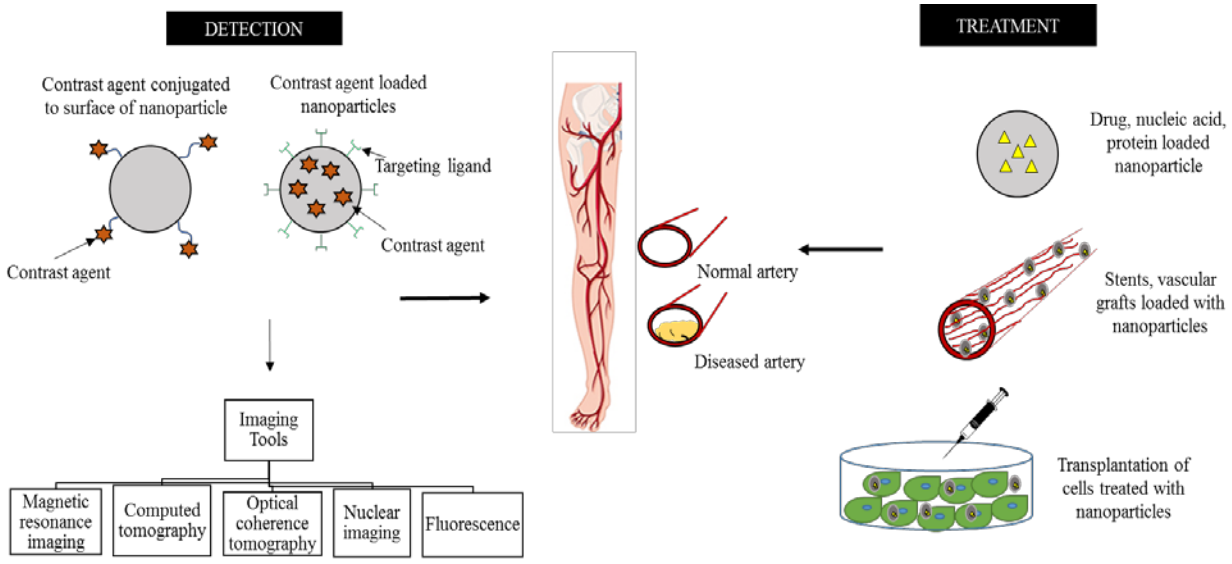

Figure 1. 1. Nanotechnology applications towards PAD. Schematic illustration of the various directions that nanoparticles can be applied towards PAD detection and treatment.

1.2. Application of Nanoparticles for PAD Detection

With its emerging uses in the prevention, diagnosis and treatment of several diseases, nanotechnology shows excellent promise in improving health globally for PAD patients, including morbidity and mortality rates. Previous PAD detection tools produced images of changes in tissue appearance but could not confirm whether those changes represent a disease state. Thus, there is an absolute need for new, improved diagnostic strategies for PAD, especially those that can identify various stages of this disease. Through nanotechnology, investigators and clinicians employ the use of very small structures often less than 100 nm, to effectively localize and determine events occurring in ailing vessels.[48] Developed imaging tools help to detect PAD early and determine what therapeutic route will work best for eradicating disease in the patient in particular, and the overall population in general (**Figure 1.2**).

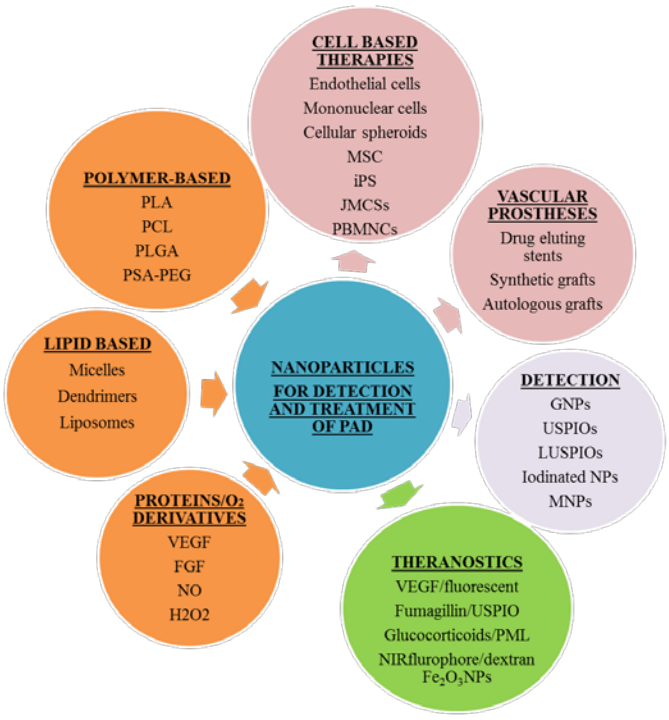

Figure 1. 2. Potential NP paths used in PAD detection and treatment. NPs made from various biomaterials such as lipids and polymers have been developed for delivery of therapeutic payloads, including proteins, to cells and vascular prostheses and for detection, treatment and theranostic applications. Abbreviations: fibroblast growth factor (FGF), gold nanoparticles (GNPs), hydrogen peroxide (H_2O_2), induced pluripotent stem cell (iPS), janus magnetic cellular spheroid (JMCS), lipid ultra-small paramagnetic iron oxide (LUSPIO), magnetic nanoparticle (MNP), mesenchymal stem cell (MSC), nitric oxide (NO), paramagnetic liposome (PML), peripheral blood derived mononuclear cells (PBMNCs), polycaprolactone (PCL), poly(lactic) acid (PLA), poly(lactic-co-glycolic) acid (PLGA), poly(sebatic) acid-polyethylene glycol (PSA-PEG), ultra-small paramagnetic iron oxide (USPIO), and vascular endothelial growth factor (VEGF).

Diseased vessels are usually characterized by lipid retention, expression of cellular adhesion molecules, destruction of endothelial cells, production of macrophages, and formation of plaque. Often observed during the different stages of inflammation, these characteristics serve as potential molecular imaging probes for detecting PAD. Molecular imaging is a subset of imaging which involves the depiction and evaluation of any biological process at the cellular and sub-cellular levels via the application use of imaging modalities

including cardiac magnetic resonance molecular imaging (CMRI), computed tomography (CT), optical coherence tomography (OCT), nuclear techniques, magnetic resonance imaging (MRI), and fluorescence.[49] In other words, these non-invasive imaging modalities permit the visualization of cells and sub-cellular components ranging from angstroms to centimeters in any living organism. Unlike the traditional approach of diagnostics using bare contrast agents, which have poor half-lives and high levels of toxicity, researchers sought to incorporate these imaging probes into nanoparticles (particles <100 nm in dimension) to overcome these limitations.[50] Despite being in its infancy stages, the application of nano-platforms as diagnostic tools for PAD has growing potential. The integration of these various contrast/imaging reagents to nanoparticles produces images that are used to evaluate the progress of PAD in mice and to monitor the delivery of the therapeutic agents effectively (**Figure 1.3**).[51] These nanoprobes have more advantageous biomedical applications due to amplified signals, enhanced binding affinity/specificity, and increased imaging capacity via the use of a single nanoparticle attached with several imaging labels for multiple imaging modalities.[52] Furthermore, nanotechnology has tapped into the use of multiple biomarkers such as: B type natriuretic peptide, homocysteine, and C- reactive protein, due to the unsatisfactory detective power of individual biomarkers.[53] Detection of an existing arterial injury could also be achieved via these new nanosensory devices (**Table 1.1**). This revolution was further reported in the *in vivo* detection of biomarkers using a selective ion detection nanoparticle probe to quantify the level of potassium during hypoxic conditions.[54]

Table 1. 1 Common Nanoparticles used in Detecting PAD

Types of NPs	Size [nm]	Contrast agent	Targeting ligand	Tool	Results	Reference
Liposome with MNPs	300–350	Gd	LM609	MRI	-Detected angiogenic regions. -Enhanced and detailed images of rabbit arteries.	[57]
PM-PFCNPs	175–200	Gd	Fumagilin	MRI	-Strong MRI signal compared to that of control NPs.	[58]
MION-47	27	Fe_2O_3	N/A	MRI	-Quantified macrophages by T_2 signal intensity. -Decreased T_2 signal intensity in atherosclerotic lesions.	[68]
USPIO	107	Gd	MSR (CD204)	MRI	-79% signal intensity increased from arterial wall. -Localization of NPs in macrophage regions.	[64]
LUSPIO	≈10	Fe_2O_3	[MDA]2 E06/IK 17 antibody	MRI	-Great arterial wall diffusion. -Minimal signal at injured sites	[70]
SPIO	<100	Fe_2O_3	Aminopropyl trimethoxusilane (APTS)	MRI	-At least four weeks monitoring capacity. -Wide hypointensity from treatment site.	[71]
Lipid based	125	Gd	CD36	MRI	-Targeted human macrophages located at the plaque. -Large signal intensity at fibrous plaque region.	[63]
VUSPIO	7.5	maghemite γ-Fe_2O_3	rIgG4 TEG4 antibody	MRI	-Fluorescent shift observed when compared to that of blank NPs. -Gross signal loss from treated platelets.	[84]
GNP	≈20	Au	N/A	CT	-5× higher deflection slope post treatment. -Macrophages within tissues were independent of the optical properties of tissues.	[81]
GNR	40 × 18 (L × W)	Au	N/A	CT	-Higher GNR average slopes than baseline slope (0.827 vs 0.196). -Discrimination detection of GNR.	[82]
GNP	7.2	Au-HDL	N/A	CT	-Primarily localized in macrophages. -Detailed macrophage composition.	[83]
GNS	60	Au	Anti-eGFR	OCT	-Increase in photothermal emission (300%) from labeled GNS-treated cells over that of controls.	[95]
PMMA/PEG	20	^{64}Cu	C-type atrial natriuretic factor (CANF)	PET	-PET imaging confirmed blood flow restoration in ischemic limb after treatment. -Significant tracer uptake by ischemic mice over that of controls.	[101]
Micelles	11–110	Dioctadecyl oxacarbo-cyanine perchlorate (DiO)	oxLDL	Fluorescence	-Upon release and diffusion of DiO, energy transfer caused shift in emission peak. -Threefold to fourfold inhibition of oxLDL uptake.	[122]
Micelles	17	Cy7 labeled CREKA	Pentapeptide	Fluorescence	-High fluorescent intensity in atherosclerotic regions. -Fluorescent micelles vs blank micelle (209 000 vs 5100 au).	[125]
PAM micelles	15	Cy7	MCP-1	Fluorescence	-Detected early and late atherosclerosis. -Cy7 micelles bound more to injured arteries in late stage than early stage atherosclerosis (5×10^7 radiance (p/s/cm^2/sr) vs 3×10^7 radiance (p/s/cm^2/sr)).	[126]

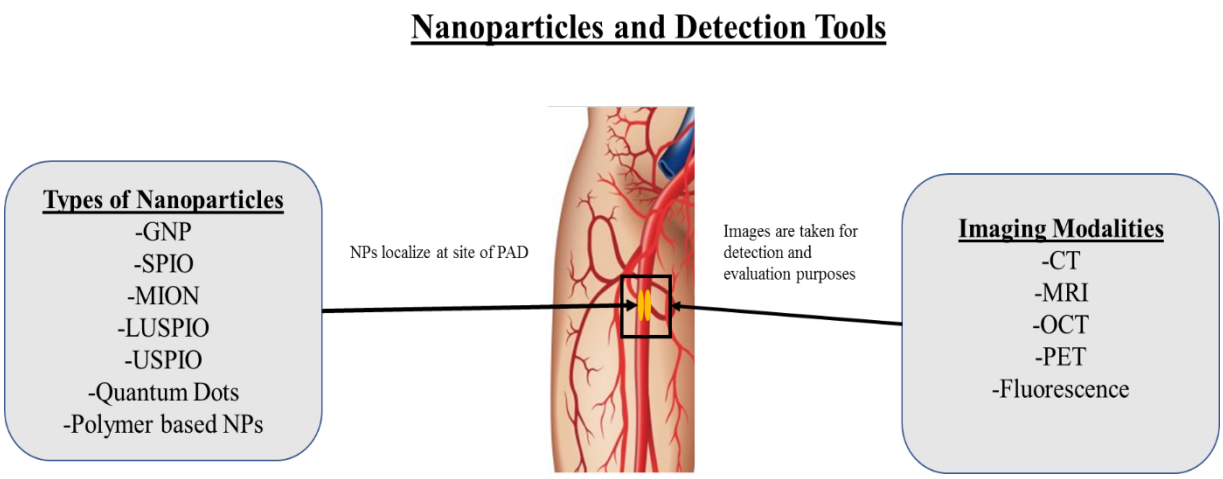

Figure 1. 3. Nanoparticles and their current detection tools. NPs can be fabricated using different synthetic and metal-based biomaterials. These NPs can be analyzed via the use of imaging tools such as optical imaging, magnetic resonance imaging (MRI), computed tomography (CT), optical coherence tomography (OCT), positron electron tomography (PET), and many more. Abbreviation: gold nanoparticle (GNP), lipid ultra-small paramagnetic iron oxide (LUSPIO), magnetic iron oxide nanoparticle (MION), super paramagnetic iron oxide (SPIO), and ultra-small paramagnetic iron oxide (USPIO).

1.2.1. Nanoparticles and Magnetic Resonance Imaging (MRI)

MRI is a noninvasive technique involving high spatial resolution and excellent soft tissue contrast expressed via signal loss. This signal is produced by contrast agents following their accumulation in vasculature, and detected by the MRI modality providing functional, phenotypical and molecular information. Although MRI is a commonly used imaging tool, these have been reported to produce ineffective and imprecise images due to endogenous contrast agents. Therefore, exogenous contrast agents have been studied to produce improved images, with the potential to detect both the localization and characterization of atherosclerotic plaque.[55] For instance, in a normal artery, the expression of $\alpha_v\beta_3$ integrin is minimal, whereas in atherosclerotic vessels, this integrin is highly expressed, and thus serves as a biomarker for

detection of damaged vasculature.[56] Tagged with $\alpha_v\beta_3$ antibodies, Gd-loaded liposome nanoparticles enhanced visibility of injured vessels in rabbits using MRI.[57] Moreover, the expression of $\alpha_v\beta_3$ vessels has been studied with designed paramagnetic perfluorocarbon nanoparticles (PM-PFCNPs) for early detection of atherosclerosis.[58] Imaging from MRI reported that fumagillin-loaded PM-PFCNPs (175-200 nm) administered to rabbits resulted in decreased signals (~3%) when compared to that of untreated rabbits (~18%).

MRI application using nanoparticles has granted researchers and clinicians the ability to monitor the progress of PAD effectively via the inclusion of imaging agents, which are classified as T1 and T2 shortening agents. The former is based on the use of gadolinium, (Gd^{3+}), a contrast agent with the ability to brighten MRI images, while the latter revolves around iron oxide nanoparticles (**Figure 1.4**). T2 shortening agents such as magnetic iron oxide (Fe_2O_3, Fe_3O_4) participate in this imaging tool by facilitating extravasation within the vascular tissues, where they are up taken by macrophatic cells.[59]

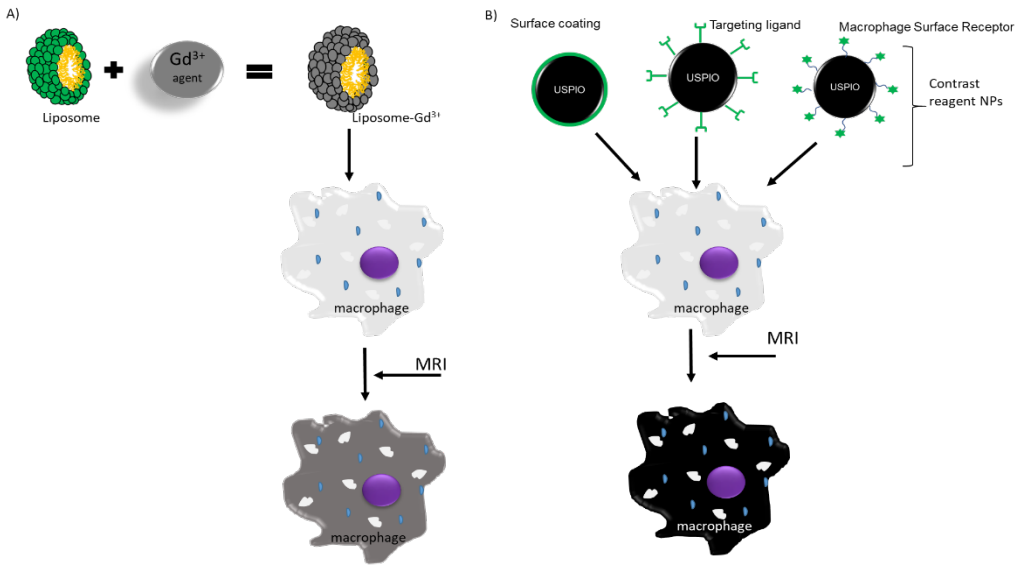

Figure 1. 4. Nanoparticles and MRI. Nanostructures fabricated into A) liposomes loaded with T1 agent (gadolinium) and B) T2 agent (iron oxide) NPs can be modified by surface coating, targeting ligands and macrophage surface receptors to target cells within the blood vessels. Upon internalization of these T1 and T2 NPs, signal intensity varies within cells as Gadolinium produces brighter images while iron oxide produces darker MRI images.

Gd^{3+} is a positive contrast agent with seven unpaired electrons, where in the presence of water-based environments, produces strong magnetic fields that impact the water protons relaxation rate and produces long relaxation time (hence longer signals).[60, 61] When bound to disease vasculature, Gd^{3+} produce brighter images upon signal detection by MRI. As a chelate, this heavy metal molecule may cause serious systemic toxicity issues. This issue is resolved by synthesis of nano-probes such as micelles, liposomes, and polymeric particles incorporated with Mn^{2+} or Gd^{3+} to produce nanoparticles with properties that provide brighter and more accurate T1-weigthed MRI images.[62] Incorporating Gd^{3+} within nanoparticles will minimize risk of toxicity when deployed to diseased vasculature. Furthermore, NPs have been credited for their easy surface modification and high targeting capacity. For instance, Gadolinium Gd^{3+}-lipid nanoparticles labeled with CD36 antibodies were used to target human macrophages.[63] MRI images from this study showed that the CD36-labeled lipid nanoparticles were able to detect and characterize atherosclerotic plaque, which could be used to further plan therapeutic options to prevent atherothrombotic events. The easy customization of NPs surface was also reported in micelles loaded with Gd^{3+} to target the macrophage scavenger receptor (MSR) in atherosclerotic mouse models.[64] NPs are so versatile for *in vivo* imaging because they can carry a larger amount of contrast agents than a single small molecule while minimizing systemic toxicity. T2 contrast agents, on the other hand, are negative contrast agents that produce dark images upon accumulation at a disease site. Due to their elevated magnetization properties, iron oxide NPs are commonly used as T2 agents.[65, 66] Customization of these nanoprobes is important as their shape, surface charge, and size has been found to affect the MRI signal. For instance, the improved tissue distinction properties of these iron oxide NPs are often attributed to their surfaces that are often coated with dextran or siloxane on the magnetite iron oxide core.[67] The size of NPs is crucial in MRI application because magnetic concentration increases with the size of the nanoparticles. Detection of macrophages via

monocrystalline iron oxide nanoparticles (MION-47), superparamagnetic iron oxide (USPIO) NPs (~5 nm diameter core with a coated dextran layer ~10 nm thick), and 3-T MRI has been used for quantification of accumulated foam cells and the progressive assessment of atherosclerosis.[68] Qualitative and informative images of rosuvastatin treated arteries revealed decreased macrophage content post-administration of MION-47 when compared to those of rabbit arteries that did not receive rosuvastatin (controls). Amirbekian et al.[64] explored the uptake of macrophage scavenger receptor (MSR)-conjugated USPIO NPs by macrophatic foam cells to depict atherosclerosis in mice. There was approximately 79% of signal intensity upregulation compared to that of controls (non-targeted micelles) 24 hours post administration. Application of pro-angiogenic and pro-inflammatory oxidation specific epitopes (OSE) for PAD detection has also been explored.[69] NPs are advantageous in *in vivo* detection because they can appropriately load large amounts of contrast and maintain their ability to travel systemically in the body as opposed to much larger structures. Designed lipid ultra-small iron oxide particles (LUSPIO NPs) conjugated with malondialdehyde [MDA]2 E06 and single-chain (IK17) Fv antibodies were specific for the detection of PAD and atherosclerotic plaque at high risk for rupture in this study. MRI images further showed a specific NP uptake localization at the injured areas compared to that of untargeted LUSPIOs (controls).[70] Recently, aminopropyltrimethoxysilane (APTS)-coated iron oxide nanoparticles (APTS NPs) were employed to monitor cells transplanted within the ischemic hindlimb in mice.[71] Reduced signals from 3T MRI scans revealed the localization and migration of the transplanted cells up to 4 weeks. A drawback using SPIOs with MRI is that local nanoparticle accumulation resulted in dark contrast images, making it difficult for quantitative analysis.

NPs for MRI have shown to be customizable to assess for biodistribution, bioavailability, biophysiology, and *in vivo* detection. Despite, the positive attributes associated with nanoparticles and MRI, there still exist some limitations with using Gd^{3+} as a contrast agent.

This includes report of Gd^{3+} linked to brain hypersensitivity and neural toxicity apoptosis,[72] further complication in PAD patients with kidney diseases,[73] and reactions for some patients.[74] It should be noted that scientists are taking various measures to overcome these challenges by fabricating manganese (Mn^{2+}) based NPs, which have been found to be more biocompatible than Gd^{3+} for *in vivo* detection and result in minimal renal failure.[75] Limitations to iron oxide based NPs typically involve their poor integration into the clinical field and their synthesis process where ferrous/ferric salts are dissolved in alkaline solution creating poor crystallinity and size variation. These issues could be rectified by adding surfactant into the reaction chemistry, e.g. polyvinylpyrrolidone (PVP) and sodium cholate to enhance NP dispersity, crystallinity, aggregation.[76] Also, iron alloys could be applied as alternatives to iron oxide based NPs in MRI detection due to their biocompatibility, higher physical properties and outstanding magnetic properties when compared to that of iron oxides.[77]

1.2.2. Nanoparticles and Computed Tomography (CT)

In addition to MRI, nanoparticles have been used with CT scans for the detection of stenosed and occluded vessels. CT is a very common non-invasive imagive modality that uses computational algorithms to convert absorbed x-rays from various angles of the body into a high resolution 3D structure. With the ability to distinguish between hard tissues (e.g. bone) from soft tissues (e.g. vasculature), this modality is limited with poor contrast of soft tissues imaging. To overcome this limitation, NPs can be loaded with heavy/dense materials and be used for CT. Due to their high absorption coefficient, some commonly used dense contrast materials are composed of iodine, bismuth or gold nanoparticles.[78] Iodinated contrast agents are usually employed for vascular visualization, however, their short blood circulation time and quick clearance by the kidneys renders them less attractive. On the other hand, gold contrast agents have a relatively high x-ray attenuation coefficient which makes them suitable

for clinical CT. Common isues in detecting atherosclerosis during its early stages are often linked to the small plaque sizes and deficiency of suitable tracers/markers to the tiny, unstable plaque. NPs can play a great role as contrast agents in CT detection of PAD and overcome these limitations because their prolonged circulation within the blood makes them excellent blood pool agents. Also, with longer circulation time; these NPs allow for precise depiction of soft tissues such as blood vessels.

Gold nanoparticles (GNPs) at various sizes and shapes have been developed for overcoming these limitations[79] of early plaque detection and inadequate tracers. GNPs not only possess excellent optical and chemical properties, but also have been known to be easily taken up by the major component of atherosclerotic plaque, macrophages, due to their metallic physical nature.[80] Targeting of macrophages for detection is easier since these NPs are naturally taken up by macrophages. As reported by Ankri et al.[81] there is a positive correlation between GNP concentrations and macrophage uptake. Also, post administration of GNPs in injured or damaged arteries revealed a diffuse reflection (DR) slope five times higher than that of normal arteries. This same group targeted macrophages using gold nanorods (GNRs);[82] a significant change from 0.196 to 0.827 represented a shift from macrophages only to macrophage-labelled GNRs via the analyzed diffuse reflection slope. This leads to the conclusion that CT scans via nanoprobes fortified the sensitivity of the DR for detection of atherosclerotic inflicted vessels. Furthermore, GNPs were extensively used for the characterization of macrophages' composition and calcification after intravenously (IV) administered into atherosclerotic mice.[83] CT images reported the localization of these NPs to be primarily in macrophages at the atherosclerotic region when compared to that of controls. Modification of GNP surfaces with either PEG, glucosamine, hydroxypropylamine, ethanediamine, or taurine has also been used to improve circulation time, biocompatibility, and uptake by cells; hence, permitting better visualization and quantification via CT images.

These reports reiterate the potential of GNPs in addressing limitations associated with the traditional mode of CT technique. NPs for CT application can be easily synthesized and customized according to a desired function. Recently, recombinant human rlgG4 TEG4 antibody was functionalized onto a versatile USPIO NPs (VUSPIONPs) surface to target activated platelets.[84] *In vitro* analysis confirmed their interactions towards platelets, whereas MRI images of treated ApoE(-/-) mouse models showed selective binding of TEG4-VUSPIO NPs to the plaque. Nanoparticles for CT detection are advantageous over MRI because tissue scanning can be completed within seconds unlike MRI that requires a longer time due to breathing by patients when obtaining images. Since PAD is characterized with macrophage accumulation within blood vessels, early PAD development can be easily detected by applying macrophage specific nanoprobes. However, the small detectable concentration difference (5.9 mM) of these NPs between targerted tissues and background is on the order of mM which could result in a lack of sensitivity from the imaging modality.[85] Also, only one parameter can be visualized at a time. This however can be modified by using nanoparticles for multiplexing CT imaging.

1.2.3. Nanoparticles and Optical Coherence Tomography (OCT)

In addition to the aforementioned techniques, OCT applies an interferometry technique which relies on the input of near infra-red light within a substrate to produce images via optical interferences from backscattering of light beams from tissues components, which could then be converted to 2D or 3D images.[86] Light scattering arises as a result of the variance from the refractive index on a scale of wavelength probing light.[87] Nanoparticles have been combined with OCT to reduce potential issues of photobleaching.[88] Upon application with noble metals such as gold or silver, their surface plasmon resonance (SPR) is often restricted within a small area where excitation by light occurs from re-emission, or absorbance. OCT is often used to

visualize the state of vessels that have undergone stent implantation and/or post-stent implantation effects.[89, 90] This invasive catheter-based method of viewing the arterial lumen uses near infrared light with a high image resolution of 15-20 □m.[91] It has been proven to be effective in the detection of atherosclerotic vessels, incomplete stent apposition, neointimal hyperplasia, thrombus formation, and stent endothelization.[92] NPs serve as great contrast agents in OCT because despite their size, the level of backscattered light produced is comparable to that of large fluorophores.[93] There has been confirmation that a GNP of about 80 nm has equivalent signal intensity as that of 10^6 fluorophores, thereby overcoming toxicity issues via the use of a lower dosage.[94] Also, NPs are biocompatible and dispense rapid thermal responses to external thermal excitation when administering within diseased vasculature. In a study by Skala et al.[95] phantom-like tissues were exposed to gold nanospheres (GNSs) conjugated with anti-epidermal growth factor receptor (EGFR). A high photothermal release (300%) was observed in cells overexpressing the receptor when compared to controls (nonconjugated, free EGFR); hence, proving that this mode of imaging has the potential to specifically visualize diseased tissues. The versatility of NPs in OCT applications makes it possible to easily tune its shape and size for precise resonant wavelength, scattering and absorption efficiency.[96] GNPs and OCT application can be quite versatile, with a shift of SPR towards shorter wavelength applications for higher resolution OCT; shifting SPR toward longer wavelengths applies to OCT systems with larger penetration depths. Despite being deemed suitable for the detection of vulnerable plaque, this imaging technique has some limitations including the inability to penetrate deep into the vessel wall and failure to differentiate between minimal neointimal proliferation and simple fibrin clot post implantation of drug eluting stents (DES).[97]

1.2.4. Nanoparticles and Nuclear Imaging (NI)

Positron emission tomography (PET) and single photon emission computed tomography (SPECT) are imaging tools that use radioactive tracers for assessment of the molecular and physiological state of healthy and diseased tissues. These radioactive tracers emit gamma rays upon injection, cell receptor binding, or uptake by cells where their kinetics and distribution within these tissues are then translated to 3D images.[98] SPECT and PET have been frequently used with NPs in *in vivo* studies and clinical settings due to their good spatial resolution, high level of sensitivity, and effectiveness in PAD detection.[99] Furthermore, nanoparticles can be modified with targeting ligands for specific functional imaging. This evidence is illustrated by amphiphilic nanoparticles designed to target the chemokine receptor 5 (CCR5), a key player in late stages of atherosclerosis and a marker for plaque stability. Luehmann et al.[100] synthesized a poly (methyl methaxrylate) (PMMA)-core/polyethylene glycol (PEG) shell nanoparticle conjugated with D-Ala 1-peptide T-amide (DAPTA) peptide, a ligand to CCR5, for administering in ApoE(-/-) wire-injured mice. PET images revealed great sensitivity and specificity towards an up-regulation of the CCR5 and demonstrated higher uptake of the nanoparticles at injured sites. The specific relationship between angiogenesis and natriuretic peptide clearance receptor (NPC-R) was also explored through the application of multifunctional core-shell nanoparticles of a PMMA core and PEG end chains.[101] These copper-labeled nanoparticles demonstrated specificity in hindlimb ischemic mouse models via PET images with a high accumulation at ischemic sites. PET can quantitatively confirm biodistribution of NPs overtime within the animal model making it a superior technology. For example, Orbay et al.[102] have previously explored the PET imaging modality through the use of ^{64}CuNOTA-TRC105 for quantitative/monitoring of angiogenesis in mice hindlimb, where the nanoparticle uptake was highest in the early hours post-surgery. NPs can also be designed specifically to bind to macrophages to assess PAD since this disease is highly involved in

immune responses. Elsewhere, high specificity and sensitivity for atherosclerosis detection in mice has recently been reported.[103] Tagged with macrophage inflammatory protein II (vMIP-II), poly (methyl methacrylate)-core/polyethylene glycol shell NPs (^{64}CU-vMIP-II-NPs) were administered to ApoE(-/-) vascular injured and atherosclerotic models. Imaging from PET revealed distinct signals and the build-up of ^{64}CU- vMIP-II-comb in the atherosclerotic plaque.

Additionally, most NPs used for PET are composed of chelate materials. This chelation can help improve tracking of NPs. To get higher sensitivity and better resolution of atherosclerosis progression, a copper comb-like NP labelled with the peptide D-Ala_1 – peptode T-amide (DAPTA) (^{64}CU-DAPTA-comb) was explored, and the results revealed that it was an effective imaging probe for atherosclerosis.[104] Also, specific vascular inflammation can be observed by combining PET, CT, and MRI.[105] Such a combination is more advantageous compared to that of a single one due to their high detectability and sensitivity of disease stages since PET and CT were reported to enhance morphological images and to be used for determining disease state via biomarkers (VCAM-1, MMPs, VAP-1, SSTR, TSPO, choline and glucose metabolism), while PET, MR and CT all increased sensitivity.[106-108] Therefore, combinations of different imaging modalities promote a better insight (anatomical and physiological) into the pathophysiology of PAD and a greater understanding about how to restore healing in these vessels. Recently, the multi-modal ^{64}CU-RGO-IONP-PEG nanoparticles (68 ± 7nm)[109] have been explored for better quantitative analysis of PAD detection. Administration of ^{64}CU-RGO-IONP-PEG nanoparticles in hindlimb mice models resulted in increased nanoparticle accumulation over time in ischemic hindlimb, when compared to the minimal signal observed in control limbs (non-ischemic) as confirmed by PET data. Photoacoustic signals also revealed an increase in the ischemic hindlimb three days post NP administration when compared to the minimal signal from the control limb (non-ischemic). Therefore, photoacoustic images provided anatomical characteristics with the highest

photoacoustic signaling found in the ischemic limb when compared to controls, whereas PET images confirmed the inverse relationship between uptake and disease stage as indicated by the increased ^{64}CU-RGO-IONP-PEG uptake observed when administered at early onset of the disease (day 3) versus at a later time (17 days). Lastly, Im et al.[110] reported that the administration of PEGylated RGO-IONPs (93± 33nm) into ischemic mice lead to their increased accumulation at ischemic sites, improved circulation time and reduced accumulation in the liver compared to that of the control. PET-CT imaging was also able to show accumulation of the hybrid Cu-TNP in atherosclerotic arteries of apoE-/- mice.[111]

A major advantage of PET/SPECT based nanoparticles is that they a have high surface to volume ratio which makes it easy for modification and carrying of large payloads of isotopes for single or multiple tagerting for detection or therapeutics to arterial vessels. Their encapsulation property helps in minimizing trace amounts of free radioactive material required in PET. Furthermore, the longer circulation half-life of NPs makes them more applicable than naked radioisotope molecules and/or nanoprobes; hence improving targeting binding affinity. Despite such qualities, these NPs also have some shortcomings. First, chelate biomaterials for NPs can cause the radiolabelled isotope to disassemble from NPs causing transchelation of native protein leading to erroneous localization and quantification at the disease site.[112] Furthermore, NP stability is of upmost importance in PET detection of PAD because uncoupling attached radiolabels could falsify quatification results. To overcome this limitation, scientists have taken measures to improve stability by fabricating bifunctional chelator to label silicon based quantum dots.[79]

1.2.5. Nanoparticles and Optical Imaging

Laser doppler perfusion imaging (LDPI) and near infra-red fluorescence (NIRF) are two common optical imaging modalities often applied in the detection of PAD. The former involves

a change in laser frequency resulting from movement of particles, while the latter uses fluorescent contrast agents that are excited by NIR light within a known wavelength range (700-1000 nm) when targeting molecular markers. Nanoparticles act as effective contrast agents to provide early detection of atherosclerotic plaque and a real-time illustration on the NP location and its released drug. Of these nanostructures, quantum dots (QD), a group of inorganic fluorescent semiconductor nanoparticles (2-10 nm crystals with CdSe cores and ZnS shells), possess exceptional photochemical and photophysical properties superior to those of organic fluorophores.[52, 113] These photostable crystals are believed to trace plaque better than contrast agents or dyes through the emission of multicolor fluorescence to boost the sensitivity of biological detection and visualization.[114] Furthermore, optical imaging of PAD is often limited with deep tissue penetration. By applying NPs, deep tissue visualization is possible when combined with red-shift NIR QD. This is demonstrated by Ximendes et al.[115] who reported early detection of ischemia by deploying near the infrared emitting quantum dots (NIR-QDs) to mice hindlimb. These NIR-QDs proved capable of tracking stages of revascularization and tissue recovery processes, advanced thermal dynamics and high penetration. This mode of imaging presents admirable properties such as long-term fluorescent exposure, flexible manipulation to desired wavelength range, and resistance to photobleaching.

Since QDs are often found to be toxic in both *in vitro* and *in vivo* studies, QDs have been modified with polyethylene glycol (PEG) to induce their colloidal stability,[116] with specific antibodies and ligands (E-cadherin, N-Cadherin, Vimetin, RANKL)[117] and nucleic acids[118] to enhance cell specificity, and with cationic peptides to facilitate particle internalization[119] and to monitor regions prone to developing plaque.[120] Some advantages of applying QDs in optical imaging for PAD are their highly photostable property and photobleaching resolution. Some QDs, especially red shifted NIR QDs, resolve issues of deep tissue penetration. Also, the dual nature of designed lipidic NPs improves the NP stability and drug/dye loading capacity

from the void created by the highly disorderd lipid matrix.[121] However, these same inorganic NPs are debated for clinical application due to their potential toxicity to tissues. Silver and carbon based QDs are proposed as alternatives to QDs due to their biocompatibility and optical intensity characteristics.

Lipidic NPs have also been explored in PAD detection due to their hydrophobic core and hydrophillic surface/shell. This dual nature permits the loading of both hydrophobic and hydrophillic contrast agents in respective regions. Recently, reports on anti-atherosclerotic activity of fluorescent-oxLDL functionalized micelles (11-110 nm) were confirmed with a significant decrease (28%) in uptake of micelles by human monocyte derived macrophages (HMDM) when exposed to serum and lipase solution compared with that of the control group (unlabeled micelles).[122] Other studies have reiterated such findings with amphiphilic micelles ranging from 10-200 nm.[123, 124] Additionally, the dual nature of lipid NPs groups them as multimodal vehicles. A multifunctional, self-assembled micelle (17 nm) with an attached pentapeptide, cysteine-arginine-glutamic acid-lysine-alanine, for targeting and treating atherosclerotic plaque in $Apo^{-/-}$ mice resulted in complete covering, accumulation and eradication of plaque in injured blood vessels.[125] In this study, a significant fluorescence signal (intensity of 209,000) and anti-thrombotic activity was observed in mice treated with labeled micelles, whereas only low fluorescence (intensity of 5,100) was observed for those of unlabeled micelle treated vessels. Furthermore, peptide amphiphilic micelles (PAMs) for targeting monocytes via the labeled MCP-1 ligand were fabricated (15 nm) for the detection and differentiation of atherosclerosis in ApoE mice.[126] Confocal microscopy confirmed the specific monocyte binding *in vitro* one hour post treatment versus minimal fluorescence observed in the unlabeled PAM micelles. After IV injection of these nanoparticles to mice arteries for 24 hours, *ex vivo* imaging revealed the binding specificity of labelled PAM micelles onto monocytes at both early and late staged atherosclerotic events, with a higher binding in

the late stage [5× 10^7 ± 1 × 10^7 radiance (p/s/cm^2/sr] than in the early stage [3 × 10^7 ± 0.5 × 10^7 radiance (p/s/cm^2/sr]. Despite its admirable qualities, this method of imaging could result in high background signals, loss of labels to neighboring cells, signal reduction due to the result of compounds such as water or hemoglobin, and absorbing visible light.[127]

1.3. Application of Nanoparticles for the Treatment of PAD

With high morbidity and mortality rates linked to cardiovascular diseases in the Western world, the recent influx of nanomedicine/nanotechnology serves as an alternative pathway for applying therapeutic solutions to this trauma. Investigators and clinicians are constantly at work to invoke different forms of treatment using various types of nanostructures, including polymer nanoparticles (**Table 1.2**), to achieve more specific drug delivery and to induce therapeutic effects while reducing toxicity and drug side effects (**Figure 1.5**).

Table 1. 2 Common Nanoparticles used in PAD Treatment

Types of NPs	Size [nm]	Payload	Result	Reference
Liposome	150	$\alpha_{IIb}\beta 3$ & P-selectin	-Enhanced selectivity and adhesion for platelets under flow overtime. -Site selective delivery of $\alpha_{IIb}\beta_3$ and P-selectin.	[132]
Chitosan	182	Secretonium peptide	-Formation of highly dense arterioles -Decreased tissue necrosis.	[138]
PLGA	200	Heparin	-Attenuated proliferation of SMCs. -Inhibited restenosis.	[144]
PLGA	200	Pioglitazone	-Increased blood flow restoration. -Promoted tube formation.	[145]
PVAX	200	H_2O_2 scavenger	-Decreased H_2O_2 in ischemic tissues. -Increased cell viability, cell migration and blood flow.	[147]
HPOX	<100	*p*-Hydroxybenzyl alcohol	-Promoted blood flow perfusion and capillary density. -Augmented EC recruitment and proangiogenicv growth factor secretion.	[149]

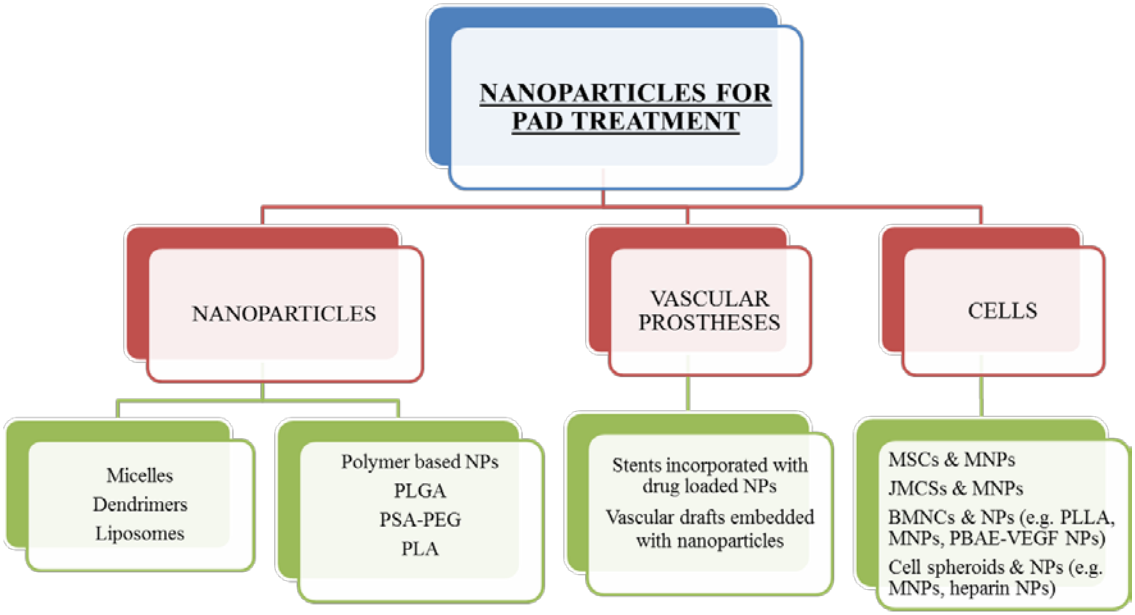

Figure 1. 5. Applications of nanoparticles for PAD treatment. NPs can be designed as drug/payload vehicles from lipids as well as synthetic and natural biomaterials, which could be applied in delivery carriers, cell-based therapy and vascular prostheses. Abbreviations: poly(lactic) acid (PLA), poly(lactic-co-glycolic) acid (PLGA), and poly(sebatic) acid-polyethylene glycol (PSA-PEG).

1.3.1. Nanoparticles as Therapeutic Carriers

1.3.1.1. Nanoparticles as Carriers for Nucleic Acids and Peptides

Over the last decade, there has been a vast application of nucleic acids and protein delivery to induce efficacy of PAD therapy in research and clinical studies. However, administration of these naked molecules has not produced any acceptable clinical outcome due to the poor circulation half-life of these molecules. To date, a variety of NPs have been developed and used to deliver nucleic acids and proteins. Dendrimers have been applied as carriers for delivery of siRNA and cDNA plasmid due to their outstanding properties, including their highly branched polymers consisting of three main regions (the core, branching zone and branch extremities) where modification can occur.[128] These multivalent structures have been reported in coronary artery disease treatment and have shown their effectiveness in gene

delivery to SMCs in arteries of rabbits when compared to that of transfection using DOTMA/ DOPE liposomes;[129] hence, their potential as an alternative treatment for PAD. Furthermore, these nanostructures are often referred to as effective transfection agents mostly due to the electrostatic interactions between their primary amine end groups with the incorporated DNA or siRNA.

Besides dendrimers, liposomes have often been employed as vascular delivery carriers, due to their biocompatibility and their broad vascular applications. By encapsulating proteins within NPs, they are protected from undesired enzyme degradation and ensured the controlled release within cells for higher therapeutic efficacy. To treat PAD, scientists have designed cyclic RGD peptide conjugated liposomes with affinity to P-selectin and integrin GPIIb-IIIa receptors on activated platelets.[130, 131] Specific vascular delivery was demonstrated in rat vessels through enhanced brightness and site specific targeting of platelets when compared to samples of either RGE-liposomes or linear RGD (lRGD)-liposomes. In addition, the versatility of NPs allows them to be chemically and physically modified via multi-targeting of arteries to ensure stronger signaling responses. Liposomal constructs have been developed via the use of multiple targeting peptides such as integrin $\alpha_{IIb}\beta 3$ and P-selectin.[132] These carriers were found to have a synergistic mechanism that enhances selectivity and strong adhesion to the injured site under flow when compared to those of a single labeled peptide. Recently, $VEGF_{165}$ peptides were delivered via PEGylated liposomes to ischemic rat hind limbs and resulted in improved blood perfusion, increased CD31 expression and induced tube formation by 174%, 143% and 168% respectively, when compared to that of controls.[133]

Polymer nanoparticles such as poly(lactic-co-glycolic acid) nanoparticles (PLGA NPs) have also been used for targeted delivery of therapeutic agents, including genes to ischemic sites in peripheral arteries to overcome safety issues of viral vectors for gene delivery.[134-136] The VEGF cDNA loaded NPs promoted significant angiogenesis with dense capillaries,

improved collateral circulation, and improved expression of the VEGF gene in rabbit ischemic models when compared to that of naked plasmid administration.[137] NPs provide controlled release of payloads at durations suitable to achieve therapeutic outcomes. Recently, chitosan thioglucolic acid mercaptonicotinic acid (CS-TGA-MNA) nanoparticles, 182 ± 9 nm, encapsulating a secretoneurin peptide were used to enhance angiogenesis in mice hind limb.[138] One week post administration of CS-TGA-MNA, there was a significant increase in tube formation with highly dense arterioles and decreased tissue necrosis when compared to that of control groups.

NPs for gene and protein delivery have demonstrated to be efficient in protecting these therapeutic agents from undesired degradation, providing cell specificity, and promoting co-delivery of therapeutic payloads for enhanced cellular responses. NPs can be tailored for desired physical and chemical properties to achieve the highest therapeutic efficiency. For instance, genes or proteins can be loaded both inside and outside a NP and still maintain their bioactivity. Also, most of the biomaterials used in fabricating NPs are biocompatible, however, there is not a single polymer that demonstrates excellent properties. For instance, due to their hydrophilic heads, cationic polymers would provide high loading and transfection efficiency, but might pose some toxicity issues especially those with high molecular weight. This could be rectified by combining with negatively charged biomaterials. Furthermore, the NPs release profile *in vitro* may differ from that of *in vivo* animal models due to the biological and chemical composition variance, impacting their applications for clinical studies. Moreover, NP loaded proteins/genes can be limited with the dosage required to achieve outstanding results in co-morbid PAD patients.[139] Lastly, PAD therapy requires longer time to observe therapeutic efficacy which is rarely reported. Depletion of these proteins or nucleic acid within NPs could occur before the desired therapeutic duration.[140] This could be corrected by adjusting their

polymer ratio/composition to regulate release kinetics of therapeutic agents from NPs and stoichiometry.[141]

1.3.1.2. Nanoparticles as Carriers for Other Therapeutic Reagents

A broad range of materials, including PLGA can used to synthesize NPs for loading with other therapeutic molecules such as heparin and thrombolytic agents due to their excellent properties such as controlled payload delivery, easy surface modification for specific/targeting, high stability and approval by the FDA for human use.[142] PLGA-probucol nanoparticles administered to rabbit arteries demonstrated superior efficiency over their liposomal counterpart in terms of the intramural retention, and there was about a 29% and 154% radioactivity in femoral arteries and hindlimb muscles, respectively.[143] PLGA-heparin NPs (297 nm) were also reported with potential angiogenic properties in ischemic mice limbs.[144] Due to their controlled release properties, polymeric NPs promote longer bioavailability of therapeutic agents to cells and tissues. A significant rise in both the expression of hepatocyte growth factor (HGF) and HGF/tubulin ratio by the PLGA-heparin treated group was observed in treated mice compared to that of controls. In addition, PLGA-pioglitazone NPs were tested as neovascularization therapeutic reagents in ischemic murine models.[145] Post administration (1 μg/kg) to mice, significant blood flow restoration was observed when compared to controls (PBS injections), and the amount of tubes formed were comparable to that produced by VEGF. This PLGA-pioglitazone NP has anti-intimal hyperplasia properties via downregulation of cyclin D1 mRNA in VSMCs by 65%.[146]

Aside from genes, proteins and thrombolytic agents, payloads such as oxygen derivatives have also been delivered to ischemic sites. Recently, hydrogen peroxide (H_2O_2)-responsive (polyoxalate containing vanillyl alcohol) nanoparticles (PVAX NPs) (~200 nm) were intraperitoneally injected in mice femoral arteries.[147] A significant decrease in the production of H_2O_2 in ischemic tissues and a significant increase in cell viability, cell migration, blood

perfusion, and VEGF secretion were observed in mice arteries treated with PVAX NPs compared with those of control groups (untreated arteries). Further studies into endothelial cells' protection from injury were explored via the application of grapeseed extracts, polyphenols, loaded into nanoparticles.[148] Other recent studies explored the use of *p*-Hydroxybenzyl alcohol incorporated co-polyoxalate (HPOX) nanoparticles to restore blood flow and neo-vasculature in ischemic mice hindlimb.[149] *In vivo* studies showed that these HPOX NPs augmented blood flow perfusion seven days post-treatment, increased capillary density, increased endothelial cell recruitment and elevated VEGF, VEGFR-2, CD-31 and HO-1 mRNA levels when compared to that of controls (treated with saline). Moreover, generation-4 polyamidoamine dendrimers conjugated to S-nitrosothio (G4-SNAP) have also been reported as NO delivery vehicles to mitigate ischemic and reperfusion injury.[150] Nanoparticles are proven to be superior in delivering various ranges of therapeutic agents due to their controlled release mechanism and prolonged bioavailability of therapeutic agents to cells. NPs could also be used to load several therapeutic agents for synergic cellular responses. However, due to their multi-payload delivery, there could be potential interactions between reagents, thereby creating unknown chemical reactions that could have serious side effects. Non-degradable NPs can cause biodistribution issues by accumulating in organs such as the spleen. In addition, NP properties including size, could significantly impact their targeting capacity, how fast they are cleared from the system or bio distributed; however, maintaining a specific size NP could be challenging.

1.3.2. Nanoparticles and Vascular Prostheses

1.3.2.1. Nanoparticles and Drug-eluting Stents

The shortcomings associated with bare metal stents (BMS) and drug-eluting stents (DES), including stent thrombosis and restenosis, led to the development of novel systems

deployed to arteries to overcome such limitations. Some common DES currently approved by the FDA include stents eluting sirolimus, paclitaxel, zotarolimus and everolimus.[151] However, these metal pieces, often coated with polymers carrying therapeutic agents, often result in limited drug release/availability. Drug loaded NPs have been developed and used to coat stents to overcome these limitations as summarized in **Table 1.3**. These NPs protect the drug from rapid clearance, hence optimizing therapeutic efficacy. Paclitaxel (PTX) loaded magnetic nanoparticle (MNPs) coated stents improved retention of MNPs with about a 10-fold improvement in arterial tissue retention, inhibited SMC growth at the injury site, and subsequently inhibited restenosis when compared to that of naked PTX.[152] In addition, introducing NPs to BMS could provide local drug delivery since the NPs would be directly at the site of injury. For instance, coating of stents with PTX loaded PLGA NPs resulted in the inhibition of SMC migration into the arterial lumen by 80% and promoted EC migration and proliferation when compared to stents eluting PTX.[153] Furthermore, enhanced therapeutics is achieved when NPs are combine with BMS. Reports of deploying stents with liposomal alendronate (161 nm) in arteries of lipid-fed rabbits increased the lumen diameter significantly, decreased monocyte counts (~90%), and reduced macrophage infiltration and neointimal hyperplasia in these treated rabbits.[154] Moreover, unlike the controls (rabbits receiving 0.9% saline), reduction in neointimal thickness was also observed in stents coated with PTX-loaded albumin NPs deployed into rabbit arteries.[155] Pitavastatin-loaded NP-eluting stents improved the endothelial cell healing rate and decreased stenotic events in porcine arteries.[156] Furthermore, in atherosclerotic rabbits, neointimal hyperplasia was decreased post implantation of the stents with TRM-484 containing prednisolone nanoparticles when compared to that of non-stented arteries (controls).[157] The addition of NPs to BMS provides the inhibition of thrombosis and restenosis while promoting endothelialization. For instance, titanium vascular stents coated with polydopamine immobilized heparine/poly-I-Lysisne NPs,

supported endothelial regeneration, and prevented thrombus formation and neointimal hyperplasia in dog femoral arteries, when compared to arteries treated with a dopamine coated titanium stent (control).[158] In addition, stents coated with magnetic mesoporous silica nanoparticles (MMSNs) and carbon nanotubes (CNTs) have been explored.[159] With excellent mechanical flexibility and hemocompatibility, *in vivo* studies demonstrated a rapid endothelialization of vessels treated with these stents compared to that of DES.

The advantages of incorporating NPs with BMS include reduced chances of drug clearance by cells provided drug proximity to the injured artery and prolonged drug release to inhibit progression of thrombosis and restenosis. However, there are still some limitations that prevent the technique from being superior to previously mentioned techniques. First, this is an invasive procedure that causes so much pain to patients. Also, the stents are made of metal with higher chances of anastomis, which could further complicate the disease.[160] Furthermore, the lack of an endothelium makes blood directly in contact with the injured lumen and the material composition of these stents could promote protein adhesion/deposition and blood coagulation, further occluding the diseased artery. This technique application is limited on micro blood vessels; hence it is not available to all PAD patients. Last but not least, the NPs may not be evenly distributed throughout the stent which could cause partial therapy within the artery.

1.3.2.2. Nanoparticles and Vascular Grafts

In addition to being incorporated onto stents, NPs have also been added to vascular grafts for inhibiting intimal hyperplasia and restenosis (**Table 1.3**).

Table 1. 3 Nanotechnology used in Stents and Vascular Grafts for PAD Treatment

Types of stents	Drugs used	NP type	Results	Reference
304-grade stainless steel	Paclitaxel	MNP	-Improved localization rates. -Fourfold to tenfold higher arterial tissue retention.	[152]
304-grade stainless steel	Paclitaxel	MNP	-Inhibited 80% of SMCs; increased lumen diameter. -Diminished macrophage infiltration, proliferation, and arterial stenosis.	[153]
Nirflex medinol	Alendronate	Liposome	-Over 90% decrease in monocytes. -Decreased arterial stenosis; increased lumen diameter.	[154]
ACS multilink duet	Paclitaxel	Albumin	-Sustained suppression of neointimal thickness. -Promoted neointimal healing over time.	[155]
BMS	TRM-484	Liposome/PEG	-Improved tissue concentration by 100-fold. -Diminished stenosis in arterial wall.	[157]
Titanium	Heparin	Heparin/poly L-lysine	-Impeded thrombosis & restenosis. -Promoted endothelialization.	[158]
Types of vascular grafts	**Cells used**	**NP/payload used**	**Results**	**Reference**
Autologous vascular graft	Vascular smooth muscles	MAPK-activated protein kinase 2 inhibitory peptide (MK2i)	-Intima hyperplasia inhibition. -Inhibition of proinflammatory cytokines.	[161]
Pullan-dextran Porous grafts	Endothelial	Fe_2O_3	-Exhibited natural vascular architecture. -Continuous endothelium via increased ECs population within 7 d.	[162]

These biocompatible, biodegradable nano-vascular grafts promote integration with native blood vessels. For instance, nanopolyplexes of poly (propylacrylic acid) (PPAA) have been used to deliver the inhibitory peptide (MK2i) to vascular cells and tissues to prevent undergoing intimal hyperplasia (IH) via a vascular construct.[161] The MK2i NPs were significantly up-taken and retained by human VSMCs. They also efficiently reduced the expression of pro-inflammatory cytokines and their influx in vascular cells, leading to the prevention of intima hyperplasia. The same treatment showed inhibition of intimal hyperplasia in rabbit arteries 28 days post transplantation of MK2i NP vascular grafts, when compared to those of untreated or free MK2i-treated grafts. Nano-vascular grafts have also been made to mimic the native blood

vessel environment by incorporating various extracellular matrix (ECM) components, which will promote cell proliferation and ease integration within tissues. Last but not least, the size of NPs eases their integration within cells and ECM. For instance, vascular grafts incorporating NPs have also been used for restoration of vascular functions to inhibit thrombosis and restenosis[162] where iron oxide NPs (~8 nm) were used to incorporate with endothelial cells and help them attach to the luminal surface of porous vascular grafts made of pullan and dextran polymers. These grafts simulated the natural, vascular cell architecture and exhibited an increased EC population over a course of seven days translating into the formation of a continuous endothelium when compared to controls that were treated with endothelial cells without incorporation with NPs.

Nano-vascular grafts (or vascular grafts incorporated with nanostructures, including NPs) have shown great therapeutic capacity towards PAD. First, the nano-vascular grafts are biocompatible and as they degrade it gives room for new tissue regeneration. Also, these nano-vascular grafts can be easily fabricated at a laboratory and industry level through the feasible manufacture technique. Furthermore, the topography of nano-grafts promotes cell morphology, infiltration, adhesion and proliferation in the direction of blood flow. Also, as scaffolds, these nano-vascular grafts can be pre-seeded with cells which will provide both a mechanical and growth factor reservoir for neovessel formation. Limitations to this approach are that this approach just like with BMS is an invasive procedure. Also, the fabrication of nano-grafts could also be cumbersome for large scale production via phase separation and self-assembly technique. Furthermore, translation in clinical studies are limited. Even though NPs size or nano-vascular grafts show outstanding physiochemical properties, these same nanoscale materials could cause issues such as their interference with biomolecules and cells could be complicated. There could also be some inflammation[163] and immune response[164] by

generating ROS production caused by the application of these nanoparticles. These issues can be resolved by loading ROS inhibitors to the nano-vascular graft system.

1.3.3. Nanoparticles and Cell Based Therapies for PAD

Despite being highly publicized, cell therapy falls short on issues of cell viability, host tissue engraftment, and limited expression/secretion of growth factors. Hence, a blend of nanotechnology and cell-based therapy (**Figure 1.6**) has the potential to conquer such shortcomings by augmenting cell retention and providing a controlled, long-lasting release of growth factors towards PAD therapeutics (**Table 1.4**).

Table 1. 4 Cell Based Therapies and NPs to treat PAD

Types of cells used	NPs used	Results	Reference
MSCs	Liposomes+MNPs+gene	-Significant increase in VEGF mRNA levels, arterioles and tissue capillary density by MSC sheet and injected groups when compared to that of PBS control groups. -Significant increase in limb blood perfusion over time by MSC sheet and injected groups over PBS control groups.	[165]
iPS	MNPs +Flk-1$^{(+)+}$	-Accelerated revascularization. -Induced expression of angiogenic factors (VEGF, FGF) in the ischemic hindlimb when compared to control groups of ECM gel sheets. -Transplanted sheets of Flk-1$^{(+)+}$ promoted angiogenesis better than injected Flk-1$^{(+)+}$ groups.	[166]
Hepatocyte spheroid	Nanomicelles loaded with EPO cDNA	-Promoted tissue viability and DNA copies in ischemic limb. -Increased hematocrit and hemoglobin levels in mice treated with hepatocyte spheroids when compared to that hepatocyte cell suspension.	[168]
BMNCs	PLLA nano scaffold coated with nano HAp	-Induced neoangiogenesis & blood flow. -Fivefold increase in eGFP muscles cells one week post implantation. -Prevented necrosis.	[175]
ECs	eNOS-MNPs	-Circumferentially attached cells to denuded vascular wall. -95-fold increase of eNOS mRNA and protein expression. -Increased contractions similar to that of native vessels.	[176]
HAECs	ω-3-fatty acid-rich, 17-β-estradiol (17-βE) and CREKA-peptide	-Significant NO production. -Diminished plaque size. -Decreased plasma cholesterol level. -Downregulation of proatherosclerotic genes within walls.	[177]
C2C12 myoblast	PBAE-VEGF NPs	-Increased paracrine secretion. -Promoted neocapillary formation. -71% limb salvage.	[178]

For instance, multilayered sheets containing MSCs treated with liposomal MNPs were implanted into mice hindlimbs and resulted in higher angiogenic characteristics and arterial competence than their control groups (injected MSCs).[165] Induced pluripotent stem (iPS)

cells (1×10^6 cells) consisting of positive fetal liver kinase-1 (FlK-$1^{(+)}$) treated with MNPs resulted in accelerated revascularization and expression of angiogenic factors in the ischemic hindlimb.[166] In addition to engineered stem cell based therapy, other researchers have proposed the use of aggregate cells or cellular spheroids as an alternative treatment for PAD due to their tissue construction capabilities and their potential to closely mimic the extracellular matrix (ECM)-cell interactions. Engineered cells also serve as a reservoir for angiogenic growth factors to induce therapeutic angiogenesis as seen with Adipose derived stem cells (ADSC) in PAD therapy.[167] For example, Bhang et al.[168] developed an injectable ADSC spheroid system for transplantation into the ischemic hindlimb of mice. An improvement in cell survival, cell retention and upregulation of proangiogenic factors was observed compared to that of transplants of a monolayer ADSC (control). Recently, aggregates of ADSCs ($4x10^6$ cells) and heparin/protamine nanoparticles (ADSC/LH/P-NP) were transplanted into mice ischemic hindlimbs for therapeutic angiogenesis.[169] At 14 days post transplantation, there was no evidence of tissue necrosis, and blood perfusion was recovered in ADSC/LH/P-NP groups when compared to that of control groups (contralateral non-ischemic limb). Also, ADSC/LH/P-NP groups resulted in a medial limb survival of 28 days when compared to that of the sham. The inclusion of NPs to cells provides the necessary mechanical and structural support required for cell therapy. Cellular spheroid therapy demonstrates therapeutic potential via its efficacy and longevity of secreted bioactive factors such as endogenous factors, expressions of transgenes, functional proteins, peptides, and coagulation factors upon transplantation.[170] Spheroids generated by cell internalization of janus magnetics to obtain janus magnetic cellular spheroids (JMCSs) with about 20,000 cells per spheroid have also been applied towards PAD treatment.[171] By combining MNPs to cells, cell retention and functions can be enhanced. JMCSs have been used to form vascular constructs and have shown an unaffected cell viability over the course of 7 weeks. However, the limitation to this application is that spheroids with

diameters >100 μm can be deleterious since they can promote necrosis at the inner core, thereby leading to some form of late thrombosis and restenosis (due to the diffusion limitation of nutrients, cells at the core may be exposed to hypoxia leading to necrosis).[172] There is also the issue of transportation of nutrients and their diffusion due to the extensive length, vulnerability to hypoxia and cell death.[173]

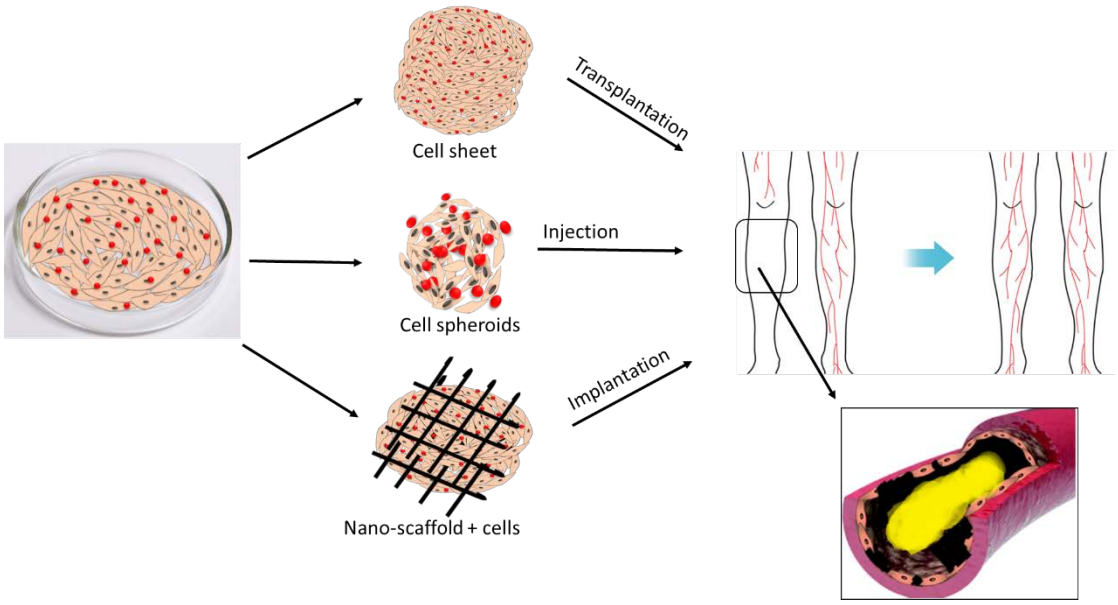

Figure 1. 6. Nanoparticles and cell-based therapies. Nanoparticles for cell therapy application can be designed in several methods such as cell sheets, cellular spheroids and cells seeded within nanoscaffolds. With nanoparticles, cells can be pre-programmed to promote healing and angiogenesis by recruiting endogenous cells and augmenting the bioavailability of growth factors and/or angiogenic factors**.**

In addition, therapeutic NPs can act as re-programmers to cells by enhancing higher cell expression of angiogenic factors and promoting cell viability while inhibiting apoptosis. Bone marrow mononuclear cells (BM-MNCs) and peripheral blood derived mononuclear cells (PBMNCs) have been used with NPs to induce neo-angiogenesis for PAD therapy.[174] BMNCs (5×10^6 cells) seeded in poly(l-lactic acid) (PLLA) nano-scaffolds coated with nano-hydroxyapatite (HAp) were implanted in ischemic injured limbs of mice for therapeutic angiogenesis.[175] Via a fluorescence (EGFP) tag of these cells, results showed higher cell retention at injured limb sites with about a 5-fold increase in 1 week post-implantation, a

significant prevention of necrotic limbs, the upregulation of angiogenesis, and an increase of blood flow in ischemic tissues, when compared to that of PLLA microspheres (controls).

The addition of NPs to cell therapy can improve cell-to-cell interaction and signaling in a more balanced and physiological manner which could improve engraftment. Recently, MNPs have been loaded in eNOS over-expressing endothelial cells (ECs) for the reconstruction of injured vessels.[176] MNP treated eNOS overexpressing ECs circumferentially attached to the injured vascular walls in mice and induced eNOS mRNA and protein levels, leading to increased contractions similar to that of native vessels with unimpaired endothelium. Nanoparticles can also act as ROS scavengers in cell therapy, thereby reducing PAD symptoms as seen when a multimodal delivery system (176 nm) for ω-3-fatty acid-rich, 17-β-estradiol (17-βE) and CREKA-peptide were used with human aortic endothelial cells (HAECs) for implantation in atherosclerotic ApoE$^{-/-}$ mice.[177] Significant NO production was observed in 17-βE–CREKA treated HAECs at low concentrations of 0.001uM. Plaque occlusion was observed to be ~20% in 17-βE–CREKA treated mice compared to over 35% in untreated and blank nanosystem treated vessels. Plaque size also diminished in vessels treated with 17-βE–CREKA. Moreover, a significant decrease in plasma cholesterol levels and downregulation of pro-atherosclerotic related genes (Selplg, Tnf, ICAM-1, VCAM-1, IL-6, Ifng) within the vessel wall were recorded in treated groups compared to that of untreated mice.

Last but not least, NPs serve as non-viral vectors for cell transfection. A genetically engineered, temperature sensitive, Tetronic-tyramine (Tet-TA) hydrogel system containing cell adhesive peptides (RGD) and cells transfected with VEGF cDNA loaded poly beta amino esters (PBAE-VEGF) nanoparticles, were studied to enhance angiogenesis in mice and their therapeutic efficacy to the ischemic hindlimb muscles.[178] Cells transfected (1.0×10^5 cells/cm^2) using PBAE-VEGF NPs (~200-300 nm) resulted in an increased paracrine secretion of VEGF and formation of neo-capillaries, 71% limb salvage, and no limb loss when compared to those

of control groups (untreated and empty vector transfected mice). As mentioned above, NPs show pivotal potential in cell therapy due to their reprogramming of cell mechanisms, improvement of cell to cell interactions, stimulation of the secretion of growth factors and cytokines, regulation of the disease environment by acting as ROS scavengers, promotion of mechanical support necessary for tissue regeneration, and for acting as a non-viral vector thereby reducing the probability of immune responses. Even though this approach seems more applicable than NPs as gene/protein carrier, or NPs and BMS, there are still issues associated with its effectiveness, safety, and feasibility. Challenges remain due to many limitations including several multiple steps involved in the harvesting and transferring of these cells, difficulty in maintaining cell viability post transplantation,[179] and an unclear understanding of the mechanisms involved in enhancing efficacy and support of angiogenesis in ischemic vascular beds.[127] Also, there is absolutely a high need for quality control of these cells.

1.4. Application of Nano-Theranostics for PAD Detection and Therapy

The English phrase “kill two birds with one stone” adequately reflects the purpose of nanoparticles for theranostic applications. The debut and prominence of nano-theranostics (**Figure 1.7**) in cancer applications have been greatly recorded; however, this technology is new in PAD. The term nano-theranostic is used to describe the input of nano-sized structures for the sole purpose of exerting both targeted therapy and diagnosis of diseases.[180] This approach focuses on manipulating contrast agent-loaded NPs for detection of disease, providing therapeutic payload, assessing therapeutic efficacy, and monitoring biodistribution of these nano-systems in the body over time (**Figure 1.8**).

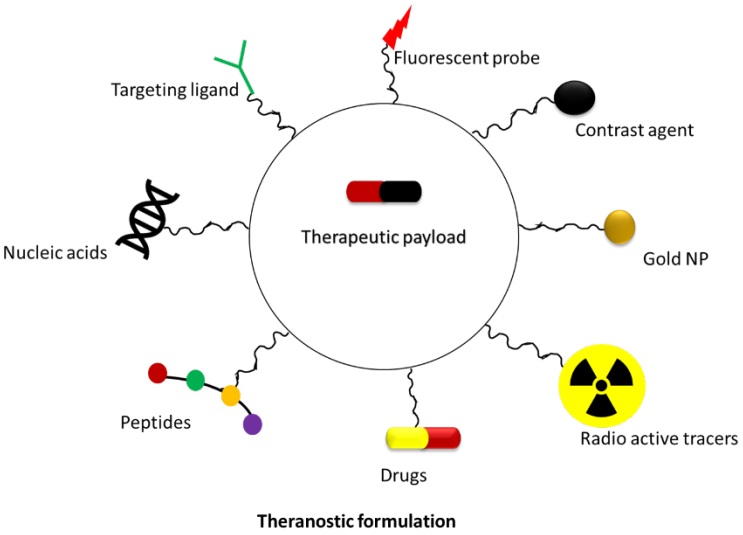

Figure 1. 7. A nano-theranostic particle for PAD detection and treatment. NPs for theranostic application demonstrate superiority over the conventional detection and treatment approaches. A single nano-theranostic can incorporate multiple imaging labels for different imaging modalities, different targeting ligands while overcoming biological barriers causing amplified signals, better specificity and binding, improved targeting effects respectively. Nano-theranostic promotes an efficient, controlled delivery of therapeutic payloads with real time monitoring.

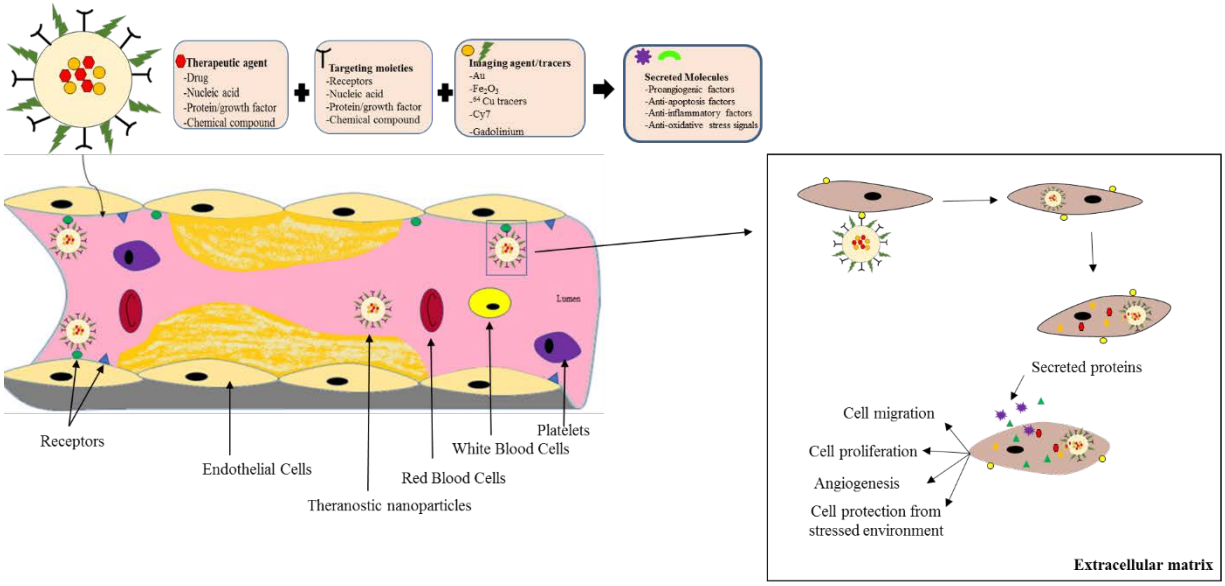

Figure 1. 8. Nano-theranostics for PAD detection and treatment. NPs for theranostic application can be designed to carry different payloads in different regions of the nanoparticle. The figure above shows a nanoparticle functionalized with a specific cell receptor and image tracers. Upon binding to cells, the cells uptake of theranostic NPs occurs. Within the cells, the NPs undergo biodegradation, releasing their payloads within the cell's cytoplasm. This payload can be identified in the cells via the detection tool described in Figure 3, and therapeutic efficacy can be analyzed via the quantification of angiogenesis, capillary density, cell survival, tube formation and cell migration.

The use of theranostics to deliver various types of therapeutic agents while also providing the capability of imaging is being heavily investigated in various diseases ranging from cancer to diabetes. It seems only natural to apply this technology to PAD in order to track drug efficacy in areas such as plaque. Lanza et al.[181] reported the use of paclitaxel (PTX) and doxorubicin loaded perfluorocarbon NPs (250 nm) to target tissue factors expressed by VSMCs post-angioplasty. MRI images were able to detect cell uptake of these NPs while the ^{19}F MRI was able to distinguish NPs within the material tissues. On the other hand, the anti-proliferative effects of the drugs (e.g. PTX and doxorubicin) were highly observed, especially in cells treated with PTX loaded NPs. Another study applied anti-angiogenesis therapy via paramagnetic nanoparticles (PMNPs) (175-220 nm) in an effort to restore functionality and stability in plagued vessels in hyper-lipidemic rabbits.[182] These NPs were tagged with fumagillin (detects $\alpha_v\beta_3$ integrin) and loaded with atorvastatin for PAD treatment. Data analyzed via CMRI reported that 75% of neovascular signals were reduced by the targeting of $\alpha_v\beta_3$ using fumagillin nanoparticles, and the therapeutic effects could be prolonged when combined with atorvastatin.

The use of fluorescent imaging nanoparticles has already been discussed as being used for the real-time detection of nanoparticle location as well as the ability to detect early signs of atherosclerotic plaque. Theranostic nanoparticles incorporating fluorescent contrast agents can allow for real time tracking of therapeutic agent delivery to ensure site specific delivery. Despite being in its premature stage, a study reported by Kim et al.[183] on the intravenous injection of VEGF loaded fluorescent silica nanoparticles (<200 nm) in the ischemic hindlimb of mice revealed that these NPs improved blood perfusion by 93 percent when compared to that of controls (unligated mice limb) and demonstrated both pro-angiogenic therapy and diagnosis of ischemic tissues in mice via fluorescence imaging. In order to effectively monitor the ailed site and drug release kinetics as well as distribution and efficacy of nanoparticles, novel theranostic systems have recently been reported. For example, poly(β amino esters)

nanoparticles (PBAE NPs) were used to enhance the expression of VEGF and CXCR4 in ischemic mice limbs.[184] VEGF improved vessel densities while CXCR4 upregulation improved ADSC engraftment and proliferation, blood perfusion, limb salvage, and muscle regeneration post transplantation, when compared to that of the control group (GFP transfection).

Microbubbles have been used as imaging agents via ultrasound (US) imaging; however, one of their limitations includes off-targeting and retention. Recently, magnetic microbubbles containing silicon oxide-coated MNPs (SO-Mag) have been used for the delivery of VEGF into mice via US-induced VEGF release,[185] and these microbubbles resulted in increased angiogenesis by 72 hours under flow when compared to the control microbubbles delivering GFP (60 vs 30 sprouts and 400 um^2 vs 150 um^2 vascularized area). Also, 8 days post treatment, ultrasound and magnetic imaging showed strong and local bioluminescence signals from mice treated with SO-MNPs microbubbles when compared to that of controls (GFP microbubbles without magnetic field or ultrasound exposure).

Further improvements in theranostic nanoparticle technology include the ability to incorporate multimodality agents into the nanoparticle. The use of a single nanoparticle design to incorporate multiple modalities allows for several anatomical and physiological processes to be imaged while minimizing patient compliance. Lobatto and his group[186] applied an anti-inflammatory drug-loaded paramagnetic liposome as a nanotheranostic for PAD. These glucocorticoid-loaded paramagnetic liposomes (PML) (~100 nm) were used for concurrent treatment, while imaging of plaque was achieved via MRI, NIRF, and PET/CT imaging modalities. Two days post IV administration, MRI revealed an increased signal intensity throughout the entire inflamed vessel wall due to the accumulation of glucocorticoid PMLs at the injured site. NIRF was able to explore the uptake and localization of these liposomes within the vessels, and the ^{18}F-FDG PET/CT images, which provided quantitative information on

inflammation present, revealed a decrease in ^{18}F-FDG uptake over a course of 7 days, indicating the efficacy of the treatment when compared to that of controls (free glucocorticoids).

Theranostic nanoparticles exhibit other advantages for PAD detection and therapy. One such advantage comes from the inherent properties of certain materials such as gold. Several metal-based materials, like gold and iron-oxides, have properties that allow for imaging via CT or MRI and therapeutic use as photodynamic therapy agents. Applications such as these will simplify the production process, minimize possible errors and increase ease of use.[187] Nanoparticles allow for a high accumulation at targeted sites due to the ability to conjugate targeting biomolecules onto the surface. This ability combined with the therapeutic agents and imaging agents allows for sustained drug release and prolonged imaging for monitoring the treatment and better guided therapeutic regimens. Utilizing responsive release theranostic nanoparticles allows for image based guided release of drugs at time points that a physician deems beneficial for treatment while significantly reducing side effects. The culmination of multiple imaging modalities into a single nanoparticle, as discussed previously, provide the opportunity to assess disease treatment from various imaging modalities, taking advantage of each specialization.[188] Despite its early thrust into the field of PAD, theranostic NPs elaborate their abilities of monitoring bio-distribution and NP dynamics in the body over time; hence, facilitating and speeding up preclinical development.

While interest continues to grow in theranostic nanoparticle capability, there are still concerns that need to be addressed before clinical standards can be met. Some shortcomings such as their complexity, lack of standardized testing procedures and regulations, potential toxicity of imaging probes, and variation in the manifestation of PAD between rodents and humans make their applications in clinical trials and/or human use a little longer. Toxicity of platforms such as quantum dots, as well as long-term toxicity potential of metal-based materials

and several contrast agents needs to be further explored *in vivo*. The cost of gold nanoparticles limits the usefulness of this promising material. Off-targeting and limited circulation times continue to need addressing in order to ensure that therapeutic agents are delivered to their specific target and that the nanoparticles remain around long enough to provide quality images over a specific period of time. Finally, further experiments are needed to confirm that the benefits of theranostics outweigh the increased difficulty in processing and creation of standard manufacturing procedures as well as any possible acute and chronic toxicity effects.[189]

1.5. Perspectives on NPs for PAD Detection and Therapy

Nanoparticles have shown to have superior advantages over traditional modes of detection and therapy. Their high versatility permits chemical and physical modifications that regulate activities such as controlled release of payloads for longer bioavailability and protection of genetic and protein materials within the nanoparticle. Reduction in PAD symptoms can achieved by using nanoparticles as scavengers for damage-causing ROS as well as reprogramming cells to express higher amounts of factors promoting cell viability. The ability to apply targeting moieties to nanoparticles increases their specificity to areas of disease as well as limits distribution and removal from circulation. Nanoparticles have the ability to carry larger amounts of contrast agents and/or therapeutic payloads compared to a single small molecule, while controlling the release rate, which means they are a reliable control over potential toxicity. With the application of targeting molecules conjugated onto nanoparticles, more of the contrast agent can be delivered to the area of interest better. The ability to load several contrast agents and surface modifications allows nanoparticles to be imaged by multiple modalities, increasing their usefulness and alleviating photobleaching. Utilization of nanoparticles with intrinsic properties, such as gold, allows for both imaging and photodynamic

therapies increased ease of use and production process. Combining targeting biomolecules allows for simultaneous treatment and imaging at specific diseased sites. Monitoring of the therapeutic effect while it is occurring allows for a better understanding of the overall therapeutic process. Stimuli responsive nanoparticles allow for tracking via imaging processes and controlled release of the therapeutic agent at the desired location.

Several innovative strategies from cancer therapy could be applied in PAD for example multistage vector (MSV) for gene therapy and smart nanoparticles. MSVs are typically composed of three stages: stage one is the porous microparticle housing nanoparticles, the second stage is the nanoparticle housing the therapeutic or imaging agent, and the third stage is the agent. MSVs become more advantageous when delivering siRNA for gene knockdown or knockout applications by utilizing multiple protective barriers to enzymatic degradation. Utilization of a three stage MSV loaded with EphA2 siRNA has shown to silence EphA2 genes in ovarian cancer models for 3 weeks with a single dose compared to free liposomal EphA2 siRNA injected every 3 days.[190] As gene therapy research grows for PAD, the use of MSVs could provide enhanced treatment by maintaining a much longer expression of pro-angiogenic factors compared to the delivery of proteins directly. Smart nanoparticles are defined as nanoparticles that change conformation due to the presence of a specific stimuli. This change in conformation can allow for the release of the nanoparticles payload on demand. In PAD, this stimulus could be the presence of ROS, inflammation, cytokines, or pH change. Smart nanoparticles are currently being applied in cancer therapy where they demonstrate tremendous potential. There have been very few references to smart nanoparticles in regard to PAD.[191]

Imaging precursor molecular events of plaque growth could allow for investigations into plaque instability and the various processes that contribute towards instability. Introducing molecular imaging techniques to structural imaging techniques can result in early prediction of thrombosis-prone plaque.[192] Methods to non-invasively monitor the efficacy of cell therapy

in PAD remains a deficiency. The ability to track injected cells would allow for better determination of accumulation and therapeutic responses. Molecular imaging techniques could allow for a more in-depth analysis of novel therapeutic strategies prior to clinical studies, as well as provide a guide for patient therapies during clinical studies.[193]

A major concern of NPs is their safety, especially for those of metal-based NPs. Cationic polymer NPs also pose toxic risks, especially at high molecular weights. Limited *in vivo* studies regarding release profiles prevents researchers from confidently saying *in vitro* release profiles match those of *in vivo* release profiles. Nanoparticles that carry multiple payloads need further *in vivo* investigation as to possible unknown chemical reactions between the payloads that can cause adverse side effects. Toxicity of contrast agents, including quantum dots and gadolinium, presents concerns that need to be further addressed and limited to acceptable levels. Eventhough Iron oxide-based nanoparticles require a synthesis process that overcomes poor crystallinity and size variation, there still exist some limitations. For example, errors in quantification at diseased sites has been shown to be caused by the dismantling of radiolabeled isotopes from their nanoparticle because of chelating materials used for the nanoparticle. Limitations to this growing area include concerns associated with toxicity of imaging agents and metal-based nanoparticles, cost of gold nanoparticles, potential off-targeting, and limited circulation time. A better understanding of long-term toxicity is needed via long-term *in vivo* studies. Furthermore, gold can be expensive, so the benefits need further validation that its benefits outweigh the cost of production, and more cost-effective synthesis methods need to be explored. Additionally, to ensure proper duration of therapy and imaging, nanoparticles need to be assuredly delivered to their designated target. Nanoparticles that require separate exogenous agents for therapy and imaging have a potential increased synthesis difficulty, and creation of a standard procedure for manufacturing is difficult to compose. Nevertheless, NPs have more advantages for PAD detection and therapy over their disadvantages, and might have

significant potential uses in clinical trials and human in the future the ability to view the drug build up in targeted regions and how each patient responds to treatment opens the doorway to personalized treatment strategies; hence meeting the changing needs of individual patients worldwide.

With the above stated advantages and disadvantages of how nanoparticles can be applied in PAD, we aim to study how we can affect non-invasive long-term therapy for vascular reconstruction. With such drive, we plan to test nanoparticles as protein carriers and non-viral vectors in gene therapy. Our **objective** is to study various groups of proteins and/or gene and monitor how they affect therapeutic angiogenesis in oxidative stressed environment. The study groups will constitute of singles or combination of proteins or plasmid DNA. Also, we shall test for complimentary strands of the same gene and evaluate their ability to induce angiogenesis in small animal models. The innovative aspect of this work lies in its 1) specificity of delivering a ligand and its receptor, and 2) the novelty of administering sense and antisense gene therapy in the ischemic tissue. The chosen ligands and plasmids cDNA were selected for their cytoprotective, cell proliferative, migratory and angiogenic properties. The therapeutic outcome from this work will go a long way in mitigating the existing wide gap there is from bedside to bench and the clinical demands in an effective PAD treatment.

CHAPTER 2

NANOPARTICLES AS CARRIERS OF ERYTHROPOIETIN AND ITS RECEPTOR FOR THERAPEUTIC ANGIOGENESIS

2.1. Introduction

Peripheral arterial disease (PAD) is a subtype of atherosclerotic disease with focus on arteries mainly in the lower limb.[194] Characterized by an obstructed and weakened lumen, endothelium layer dysfunction, insufficient blood flow and oxygen to nearby tissues; PAD could cause tissue necrosis, leading to amputation in advanced patients. Affecting ~12 million Americans, mostly elderly males ≥ 65 years old, PAD is prevalent with smoking, diabetes, high blood pressure and high cholesterol levels.[195, 196] Current therapeutic approaches include surgical bypass grafts, cell therapy, angioplasty and stents. However, their limitations including the invasive nature of surgeries, cell viability, stent apposition and thrombosis, make them less attractive.

Therapeutic angiogenesis, formation of new blood vessels from preexisting ones, is rapidly gaining momentum as an alternative method for tissue re-vascularizing.[197] Therapeutic angiogenesis can be achieved by administering pro-angiogenic growth factors capable of mobilizing circulating endogenous cells such as bone marrow stem cells and endothelial progenitor cells (EPCs) to injured tissue sites through pacracrine, chemokine signaling or differentiation of these cells into vascular cells, which promote angiogenesis by stimulating neovascularization.[198, 199] For example, the common vasculogenic reagent, vascular endothelial growth factor (VEGF), is well established for its potent cell proliferative and revascularization properties in vitro and *in vivo*.[200, 201] Additionally, when the chemokine CXCL12 also known as stromal cell derived factor 1α (SDF-1α) was tested for its angiogenic downstream mechanism, its results showed to enhance angiogenesis by directly

polarizing, migrating and organizing HUVECs into tubal structures.[202] Protein therapy is a common angiogenic technique due to its readily/bioavailability to cells and tissues; a requirement for angiogenesis. These proteins are often delivered as bolus injection which could be enzymatically degraded, affecting their already short circulation half-life; thereby limiting their performance/outcome[203] and requiring redosing that can cause negative feedback mechanisms. Another angiogenic approach is gene therapy (GT), delivering nucleic acids to a cell to invoke a desired response. However, the inadequate cell uptake of the naked DNA, DNA lysosomal entrapment and enzymatic denaturation, and low expression levels makes it less attractive.[204]

To overcome the limitations of current protein therapy and gene therapy, we aim to develop EpoR and/or Epo NPs that gradually release EpoR and Epo for continuous bioavailability to cells to stimulate angiogenesis and to assess their efficacy in inducing angiogenesis in endothelial cells (ECs). Erythropoietin (Epo) and its receptor (EpoR) have individually shown their potential proangiogenic capacity. Epo, a 34 kDa cytokine produced in adult kidney is expressed by hypoxic ECs,[205] and considered an outstanding proangiogenic factor for its association with vessel formation in the heart[206] and brain[207] and for its suppression of pro-apoptic gene activation in carcinomas.[208] On the other hand, 66-78 kDa transmembrane EpoR protein is upregulated in hypoxic ECs,[209, 210] has cytoprotective properties associated with apoptosis and inflammation,[211] and mediates angiogenic effects of Epo.[212] The novelty of this work includes the use of recombinant Epo protein and/or EpoR cDNA to protect ECs and facilitate angiogenesis under hypoxia and the controlled releases of EpoR cDNA and/or Epo protein from PLGA NPs for enhancing angiogenesis *in vitro* and *in vivo*. In this research, Epo NPs, EpoR NPs, and EpoR/Epo NPs were formulated, and their properties, including their effects on EC proliferation, EC migration, EC protection under

stress conditions, and tube formation potential of ECs under hypoxia, were determined using various bioassays.

2.2. Materials and methods

2.2.1. Cell culture Human umbilical vein endothelial cells (HUVECs) were purchased from ATCC, cultured in Vasculife® VEGF (LS-1020) (Lifeline cell technology), supplemented with 1% penicillin and streptomycin (Life technologies) and incubated at 21% O_2, 5% CO_2, 37ºC, 95% air humidity. For all *in vitro* studies and assays using HUVECs, cells were incubated with conditioned media (CM) containing 2% fetal bovine serum (FBS) (GElifescience).

2.2.2. Construction/purification of the human EpoR plasmid Plasmid DNA encoding the EpoR gene was cloned into the pMXs-IRES-GFP vector (Cell Biolabs Inc.).[213] These vectors were expanded using chemically competent DH5α Escherischia Coli (E.Coli) cells (Invitrogen) in SOC medium (Invitrogen) supplemented with ampicillin (Sigma). The EndoFree plasmid mega kit (Qiagen) was used to purify the plasmid DNA grown from bacteria cells.

2.2.3. Synthesis of Epo NPs poly(lactic-co-glycolic) (PLGA) NPs were prepared by the standard double emulsion (W/O/W) solvent evaporation technique.[214-217] In brief, Epo (Peprotech) was cryopreserved using protective reagents, including Bovine serum albumin (BSA), as previously described.[216] Cryopreserved Epo (0.02 mg) was dissolved in DI water (0.2mL) to form water phase 1 (W_1). W_1 was added dropwise to 40 mg PLGA 50:50 (Lakeshore Biomaterials) dissolved in 1mL dichloromethane (DCM) (EMD Millipore Corporation) to form the organic (oil) phase and sonicated at 30 watts for 1 min. This emulsion was later added dropwise to 12 mL of poly vinyl alcohol (PVA) 5% (w/v) (Sigma) solution (W_2) and sonicated at 40 W for 10 mins on ice. Particle suspension was stirred overnight at room temperature to

ensure a complete DCM evaporation. Epo NPs were recovered by centrifugation at 15,000 rpm for 30 mins at 25ºC. Supernatant was collected for determining loading efficiency. All NPs were lyophilized and stored in powder form at -20ºC when not in use and were freshly reconstituted in appropriate solvent for our experiments.

2.2.4. PEI coating and EpoR plasmid DNA loading Surface modification was made on the above PLGA NPs to produce EpoR NPs.[218] In brief, 0.05% (w/v) branched polyethyleneimine (PEI) (bPEI 1200) (Polysciences) was added to PLGA NPs according to the PLGA-PEI ratio of 25:1 (w/w). This mixture was left to rotate at room temperature for 30mins allowed for electrostatic bonding. PEI-PLGA NPs were recovered by centrifugation at 15,000 rpm for 30 mins at 25ºC. Lyophilized NPs were suspended in 25μg/mL plasmid cDNA solution and incubated for one hour at a PEI-DNA ratio 0.03:1. Nanoparticle groups fabricated were empty vector-PEI-PLGA-Epo NPs, EpoR-PEI-PLGA-BSA NPs, EpoR-PEI-PLGA-Epo NPs, and empty vector-PEI-PLGA-NPs which we shall refer to as Epo NPs, EpoR NPs, EpoR/Epo NPs, and blank NPs respectively throughout this study. pMXs-IRES-GFP also served as the control cDNA model (empty vector) for coating onto NPs.

2.2.5. Characterization NPs Size and surface charge measurements were performed using the Zeta Potential Analyzer (Brookhaven instruments co.) that applied dynamic light scattering (DLS) from NP Brownian motion. Morphology was confirmed via transmission electron microscopy (TEM), and NP stability in 0.9% solutions of saline and simulated body fluid (SBF)[219] was tested for 48 hours as previously described.[220, 221] Additionally, for *in vitro* release profiles of Epo and EpoR, 1 ml of NP suspension (1 mg/ml) for each NP type was added to dialysis bags with molecular weight cut-off of 300 kDa (Spectrum Laboratories Inc.) and dialyzed against 1X PBS at 37°C for 28 days. At each time points, 1 ml of dialysate was

collected from the samples and replaced with 1 ml of fresh 1X PBS. Pierce BCA protein assays (Fisher Scientific) and absorbance (260/280) via spectrophotometry (Tecan) quantified the released protein and cDNA, respectively. Lastly, NP loading efficiency (LE) was quantified by the amount of un-entrapped reagent from collected supernatant. The LE can be calculated as the percentage of protein/cDNA used initially during NP formulation (Equation 2.1).

$$Loading\ efficiency = \frac{protein/cDNA\ used - protein/cDNA\ in\ supernatant}{protein/cDNA\ used}\ x\ 100 \qquad (2.1)$$

2.2.6. *In vitro* studies of NPs

2.2.6.1. *Transfection efficacy of NPs for EpoR expression and Epo secretion over time.* HUVECs were seeded in tissue cultured plates one day before NP treatment. Cells were then treated with NP in Opti-mem (Thermofisher) for 4 hours. After which they were washed and re-incubated with CM and incubated for a duration of 5 days. Supernatant was collected every day and replenished with fresh CM. Collected supernatant was used to perform ELISA assays (Thermofisher) for EpoR and Epo via the manufacturer's instructions. HUVECs in 24-well plates were transfected with NPs (62.5µg/mL) in Opti-mem media for 4 hours at 37°C. Cells were washed and replenished with CM for 48 hours. Cells exposed to lipofectamine 2000 + EpoR cDNA plasmids served as a positive control. Lipofectamine 2000 (thermofisher) is a well-known and recognized transfection agent. Analysis of transfection was performed by the percentage of GFP expressing cDNA EC population (Equation 2.2).

$$\%\ Transfection = \left(\frac{Cells\ with\ GFP}{Cells\ without\ GFP + Cells\ with\ GFP}\right) \times 100 \qquad (2.2)$$

2.2.6.2. *Cellular uptake.* HUVECs were seeded in tissue culture plates 1 day before treatment. Cells were treated with NPs re-suspended at various concentrations (0-2 mg/ml) in Opti-mem

media for 4 hours. Quantification of NPs up-taken by cells were analyzed through the amount of fluorescence to the total protein correlated to the cell number from cell lysate via spectrophotometry.[222, 223]

2.2.7. Therapeutic efficacy of NPs

2.2.7.1. *On EC proliferation.* HUVECs were pre-transfecting with NPs (62.5µg/mL) for 24 hours, then the cells were incubated with CM for 3 days in a hypoxic condition (< 1% O_2, 5% CO_2 in nitrogen at 37ºC). A parallel cell culture plate was incubated in a normal oxygen environment (21% O_2, 5% CO_2, 37ºC, 95% air humidity). At each time point (1 and 3 days), MTS assays were performed to analyze the number of viable cells following the company (Promega)'s instructions. DNA quantification using Picogreen assays (Invitrogen) served as another supportive assessment. Cells treated with 25ng/mL of VEGF and CM served as positive and negative controls, respectively.

2.2.7.2. *On EC protection from ROS species.* Pre-transfected HUVECs seeded in 48 wells (as previously stated) were washed and replenished with 200µM H_2O_2 in CM for 1, 4 and 7 days at 37ºC. Cells + H_2O_2 (NT) served as negative control while quiescent cells without exposure to H_2O_2 served as positive control. After each time point, cell viability was confirmed via MTS assays.

2.2.7.3. *On the protein expression profile.* whole cell lysates of pre-transfected HUVECs exposed to hypoxia were collected to determine the protein profiles. Protein quantification via Bradford protein assays (Biorad) was performed before running lysed extracts on an SDS-PAGE gel electrophoresis. The protein bands were later transferred onto a nitrocellulose membrane (Biorad) and electrophoresed at 90V for 1 hour. After overnight membrane blockage using 5%

milk solution, the nitrocellulose membrane was treated with primary and secondary antibodies against EpoR, Epo, phosphorylated STAT-3 (pSTAT-3), HIF-1α,[224] and GAPDH (control) proteins.

2.2.7.4. *On EC migration.* In 96 well plates, pre-transfected HUVECs were scratched, using a pipette tip to create a wound as previously described,[225] washed with PBS and incubated in basal media for 24 hours at 37ºC in normal conditions. A phase contrast microscope was used to obtain the initial and final wound distances. Measurements of the recovered distance was analyzed using Image J analysis software.

2.2.7.5. *On the ability of treated cells to induce angiogenesis.* HUVECs' ability to form tubular structures via matrigels was performed as previously described.[226-228] In this study, quiescent HUVECs pre-treated with NPs (62.5 µg/mL) for 4 hours were harvested and seeded on low basement membrane matrigels with basal media in a 48-well plate. Cells were further incubated in hypoxia (< 1% O_2, 5% CO_2 in nitrogen at 37ºC) for 8 hours. Non-transfected cells (NT) and cells exposed to 25 ng/mL VEGF served as negative and positive controls, respectively. After 8 hours, phase contrast microscopy was performed to obtain and determine the level of tubes formed. Quantification of the sprouting length and density was analyzed using Image J analysis software.

2.2.8. In vitro characterization of NPs

2.2.8.1. *Hemo-compatibility of NPs* was tested using acid citrate dextrose anticoagulant (ACD) human blood exposed to various NP concentrations (0-1 mg/ml). Whole blood clotting time was evaluated by activation of 50 µL blood with $CaCl_2$, (sigma) and recorded (0-60 minutes) by absorbance (540 nm) via spectrophotometry.[229] In addition, a hemolysis assessment of red blood cells (RBCs) exposure to NPs at 37°C for 2 hours was performed by using saline (0.9%)

(sigma) diluted blood on NPs and absorbance read at 545 nm. Each sample group was studied at n=20 due to human blood variation issues. Percentage hemolysis was calculated using the equation below (Equation 2.3).

$$\%\ hemolysis = \frac{[(absorbance\ of\ tested\ NPs) - (absorbance\ of\ negative\ control)]}{absorbance\ of\ positive\ control} \quad (2.3)$$

2.2.8.2. *Cyto-compatibility of NPs,* HUVECs were seeded in culture plates and treated with various concentrations (0-1 mg/ml) of NPs for 24 hours in CM. Cell viability and death were assessed via MTS cell viability and LDH (Lactate dehydrogenase, a cytosolic enzyme indicated cell toxicity and cytolysis in media) assays, respectively.

2.2.9. Statistical analysis: All data were expressed as means±S.E.M. and were analyzed by two-way ANOVA with Fisher's adjustment, and $P < 0.05$ was considered to be statistically significant.

2.3. Results

2.3.1. Characterization of NPs. Dynamic light scattering (DLS) (**Table 2.1**) and transmission electron microscopy (**Figure 2.1A**) confirmed that most of NPs had the average diameter ~200nm.

Table 2. 1. Dynamic light scattering (DLS) analysis of NPs

PLGA-NPs	Diameter size (nm)	Zeta potential (mV)	Poly dispresity (PDI)
Blank NPs	217 ± 56	47 ± 1.12	0.144
Epo NPs	207 ± 12	45 ± 0.78	0.076
EpoR NPs	227 ± 56	48 ± 0.60	0.185
EpoR/Epo NPs	234 ± 63	46 ± 0.84	0.157

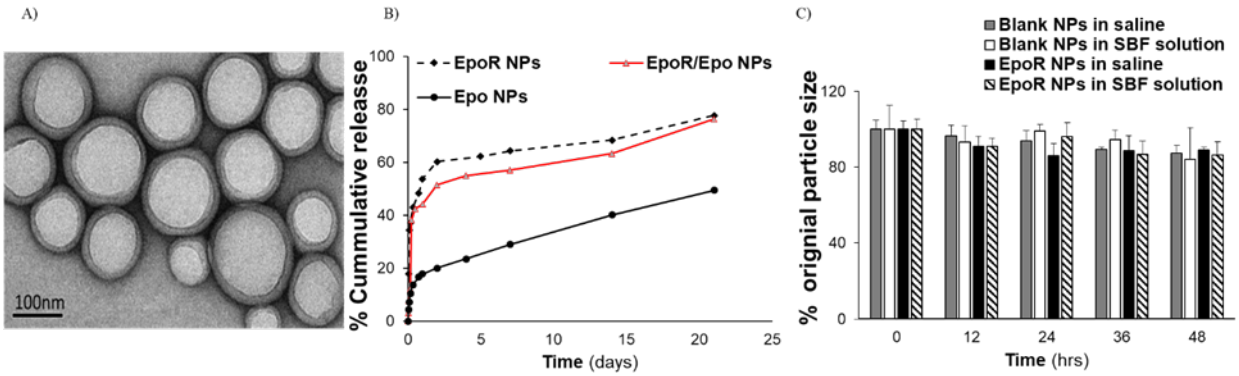

Figure 2. 1. Characterization of NPs. A) TEM of EpoR/Epo NP. **B**) Release profile of Epo and EpoR NP. Both Epo and its receptor NP showed a biphasic release over time when immersed in PBS (pH 7.4) over a course of 21 days. **C**) Nanoparticle stability in solutions of saline, SBF and media with serum (data not shown) for 48 hours.

PEI coating was confirmed via ninhydrin assays and FTIR spectroscopy (data not shown). Epo and EpoR release from NPs confirmed a biphasic profile with an initial burst then a controlled, sustained release over 21 days (**Figure 2.1B**). Lastly, in solutions of saline and SBF, NPs maintained their original size up to 48 hours of exposure (**Figure 2.1C**) demonstrating their stability in these solvents. NPs also did not increase in particle sizes when they were incubated with complete media containing serum (data not shown), indicating their stability in this solution.

2.3.1. ***In vitro*** **characterization of NPs**. At 1 and 5 days, ELISA results confirmed increasing EpoR expression and Epo secretion by HUVECs (**Figure 2.2 A-B**). This confirms that EpoR and Epo are made available to cells for therapeutic angiogenesis via EpoR/Epo pathway. In 4

hours, HUVECs were able to engulfed an average of 5µg NPs/µg protein for all NP groups (**Figure 2.2C**).

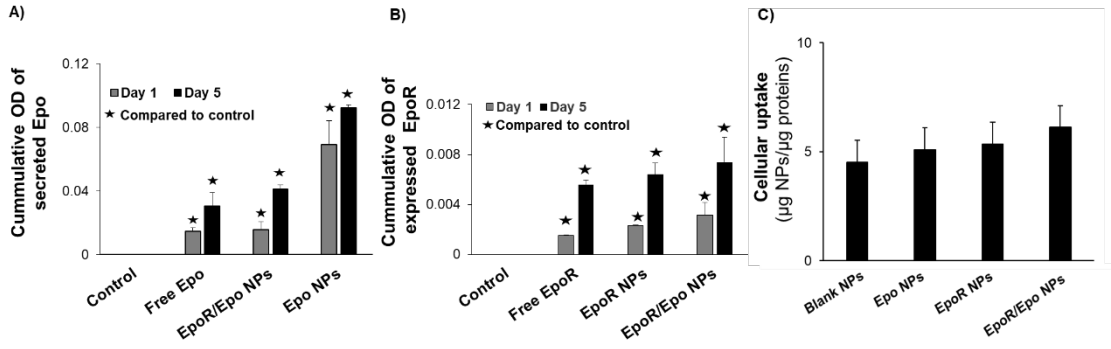

Figure 2. 2. Epo secretion and EpoR expression by ECs. Low serum supernatant was collected from HUVECs exposed to NPs for ELISA analysis of or **A**) Epo protein secretion. **B**) EpoR protein expression (n=3). ($P < 0.05$ w.r.t control; mean ± SEM) **C**) NPs uptaken by HUVECs.

2.3.2. Therapeutic efficacy of NPs on EC proliferation and protection. A significant number in cell proliferation (**Figure 2.3A**) was observed in groups of Epo NPs, EpoR NPs and EpoR/Epo NPs when compared to that of free Epo/EpoR solution and control groups at day 1 and 3. Although, VEGF out performed most of NPs at day 1, cell proliferation in most NP sample groups were comparable to that of VEGF after 3 days of exposure. Following a 200µM H_2O_2 treatment, HUVECs pretreated with Epo NPs, EpoR NPs and EpoR/Epo NPs induced cell viability compared to those exposed to blank NPs and NT groups at all time points. When comparing with VEGF at day 1, Epo NPs, EpoR NPs and EpoR/Epo NPs showed similar protectiveness, however, by days 4 and 7 they outperformed VEGF by 2.7-folds and 2.5-folds, 1.67-folds and 2.8-folds, and 2.6 and 4.4-folds, respectively (**Figure 2.3B**).

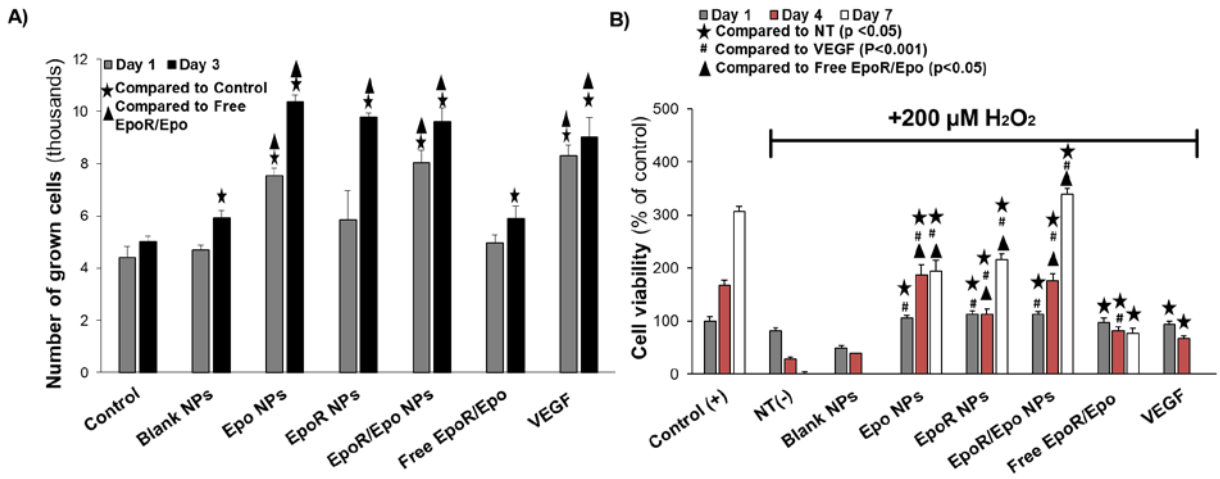

Figure 2. 3. **Therapeutic efficacy of NPs on HUVECs proliferation and protection. A**) Transfected HUVECs (10^4 cell) proliferation in low serum (LS) media in at 37ºC for 3 days and analyzed via cell proliferation MTS assays (n=4). **B**) Transfected HUVECs ($3x10^4$ cells) in LS media+H_2O_2 incubated in 21% O_2, 5% CO_2 at 37ºC for 7 days (n=4). Positive control (cells + media with serum), NT (Cells in LS media + H_2O_2. (ANOVA, P< 0.05 w.r.t. NT, Free EpoR/Epo and VEGF).

2.3.3. Therapeutic efficacy of NPs on EC migration and tube formation. Epo NPs, EpoR NPs and EpoR/Epo NPs showed to significantly reduce the initial wound gap. EpoR/Epo NPs showed highest EC migration, and its performance was like that of VEGF (**Figure 2.4A**). Within 12 hours, the total tube length of samples was in the following order: EpoR/Epo NPs > EpoR NPs >VEGF > Epo NPs and they were all significantly higher than that of blank NPs, free EpoR/Epo, or NT groups (**Figure 2.4B**).

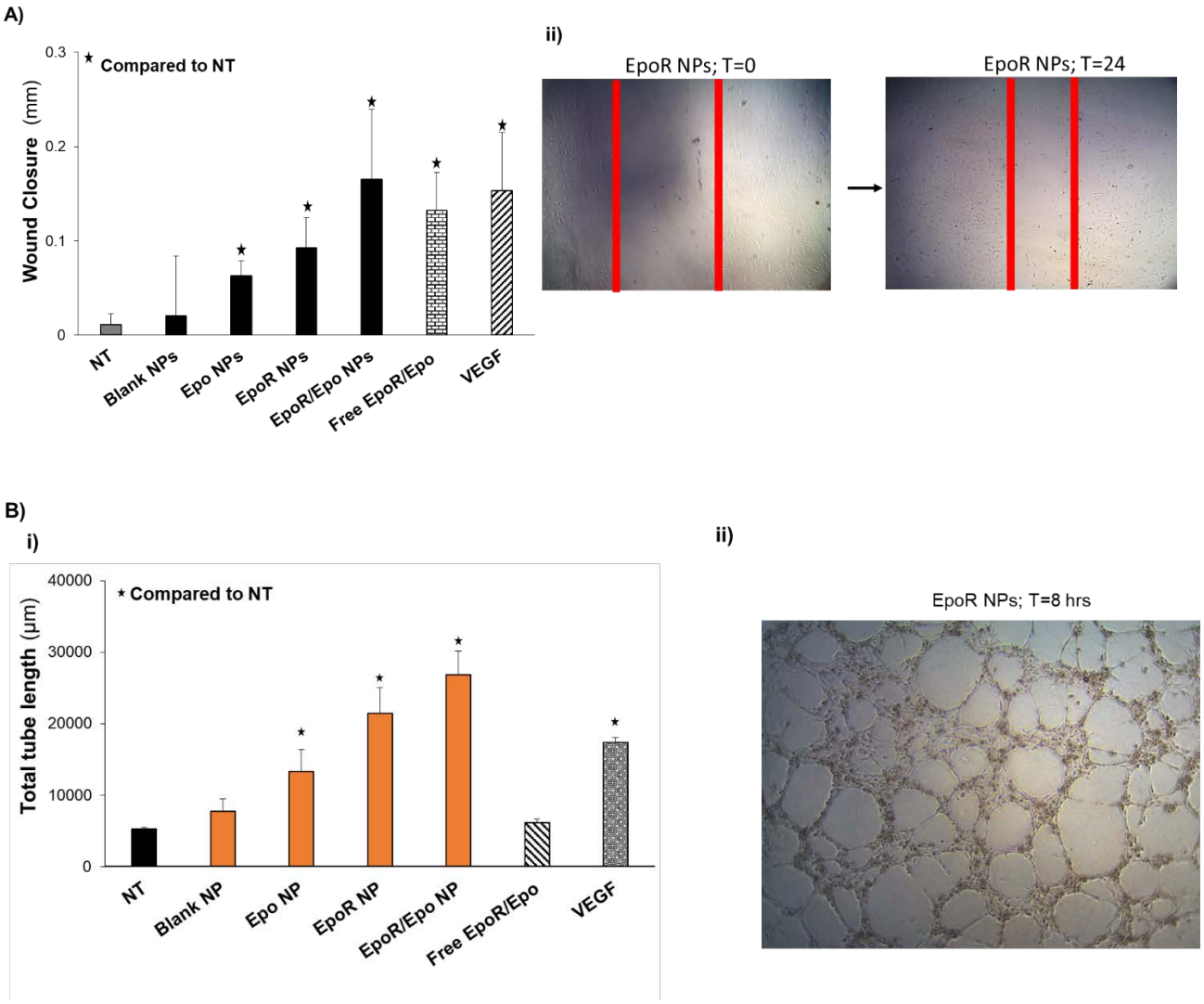

Figure 2. 4. **Therapeutic efficacy of NPs on ECs migration and tube formation**. **A**) cell migration of transfected HUVECs ($1x10^4$ cell) in basal media incubated in < 1% O_2, 5% CO_2 in nitrogen at 37ºC for 24 hours and analyzed via by phase contrast microscopy and Image J software (n=4). (i) wound closure distance for all sam[les groups. (ii) representative images of cells samples exposed to EpoR NPs from T=0 hr to T=24hrs. **B)** (i)Tube formation by transfected HUVECs ($3x10^4$ cells) in basal media incubated in <1% O_2, 5% CO_2 at 37ºC for 8 hours (n=4). Positive control (cells + VEGF) negative control (NT) (non-transfected cells in basal media) (ANOVA, P< 0.05 w.r.t. NT).(ii) representative image of transfected HUVECs seeded unto a Matrigel at T=8 hrs.

2.3.4. Hemo-and cyto-compatibility of NPs. As per the American society for testing and materials (ASTM F756-00, 2000), based on the degree of hemolysis, biomaterials can be classified as non-hemolytic (0-2% hemolysis), slightly hemolytic (2-5% hemolysis), and hemolytic (≥5% hemolysis).[230] Hemolysis results showed < 2% RBCs lysis (**Figure 2.5A**).

Also, cytocompatibility of NPs was established >80% viability at concentration ≤1mg/mL (**Figure 2.5B**).

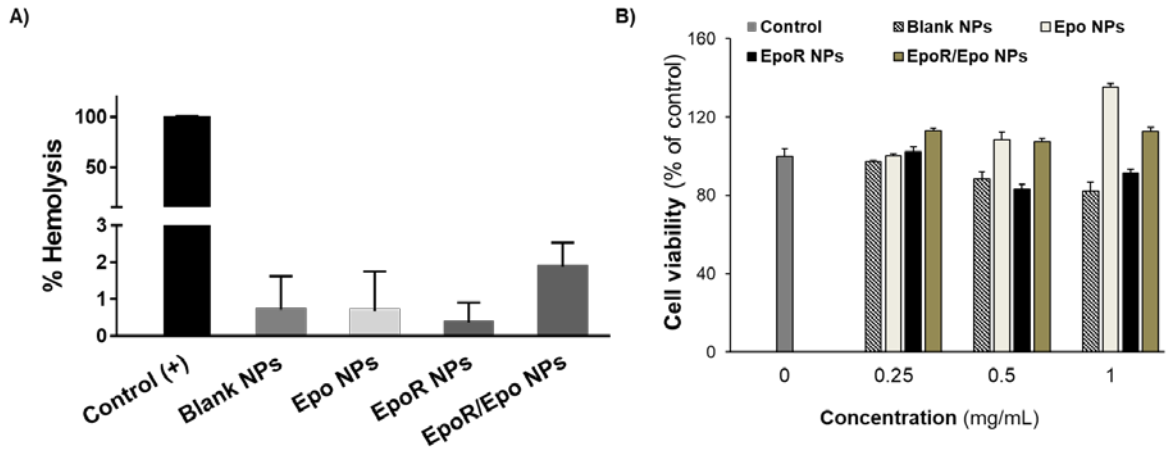

Figure 2. 5. In vitro characterization of NPs. A) Hemolysis properties of EpoR/Epo NP demonstrated to be <2% hemolytic. **B**) Cytocompatibility of NPs.

2.3.5. Protein expression by ECs treated with NPs. After 1 day of exposure to NPs under hypoxic conditions, western blot analysis (**Figure 2.6**) for expressed proteins, including EpoR, Epo, and STATs, confirmed that EpoR protein in sample groups in this order: EpoR NPs> Epo NPs > EpoR/Epo NPs =Free EpoR/Epo > NT. Epo expression in Epo NPs = EpoR NPs > EpoR/Epo NPs > free EpoR/Epo > NT. Also, pSTAT-3 produced spliced variant of the 94kDa pSTAT-3α and 86kDa pSTAT-3β protein. pSTAT-3α in Epo NPs = EpoR NPs > EpoR/Epo NPs > free EpoR/Epo > NT; while pSTAT-3β in EpoR/Epo NPs > EpoR NPs > Epo NPs > free EpoR/Epo > NT

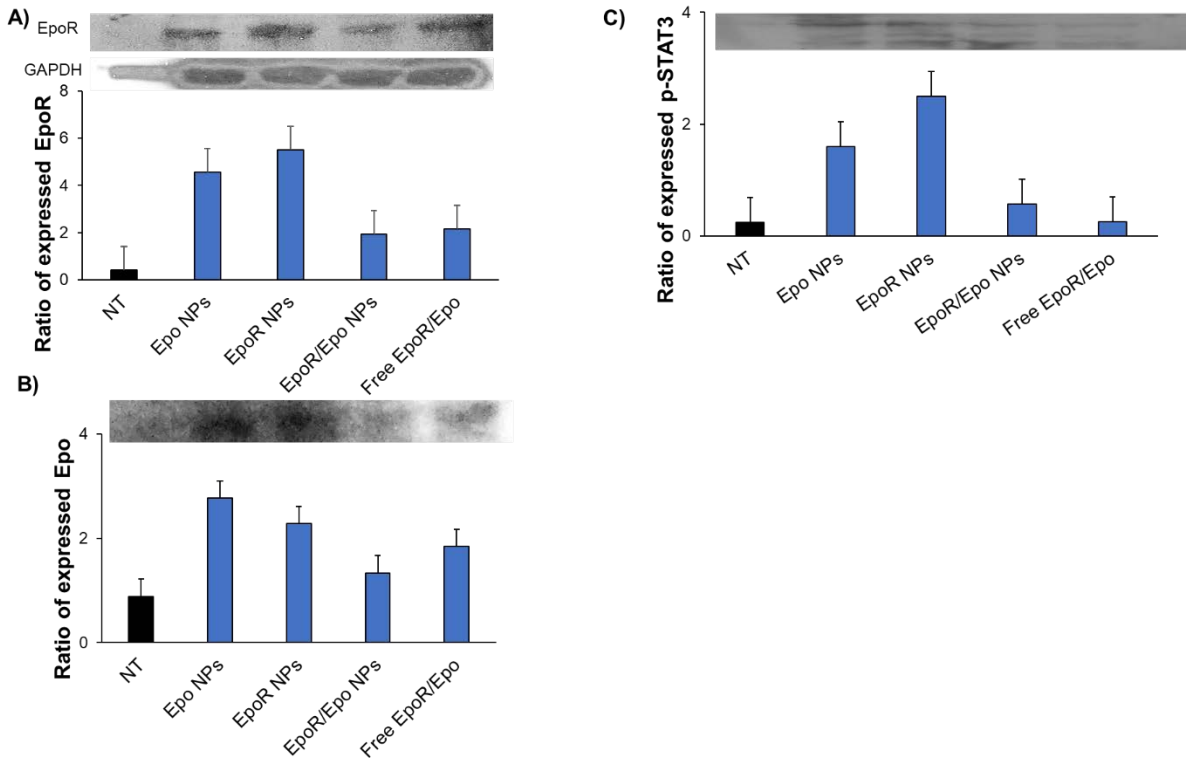

Figure 2. 6. Protein expression by EC treated NPs. Following hypoxia treatment, pre-treated HUVECs lysates were collected and analyze via western botting for fold induction of genes EpoR, Epo, STAT-3, BCL-2, and GAPDH (housekeeping gene): **A**) EpoR and **B**) Epo expression was increased in cells treated with Epo NPs and EpoR NPs. **C**) STAT-3, signal transducer involved at the transcriptional level, showed to be highest in cells treated with EpoR NPs than any other group.

2.4. Discussion

Angiogenesis is critical to various physiological and pathological assessment in the body. To the best of our knowledge, this is the first attempt at delivering both a receptor and its ligand for therapeutic angiogenesis via nanoparticles. The present study showed that the use of NPs for Epo and/or EpoR delivery was feasible for therapeutic angiogenesis to treat PAD by being stable, hemo-compatible, biocompatible, non-viral carriers with sustained release properties. The released EpoR and Epo remain functional in ECs by facilitating cell proliferation, enhancing cell protection in oxidative stress, fostering cell migration, and boosting neo-vasculature.

PLGA, an FDA approved biodegradable polymer, produced ~200nm NPs formulated by our group was similar to other NPs [136] and with a controlled degradation rate.[203] Our Epo NPs consisted of 67% encapsulation efficiency and exhibited 49% release within 21 days, whereas Epo chitosan NPs showed 63% released within 15 days.[231] Due to its anionic surface, PLGA NPs are branded as foreign by reticulo endothelial systems (RES).[232] To overcome this hurdle, surface modifications using cationic, low MW, PEI polymer was applied because of its prominent transfection properties.[233] This alteration improved the formation of spherical complexes with DNA, membrane permeability and DNA translocation to the nucleus.[234] Previous studies disclosed loading efficiency of 99% V1Jns plasmid[235] and 65% HUVECs transfection[236] supported our findings of a 97% EpoR loading efficiency using PEI in PLGA NPs and about 60% HUVEC transfection (compared to that of 58% expression by lipofectamine 2000). With a biphasic release profile from our EpoR NPs, the confirmed properties from this work are suitable to sustain gene and protein delivery in targeted tissues or cells.

Hitherto, therapeutic angiogenesis is often applied using VEGF, fibroblast growth factor (FGF), and platelet derived growth factor (PDGF). Unfortunately, the unmet clinical need to reperfusion and ensure vascular reconstruction remains challenging. Vascular growth emerges from EC proliferation and migration, which are regulated by a multitude of pro-angiogenic agents.[237] Epo stimulate angiogenesis by directly influencing VEGF and EC proliferation,[238] by inducing DNA replication, cell proliferation and cyclins' expression.[239] Our Epo NPs produced 2-fold increase in proliferation at day 3 compared to control, blank NPs and free EpoR/Epo; whereas 0.25-fold[240] and 1.5-fold[241] increase were observed by Epo gelatin hydrogel and VEGF-NPs at day 3, respectively. Enhanced endogenous cell recruitment to injury site is essential for angiogenesis. Epo-induced cell migration significantly improves healing process and upregulates VEGF mRNA.[242] This cytokine Epo regulates VEGF by

their shared tyrosine kinase, as the intracellular messenger, and boost cell migration.[242] Furthermore, Epo has increased CD31 gene expression, protein wound content and VEGF mRNA levels in injured mice.[243] Moreover, other molecules can influence major growth factor (GF) expression. For instance, LL37 peptide [244] and curcumin [245] improved wound healing by upregulating VEGF, while Glypican-1 nanoliposomes promoted migration and improved total tube formation by upregulating more FGF-2 than VEGF levels.[246] Therefore, post-injury, endogenous levels of pro-angiogenic GFs are insufficient to sustain healing, and by applying exogenous molecules, a healing stimulation is eminent. This could explain the 6-fold EC migratory increase in the Epo NPs compared those samples of NT and blank NPs.

Furthermore, oxidative stress from reactive oxygen species (ROS) compounds, hydrogen peroxide (H_2O_2) and superoxide anion, are major initiators of EC damage. H_2O_2 is selected as our stress condition because it is a small nonpolar molecule, with long biological life span, that easily diffuses into cells.[247] Its presence in ECs diminishes proliferation and reduces cell viability.[248] Epo has been found to mitigate EC susceptibility to oxidants via NO upregulation.[249] Epo NPs effectively prevented EC damage by sustaining cell viability and deactivating proinflammatory cytokines (e.g TNF).[250] Epo NPs, EpoR NPs, and EpoR/Epo NPs demonstrated their cell protection (195%, 215% and 339%, respectively) under H_2O_2 damage or exposure, especially at larger time points (day 7). When catalase (superoxide dismutase (SOD)) magnetic NPs were delivered to ECs, only 62% cells were rescued from H_2O_2 damage.[251]

Tube formation in ECs by delivering of growth factors are well-documented. For instance, VEGF NPs produced capillary-like tubes[252] and improved micro-vessel density in rabbit models,[253] while partial recovery of mice ischemic limb[254] and blood flow reperfusion in rat hindlimb[255] by FGF-PLGA NPs are documented. Like these studies, we observed 1.7-fold improvement of total tube length in 8 hours than that of NT group; and comparable to

that of VEGF. ECs formed matrigel tubules by Epo are said to be more stable and complex than FGF[256] because Epo causes an influx of Ca^{2+}, which activates Akt and increases NO bioavailability and ultimately induces angiogenesis.[257] These reports confirm that despite being major players in angiogenesis, there exist a dependency by common GF and other molecules for effective angiogenesis.

Currently, genes encoding pro-angiogenic GFs are delivered using unregulated vectors with limited expression levels, [258-260] which impedes therapeutic efficacy in cells and tissues. Consequently, sustained gene expression is essential for cell proliferation and migration, especially in hypoxia. This is the first report on EpoR cDNA plasmid application for PAD. EpoR enhances cell proliferation by increasing Epo secretion, which facilitates its synergism with VEGF in ECs.[261] The tyrosine residue on EpoR transmembrane protein serves as a docking site to other proteins which results to synergism therapeutic efficacy. At day 3, EpoR NPs enhanced better EC proliferation (by 1.1-fold) than VEGF plasmid hydrogel (0.3-fold).[262] Furthermore, EpoR acts as a signaling molecule for cell recruitment. For instance, by upregulating VEGF, the EpoR/Epo pathway also indirectly plays in endothelial progenitor cells (EPCs) recruitment.[263] EpoR NPs effected significant cell migration in ECs than that of NT and blank NPs, but due to short treatment/expression time, no difference was detected to that of VEGF group.

The production of ROS compounds within ischemic cells and tissues causes oxidative stress, influx of pro-inflammatory cells and activation of apoptotic pathways. Hence, protecting mitochondrial activity in peripheral tissue brings one step closer in promoting angiogenesis.[264] Exogenous EpoR released from our NPs protected HUVECs from H_2O_2 damage by increased cell viability (2-folds) and reduced mitochondrial dysfunction a phenomenon not observed by VEGF, blank NPs nor NT. EC transfection with EpoR NPs might produce anti-oxidative and anti-inflammatory effects in H_2O_2 stress induction. We

deduced that VEGF has no anti-oxidative properties. Our results are consistent with Zhao et al. [265] who applied SelS plasmid in HUVECs and observed similar anti-oxidative properties in the presence of H_2O_2. In stressed conditions, NO undergoes oxidative modification.[266] The defensive essence of EpoR in ECs may also be involved with the regulation of NO by ensuring its bioavailability to cells, which in turn mitigated inflammation and promoted angiogenesis.[267]

Genes constantly produce large quantities of proteins to sustain GF levels, without the need for multiple injections, to achieve neovascularization. EpoR NPs outperformed VEGF in total tube length probably due to the latter's limited protein molecules. Comparably, collateral circulation and neovessel development from VEGF plasmid NPs in ischemic rabbits,[268] and a steady 12 days expression of VEGF plasmid-PLGA nanospheres in ischemic mice limbs,[258] were superior than free VEGF plasmids. Additionally, other nucleic acid such as MiR-92a-lentivirus enhanced tube formation in H_2O_2 and activated Akt pathway;[269] miR-126-3p-microbubles improved capillary density and vascular reperfusion,[270] and miR-126-liposomes, upregulated angiogenic factors and increased blood flow.[271]

Substantial protein levels are essential for development of therapeutic angiogenesis. After 1day hypoxic treatment, NPs transfected HUVECs initiated angiogenesis by expressing various pro-angiogenic proteins and pathways. EpoR/Epo pathway activation is confirmed by expressed Epo. In hypoxia, the upregulation of EpoR on ECs has a positive feedback effect on Epo secretion. Additionally, STAT 3- is a pleitropic factor involved in quick changes in gene expression due to stimuli such as GF, cytokines or hormones. Phosphorylated STAT-3 is a major regulator in maintaining interaction between extracellular activities and cytokine induced genes expression changes.[272] STAT-3 protects mammalian cells from apoptosis and acts as a mediator for VEGF EC activation and angiogenesis.[273] Yang et al. [274] confirmed 40 times higher VEGF protein expression by plasmid VEGF NPs. Hence, its expression induced

by our Epo NPs, EpoR NPs and EpoR/Epo NPs can be deduced to have been involved in the proliferation and protection of HUVECs. We see that levels of both splice STAT-3 variants are enhanced by EpoR NPs; however, more the STAT-3α is expressed in Epo NPs while more STAT-3β is expressed by EpoR/Epo NPs. Very minimal levels of both variants are observed in free EpoR/Epo and NT groups.

Synergistic NP co-delivery of different reagents have been published. Recently, Glypican-1/FGF nanoliposome enhanced FGF mediated cell proliferation,[246] while VEGF+ angiopoietin-1 NPs increased cell growth by 90% in 2 weeks.[275] Despite no synergism, EpoR/Epo NPs demonstrated higher EC protection in H_2O_2 after 7 days of exposure(400% of control day 1), surpassing positive control (~300%). Additionally, EpoR/Epo pathway is involved in the mobilization of EPCs in angiogenesis and influences VEGF to boost cell migration.[276] More recently, VEGF plasmid/apelin NPs produced higher and more compacted tubules than VEGF plasmid alone,[277] while co-delivery of bFGF and VEGF nanogels enhanced tubular formation compare to those of single ones.[278] Enhanced tube formation by EpoR/Epo NPs is due to EpoR and Epo bioavailability to cells, resulting in a positive feedback mechanism at the EpoR/Epo pathway, which in turns results in more VEGF production. Other groups[279] have reported the co-delivery of FGF-2 fragmin/protamine NPs (FGF-2 + F/P NPs) is effective in restoring hindlimb function in rat models than single delivery (FGF-2 NPs or F/P NPs). Unlike these studies, no synergistic effect was observed in our EpoR/Epo NPs, and it might be possible either that EpoR cDNA plasmid released from our NPs did not induce enough EpoR expression for Epo synergistic effects or that Epo and EpoR cDNA interact somehow, leading to lesser, but still effective therapy.

2.5. Limitations

Regarding issues of cell toxicity from higher MW PEI, we opted for lower MW. Furthermore, no synergism was observed in EpoR/Epo NPs in most of our studies; therefore, we would further investigate the role of EpoR NPs only in the ischemic hindlimb mice model.

2.6. Conclusion and future work

PAD progresses due to various factors such as endothelium dysfunction, local ischemia, and oxidative stress. Even though GFs such as VEGF and FGF have been tested clinically, they weren't enough to restore blood flow in ischemic tissues. We developed NPs for Epo, EpoR and EpoR/Epo with improved bioavailability to cells and observed their distinguished performance in enhanced cell proliferation, refined cell protection in stressed conditions, and facilitated cell migration and tubular formation. By delivering these NPs, therapeutic angiogenesis can be achieved and applied as a noninvasive therapeutic option for most of PAD patients.

CHAPTER 3

NANOPARTICLES FOR DELIVERY OF SENSE AND ANTI-SENSE cDNA OF EpoR FOR THERAPEUTIC ANGIOGENESIS

3.1. Introduction

Atherosclerosis is known to affect many people globally. As an atherosclerosis outcome, peripheral arterial disease (PAD) is impairment in arterial function causing limited blood and oxygen reaching tissues of the lower extremities.[280] PAD can progress to become critical limb ischemia (CLI). In CLI, there are higher chances of tissue damage, amputation and other associated disorders in patients. PAD is affecting millions of patients in the U.S (~12 millions) especially elderly males of more than 60 years old,[195, 196] and there is no current effective approved therapy. For CLI, current techniques of reducing on going symptoms of PAD are via amputation, surgical bypass grafts, cell therapy, angioplasty and stents; however, these approaches are invasive with limited cell viability and poor long-term patency.[281]

Gene therapy is the modification of defective cells or tissues by delivering of nucleic acid molecules as therapeutic agents. These genes are often delivered through viral or adenoviral vectors due to their high transfection efficiency. However, concerns associated with immunogenicity and/or potential mutagenesis have caused non-viral vectors to be opted as alternative gene carriers.[282] Non-viral vectors such as nanoparticles (NPs), often are in the form of lipids or polymeric materials with minimal toxicity effects.[283, 284] Poly (lactic-co-glycolic) acid (PLGA) is an FDA approved biodegradable polymer with good encapsulation properties that provides controlled, sustained release of its payload,[203] while polyethylenimine (PEI) is a cost effective polymer with outststanding transfection properties, for its ability to

form complexes with DNA molecules through electrostatic interactions resulting into higher transfection efficiency. In addition, this polyplex (PEI-DNA) has the ability to produce a proton-sponge effect hence erading lysosomal degradation. It should also be noted PEI transfection efficiency and toxicity are dependent on its molecular weight.[285, 286] Common pro-angiogenic growth factors such as vascular endothelial growth factor (VEGF) are well known for their proliferative and reconstructive properties.[200, 201] VEGF plasmid DNA (pDNA) enhanced blood vessel formationn and recovered injured tissue in patients, who had been scheduled for below the knee amputation;[287] however, adenoviral delivery of this plasmid is ineffectiveness in improving patients' quality of life, maintaining an average ABI, reducing peripheral edemas, and improving peak walking time.[288] Also, fibroblast growth factor-2 (FGF-2) gene is mentioned for its angiogenic properties.[289] Clinically, this gene caused a gross trim in amputation and death risks; however, it demonstrated no ulcer healing properties.[290] Furthermore, platelet derived growth factor (PDGF) gene is recognized for its role in signaling perivascular cells, while hepatocyte growth factor (HGF) gene was commended for its pain reduction and ABI improvement.[291]

The outstanding potential of gene therapy in some cases is in its transisent protein expression at maintaining systemic concentration. Furthermore, there is the possibility of delivering more that one therapeutic gene. Therefore, in this work, we plan on the application of NPs delivering singles (sense or anti-sense) and combination DNA, that are complimentary strands to the erythropoietin receptor (EpoR) gene. These NPs will slowly release the loaded plasmids for constitutive bioavailability to cells to affect angiogenic outcomes in ischemic tissues. For this study, sense EpoR and anti-sense EpoR, shall be referred as EpoR and RopE, respectively. EpoR is a 66-78 kDa transmembrane protein upregulated in hypoxic ECs[209, 210] consist of cytoprotective properties to apoptosis, inflammation and mediates angiogenic effects of Epo,[212] while RopE has been reported to be concurrently upregulated with EpoR expression

in vivo following pneumonectomy.[292] The novelty of this work is portrayed using a complimentary strand of the same gene to protect, recruit and restore tissue functions via angiogenesis. In this research, we evaluated the formulated EpoR NPs, RopE NPs, and EpoR/RopE NPs for their possibility and efficacy as non-viral vectors in angiogenic gene therapy and investigated their roles in restoring ischemic limbs of mice.

3.2.Materials and method

3.2.1. Cell culture. Human umbilical vein endothelial cells (HUVECs) were purchased from ATCC, were maintained in Vasculife® VEGF (LS-1020) medium (Lifeline cell technology) at 37ºC, incubator with a 95% air humidifier and, 5% CO_2 atmosphere. HUVEC culture medium supplemented with 1% penicillin and streptomycin (Life technologies) was changed every other day. Conditioned media (CM) having 2% fetal bovine serum (FBS) (GElifescience) was used for HUVECs in all *in vitro* studies and assays.

3.2.2. Expression and purification of the human EpoR and RopE plasmids. EpoR was expressed and purified as previously described.[293] Briefly, EpoR and RopE genes were cloned into the pMXs-IRES-GFP vectors (Cell Biolabs Inc.).[213] These vectors were expanded using Chemically competent DH5α Escherischia Coli (E.Coli) cells (Invitrogen) in SOC medium (Invitrogen) supplemented with ampicillin (Sigma) were used to expand the vectors and plasmid purification was performed using EndoFree plasmid mega kit following the company (Qiagen)'s instructions.

3.2.3. Preparation of EpoR and RopE NPs

3.2.3.1. *Plasmid DNA loading.* Polymer-nucleic acids complexes were prepared via bonding.[218] Briefly, branched PEI (bPEI 1200) (Polysciences) was prepared to a final concentration of 0.05% (w/v). PEI (0.06 mg) was added to the DNA(2mg)-glucose (2mg) solution and left to form complex via electrostatic bonding at room temperature for 30mins under rotation. PEI-DNA (0.03:1) (w/w) solution (W_1) was further applied in PLGA NP synthesis.

3.2.3.2. *PLGA nanoparticle synthesis.* The standard double emulsion ($W_1/O/W_2$) solvent evaporation technique was applied in PLGA NPs synthesis.[214-217] Briefly, the above solution (W_1) was added to 40 mg PLGA 50:50 (Lakeshore Biomaterials) in 1 mL dichloromethane (DCM) (EMD Millipore Corporation) (O) to form the first emulsion and sonicated at 30 wats for 1 min on ice. Drops of this emulsion (W_1/O) was to 12 mL of poly vinyl alcohol (PVA) 5% (w/v) (Sigma) solution (water-phase 2) and sonicated at 40 W for 10 mins on ice followed by overnight stirring at room temperature to ensure complete organic solvent evaporation. Centrifugation at 15,000 rpm for 30 mins at 25ºC and freeze-drying were performed to recover PLGA-PEI-cDNA NPs. Supernatant was kept for determining the encapsulation efficiency of DNA plasmids in NPs. All lyophilized NPs were stored in at -20ºC when not in use and were freshly reconstituted in appropriate solvent for our experiments. Empty vector (GFP-encoded plasmid cDNA) was used as the control cDNA model for encapsulation within NPs. Nanoparticles groups fabricated were EpoR NPs, RopE NPs, EpoR/RopE NPs (1/2 mg EpoR plasmid and ½ mg RopE plasmid), and empty vector NPs.

3.2.4. Characterization of NPs encapsulating EpoR and RopE gene. Transmission electron microscopy (TEM) confirmed morphology and laser light scattering from NP brownian motion of Zeta Potential Analyzer (Brookhaven instruments co.) were recorded for

size and zeta potential measurements, and stability in saline solutions (0.9%) was monitored for 48 hours as previously described.[220, 221] EpoR and RopE NPs *in vitro* release profiles were studied using NP suspensions (1 mg/ml) in dialysis bags (300 kDa; EpoR M.W= 6.0 kb) (Spectrum Laboratories Inc.) and dialyzed against 1X PBS at 37°C for 28 days. At designed time, 1 ml of dialysate was replenished with 1 ml of fresh 1X PBS. An UV absorbance (260/280) via spectrophotometry (Tecan) quantified released cDNA. Lastly, un-entrapped cDNA from collected supernatant was quantified for gene loading efficiency (LE) as the percentage of cDNA initially used during NP formulation (Equation 3.1).

$$Loading\ efficiency = \frac{cDNA\ used - cDNA\ in\ supernatant}{cDNA\ used} * 100 \quad (3.1)$$

3.2.5. *In vitro* studies of EpoR and RopE NPs

3.2.5.1. *Hemo-compatibility of NPs***,** various concentrations (0-1 mg/ml) of NPs were exposed to human blood. Whole blood clotting was analyzed by activation of 50 µL blood with $CaCl_2$ (sigma), and the time for blood clotting was recorded (0-60 minutes) via absorbance at 540 nm as previously described.[229] Furthermore, a hemolysis test to study the red blood cells integrity upon exposure to NPs at 37°C for 2 hours was performed by exposing saline (0.9%) (sigma) diluted blood to NPs and read at 545 nm. Each sample group was studied at n=20 due to human blood variation issues. The absorbance was converted calculated using the equation below (Equation 3.2).

$$\%\ hemolysis\ \frac{[(absorbance\ of\ tested\ NPs) - (absorbance\ of\ (-)\ control)]}{absorbance\ of\ (+)\ control} * 100 \quad (3.2)$$

3.2.5.2. *Cyto-compatibility of our NPs*, HUVECs were seeded in culture plates and treated with various concentrations (0-2 mg/ml) of NPs for 24 hours in CM. Cell viability and death were

assessed via MTS cell viability and LDH (Lactate dehydrogenase, a cytosolic enzyme indicated cell toxicity and cytolysis in media) assays, respectively.

3.2.6. GFP cDNA plasmid expression. HUVECs were seeded in tissue culture plates one day before treatment. Cells were treated with 1 mg/mL NPs in Opti-mem solutions for 4 hours. The DNA quantification was achieved via nanodrop spectrophotometry for total DNA content when compared to that of control group.[222, 223] DNA expression was performed using a 24 well plate with NPs (62.5µg/mL) in opti-mem media for 4 hours at 37°C. Cells were washed and replenished with media with serum for 48 hours. Cells' nuclei were stained with DAPI while uptaken cells expressed GFP tagged plasmid. Analysis was performed by the fluorescence of GFP expressing cDNA in the endothelial cell population.

3.2.7. *In vitro* therapeutic efficacy of NPs

3.2.7.1. *On EC proliferation.* HUVECs were pre-transfected with NPs (62.5µg/mL) the day before, then the cells were incubated with CM for 3 days in a hypoxic (< 1% O_2, 5% CO_2 in nitrogen at 37ºC) environment; a parallel plate was incubated in a normal oxygen environment. At each time point (1 and 3 days), MTS assays were performed to analyze the number of viable cells following the company (Promega)'s instructions. DNA quantification was also determined using Picogreen assays. Cells treated with CM containing 25ng/mL VEGF and CM only served as positive and negative controls, respectively

3.2.7.2. *On EC protection from ROS species.* Pre-transfected HUVECs seeded in 48 wells (as previously stated) were washed and replenished with 200µM H_2O_2 in CM for 1 and 3 days at 37ºC. Cells + H_2O_2 served as negative control while quiescent cells without H_2O_2 exposure served as a positive control. After each time point, cell viability was confirmed via MTS assays

3.2.7.3. *On the ability of treated cells to induce angiogenesis.* Tubular structure formation on matrigels were performed as previously described.[226-228] Pre-transfected HUVECs were seeded onto low basement membrane matrigels with basal media. Cells were incubated in hypoxia (< 1% O_2, 5% CO_2 in nitrogen at 37ºC) for 8 hours. Non-transfected cells (NT) and cells exposed to 25 ng/mL of VEGF served as negative and positive controls, respectively. After 8 hours, phase contrast microscopy was performed to obtain and analyze the level of tubes formed. Quantification of the sprouting length and density was analyzed using Image J analysis software

3.2.7.4. *On EC migration.* In 96 well plates, pre-transfected HUVECs were scratched to create a wound, and the wound closure assays was assessed as previously described.[294] In brief, cells were washed with PBS and incubated in basal media for 24 hours at 37ºC after scratching. The initial distance (time 0) was recorded and the wound closure distance by migrating cells within 24 hours was studied and recorded over time. Cells without treatment in CM served as negative control while cells exposed to media containing 25 ng/mL VEGF were positive control. Measurements of distance closure were determined via phase contrast microscopy and Image J analysis.

3.2.8. Mouse ischemic hindlimb. Mice (male and female) (6-8 months old) were purchased from Charles River Laboratory (Wilmington, MA) and kept on a standard chow diet. Hindlimb ischemia (HLI) was generated as previously described.[295] Briefly, mice were securely taped down in a supine position before they were shaved, cleaned with iodine solution and 70% alcohol solution and anesthetized by isofluorane inhalation (2%) before and during surgery. Animals were administered analgesic (1µg buprenorphine /g animal weight) before surgery.

HLI was created by making an incision on the skin at the upper front thigh region. Subcutaneous fat tissues were carefully separated to expose the femoral artery. Three distal tie-offs were made on the femoral artery using sutures. Incisions were closed using bioresorbable sutures. All animals were left to recover, and observation of ischemic toes and limping were detected before returning to their assigned cages. All tests were carried out following the animal study protocol approved by the institutional animal care and use committee (IACUC) at the University of Texas at Arlington.

3.2.9. Treatment and evaluation of NPs in mouse limb ischemia. For intramuscular injections, cDNA plasmids incorporated with or without NPs were suspended in 100 µL sterile injection water and injected into 4 different sites in the ischemic hindlimb (2 front, 2 back on the thigh muscle distal to ligation) with a 27-gauge needle 5 days after femoral artery ligation. Sham-operated control animals were subjected to the same surgical protocol and administered with the same volume of sterile water.

3.2.10. Laser doppler perfusion imaging (LDPI). LDPI and necrosis score were performed before and post injury to confirm proper ligation of arteries as previously described.[296] Blood flow perfusion and color-coded images were recorded after 0, 2, 5 and 12 days. The blood flow ratio of the ischemic limb (left)/non-ischemic limb (right) was measured and determined using a laser doppler perfusion imager (Perimed). Mice were monitored by serial scanning of surface blood flow of the hindlimbs before ligation, just after ligation, and on day 0, 2, 5, 12 post NP treatment. Color coded images confirmed impaired and current blood flow as well as reperfusion over time. Assessment of ischemic tissue damage and loss was performed with 1= no necrosis or defect, 2= skin necrosis or toe amputation, 3= forefoot amputation.as previously described.[297] Outcomes of all mice were observed and recorded.

3.2.11. Tissue recovery via treadmill endurance test. At various time points post treatment (day 0, 2, 6 and 13), all mice were challenged with an acute exercise (maximal endurance) as previously described.[298] Before beginning the exercise, mice were acclimated to the treadmill for 3 mins and held constant at 10m/min. exhaustion was defined as when the mouse spent more than 30 consecutive seconds on the shock grid without trying to reengage the treadmill. The maximal running distances (in m) and number of stimulations were recorded.

3.2.12. Therapeutic effectiveness of NPs in vivo

3.2.12.1. Q*uantification of capillary density, maturity and biomarkers for ECs.* Two weeks post treatment, all mice were sacrificed, then organs and ischemic limb tissues were retrieved. Gastrocnemius muscles were fixed at 4% paraformaldehyde and embedded in optimal cutting temperature (OCT) compound, and 10 µm thickness cross sections were immunohistochemically stained for smooth muscle actin (SMA) to assess arteriole density, CD34 to assess EPC recruitment and CD31 to assess endothelization of vascular structures (Santacruz biotech) and analyzed using microscopy and image J software technique.[299] For comparison among the various treatment groups, a count of capillary/ratio was carried out. Histological evaluation of the muscle tissue was achieved by staining with hematoxylin and eosin (H & E) and performed to examine muscle degeneration and tissue fibrosis in the ischemic regions.

3.2.12.2. *Expression of Epo, Epo, and other angiogenic proteins.* Organs and tibialis anterior muscles in mice were harvested and lyzed to determine the protein profiles. Quantification of the expressed Epo and EpoR was tested via ELISA assays to support the expression levels of

molecules associated with angiogenesis and the EpoR/Epo pathway. Protein quantification via Bradford protein assays (Biorad) was performed before running lysed tissue extracts on an SDS-PAGE gel electrophoresis. The protein bands were later transferred onto a nitrocellulose membrane (Biorad) and electrophoresed at 90V for 1 hour. After overnight membrane blockage using 5% milk solution, the nitrocellulose membrane was treated with primary and secondary antibodies against EpoR, VEGF, NG2, phosphorylated STAT-3 (pSTAT-3), HIF-1α,[224] and GAPDH (control) proteins.

3.2.12.3. *Biodistribution of NPs.* PLGA loaded DiD NPs were injected intramuscularly into the ischemic limb. The ex vivo fluorescent imaging system was utilized to image the NPs treated mice at designated time intervals. At each time point (0 and 4 hours), mice were sacrificed, and tracking of NPs at various organs (e.g. lung, liver, kidneys, spleen, heart, blood) were confirmed by emitted fluorescence of the *ex vivo* imager. Following imaging of animals, organs were harvested and lyzed for the presence of fluorescent NPs via spectrophotometry. Quantification of NPs distribution were determined by the emitted fluorescence from other tissues at final time point to that same tissue of initial time point and expressed as a percentage of injected NPs per gram of tissues.

3.3. Results

3.3.1. Characterization of NPs.

In this study, we prepared EpoR and RopE NPs using poly(lactic-co-glycolic) acid (PLGA) and PEI polymers. Results from DLS (**Table 3.1**) and TEM (**Figure 3.1A**) confirmed that most of NPs had average diameter size <200nm. EpoR and RopE NPs consisted of a biphasic release with an initial burst released followed by a control release for 21 days (**Figure 3.1B**). In solutions

of saline, NPs were observed to be stable as they maintained their original size after 72 hours of exposure (**Figure 3.1C**).

Table 3. 1. Dynamic light scattering (DLS) analysis of NPs and loading efficiency

PLGA-PEI	Size (nm)	Zeta potential (mV)	Polydispersity (PDI)	Loading efficiency
Empty vector NPs	199 ± 39	14 ± 1.02	0.134	84%
EpoR NPs	199 ± 41	16 ± 1.07	0.206	77%
RopE NPs	209 ± 10	6 ± 6.25	0.064	83%
EpoR/RopE NPs	178 ± 49	7 ± 0.67	0.112	81%

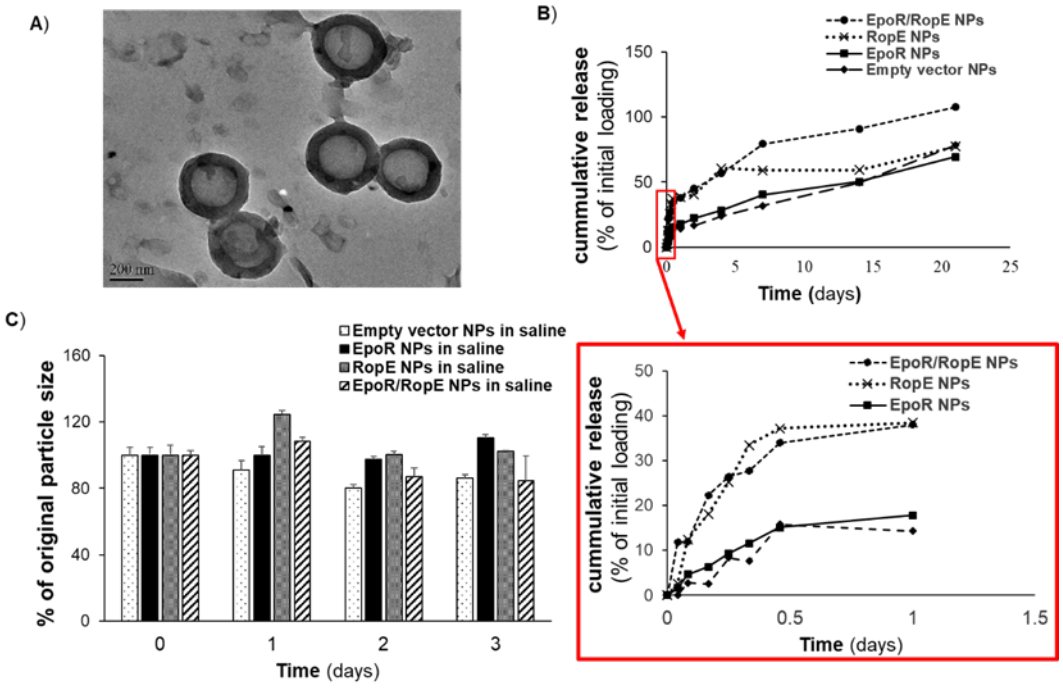

Figure 3. 1. Characterization of EpoR and RopE NPs. A) TEM image of EpoR/RopE NPs. **B**) Stability of NPs in saline (0.09%) and **C)** Release profile of NPs in PBS pH 7.4 overtime.

3.3.2. *In vitro* properties of EpoR and RopE NPs.

The cytotoxicity of synthesized particles were tested on HUVECs for a duration of 24 hours. MTS analysis confirmed that cells maintained over 80% viability after 24 hours of exposure to these NPs. LDH assay analysis also demonstrated low toxicity in cells exposed

to NPs (data not shown) confirming that our particles are cyto-compatible (**Figure 3.2A**). Transfected HUVECs were seen expressing GFP vector upon NP uptake (**Figure 3.2B)**. When exposed to whole blood, there was less than 1% red blood cell lysis observed (**Figure 3.2C)**. This confirms that our nanoparticles are safe for use *in vivo*. Following treatment with plasmid nanoparticles, we wanted to confirm the amount of DNA expressed by each group to that of controls. EpoR/RopE group demonstrated to have the highest DNA content when compared to that of other groups, including the control group (**Figure 3.2D**).

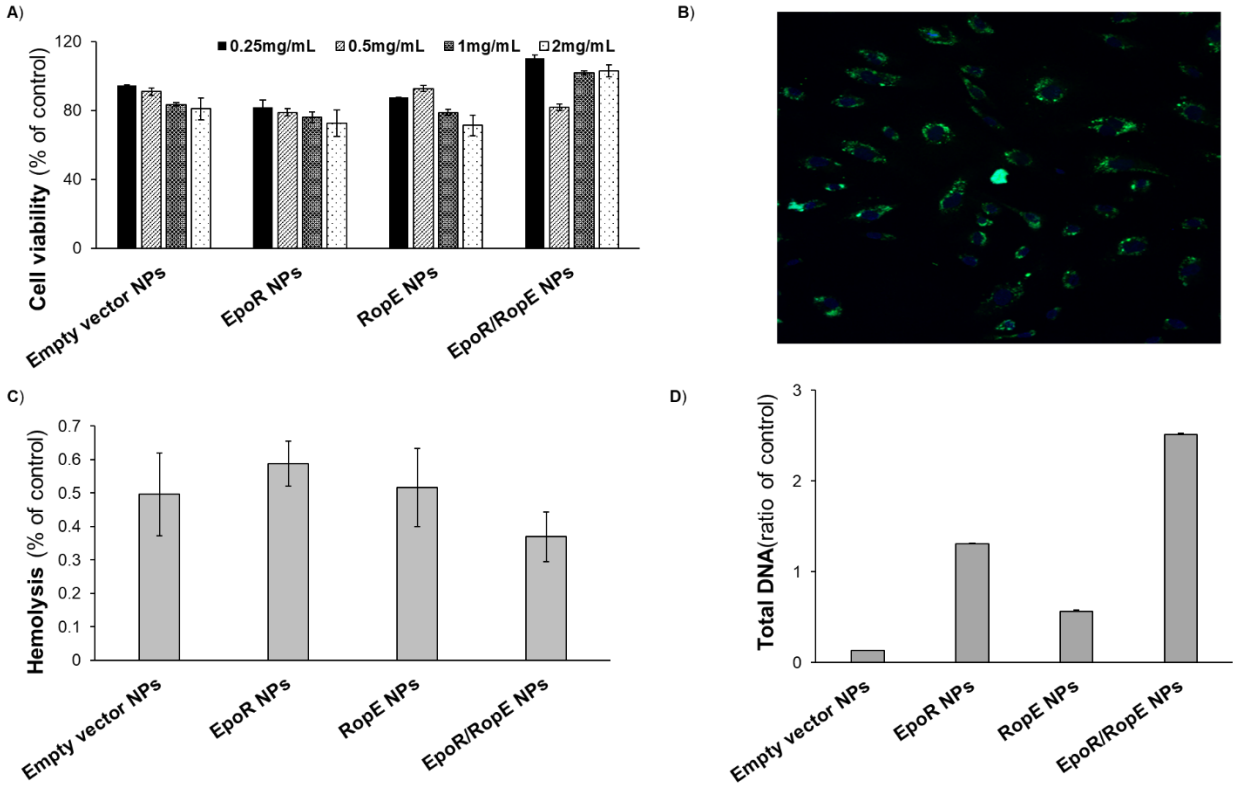

Figure 3. 2. In vitro characterization of EpoR and Rope NPs. A) 24 hours cyto-compatibility of NPs by MTS; cells without NPs treatment served as controls. **B**) ECs expressing GFP vector with DAPI nuclei stain; cells without NPs treatment served as controls. **C**) Hemolytic properties of NPs. Blood exposed to water and saline served as positive and negative control respectively. **D**) Total DNA ratio of HUVECs treated with NPs. Cells that were not exposed to NPs served as controls.

3.3.3. *In vitro* therapeutic efficacy of NPs on ECs

EpoR NPs, RopE NPs, and EpoR/RopE NPs have demonstrated to participate in cell proliferation in both hypoxic and normoxic environments. We observed that following a change in oxygen levels, cells treated with EpoR NPs, RopE NPs and EpoR/RopE NPs showed to significantly improve cell viability when compared to that of control groups and empty vector NPs (**Figure 3.3A**). Further analysis of these synthesized NPs and their roles in protecting cells in the presence of ROS species such as H_2O_2 was confirmed. All groups of DNA nanoparticles demonstrated to protect cells under stressed conditions (exposure o 200µM H_2O_2) (**Figure 3.3B**). Additionally, pre-transfected cells by all 3 NPs significantly improved cell migration when compared to the NT and other control groups. Initial wound distance closure by EpoR/RopE NPs (100%) was comparable to that of VEGF and showed a synergistic effect within 24 hours (**Figure 3.3C**). Major induction of angiogenesis via tube formation was also observed in all groups when compared to that of negative control groups (**Figure 3.3D**). Our EpoR/RopE NPs induced higher tube formation compared to that of VEGF, a positive control.

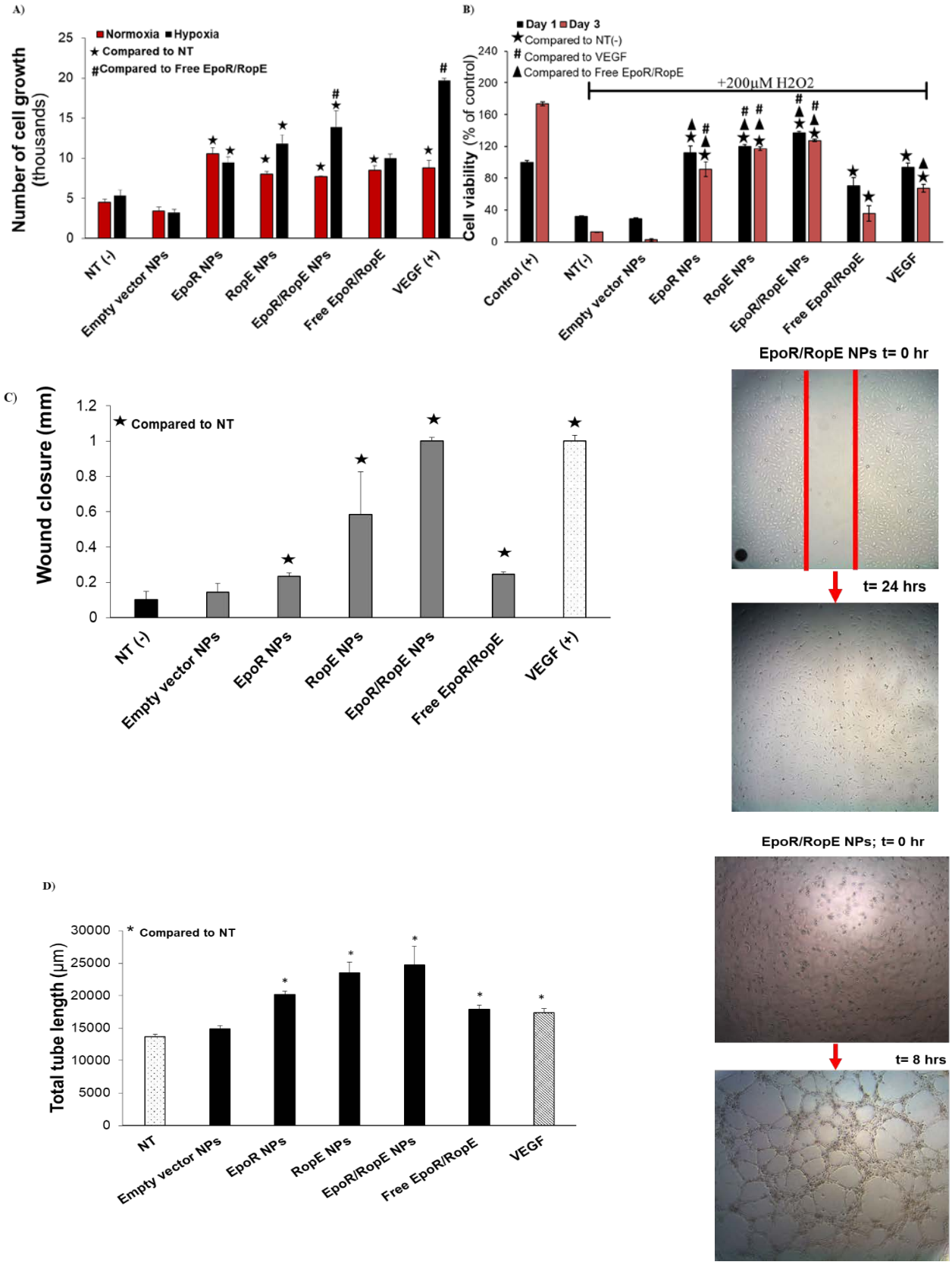

Figure 3. 3. ***In vitro*** **therapeutic efficacy activities of NPs on ECs. A)** Cell proliferation**. B)** Cell protection in stressed environment **C)** EC migration via wound scratch assays and **D)** tube formation on matrigel of endothelial cells.

3.3.4. Tissue recovery via laser doppler perfusion and treadmill endurance test.

LDPI was used to monitor the revovery of blood flow in the mice. As a result, LDPI of the footpad compared perfusion in the ishcemic limb to the non-ischemic contralaterial limb (**Figure 3.4A**). In EpoR NPs, RopE NPs, and EpoR/RopE NPs-treated mice, perfusion of the ischemic leg started to regain blood flow as early as 5 days in animals compared to those of sham and empty vector NPs (**Figure 3.4A**), and continued to improve throughout the study (**Figure 3.4B**). Animals treated with EpoR/RopE NPs regain strength with signifcantly greater treadmmill maximal endurance at 14 days (**Figure 3.4C**).

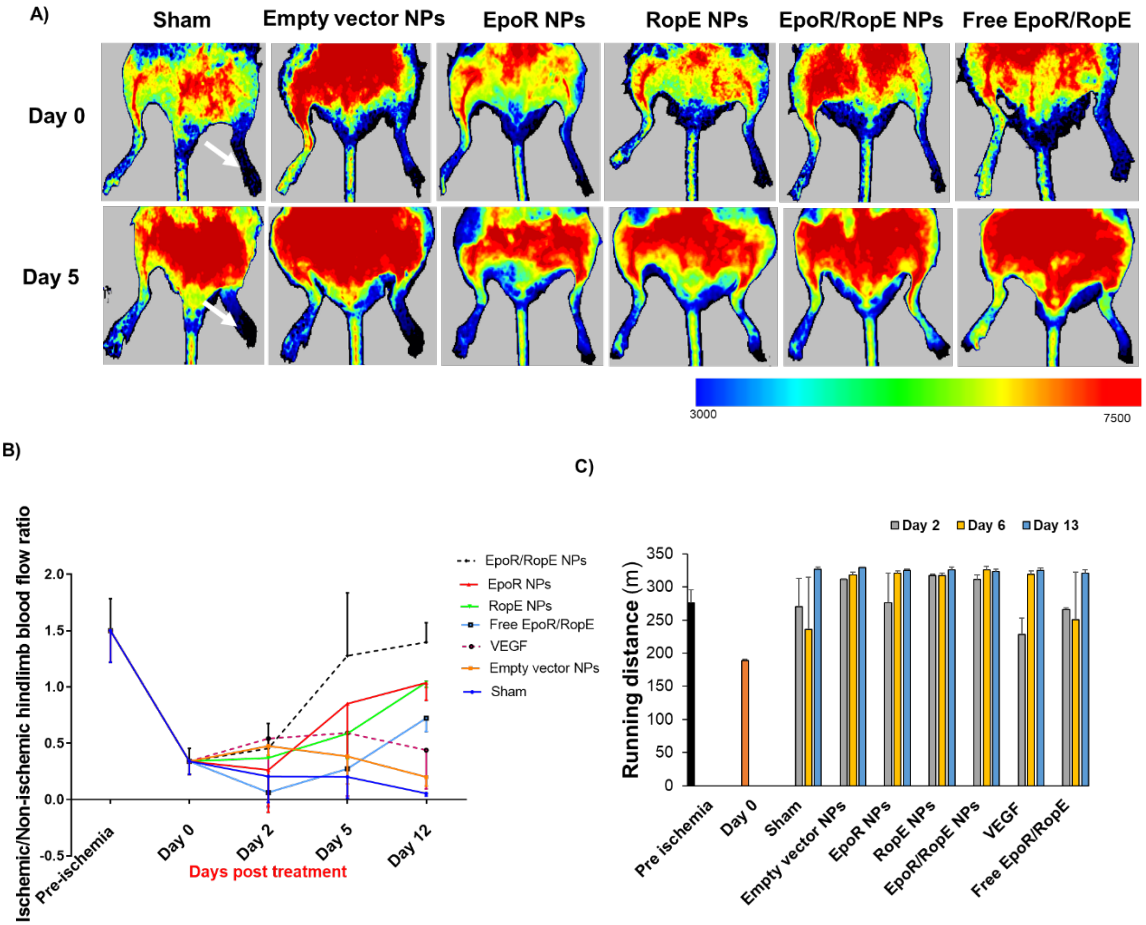

Figure 3. 4. Recovery from hindlimb ischemia after treatment with NPs. A) Representative images of Balb/C ischemic (left) and non-ischemic (right) limb on day 0, 2, 5, 12 following NPs treatment. In color coded illustrations, red indicates normal perfusion, blue indicates reduced blood flow and black indicates a marked reduction in blood flow in in the ischemic hindlimb. **B)** Time course of the ischemic-to-control leg blood flow ratio in the hindlimb. The blood flow of the ischemic hindlimb is expressed as the ratio between th eperfuion of the ischemic limb ad the uninjured limb. **C)** In mice, EpoR NPs, RopE NPs and EpoR/RopE NPs resulted in significantly greater endurance as compared to that of sham, empty vector NPs or free EpoR/RopE.

3.3.5. Histology of the gastrocnemius muscle.

To confirm whether EpoR related reagents are beneficial in stimulating angiogenesis, 14 days after treatment with NPs, we assessed angiogenesis as a fucntion of of CD-31$^+$ (PECAM-1) expression in ischemic muscles.(**Figure 3.5A**). CD-31$^+$ is known to be involved in the signalling, adhesion and motility of ECs during vascular reconstruction. Little to no CD-31$^+$ was expressed by sham and empty vector NP groups. Furthermore, EpoR NPs showed higher CD-31$^+$ expression when compared to that of RopE NPs, free EpoR/RopE and VEGF groups. In addition, EpoR/RopE NPs resulted in a significant increase in CD-31$^+$ capillary structures. These results suggest that EpoR/RopE NPs improves and stimulates angiogenesis which further enhances the restoration of blood perfusion in the ischemic hindlimb mouse. Histological analysis of ischemic hindlimb tissues were further analyzed to confirm therapeutic efficacy of EpoR related reagents and immune responses (**Figure 3.5B**). Tissue damage caused by ischemia and infiltration of inflammatory cells were observed in groups of sham and empty vector NPs. More vascular networks were observed in free EpoR/RopE treated muscles than that of the VEGF group. EpoR NPs and RopE NPs showed to preserve muscle tissue integrity and formed some vascular networks connecting tissues and superior to that of VEGF or free EpoR/RopE. EpoR/RopE NPs showed remarkable therapeutic effects by enhancing vascular tubal structures and inhibited inflammatory cell recruitment the injury site.

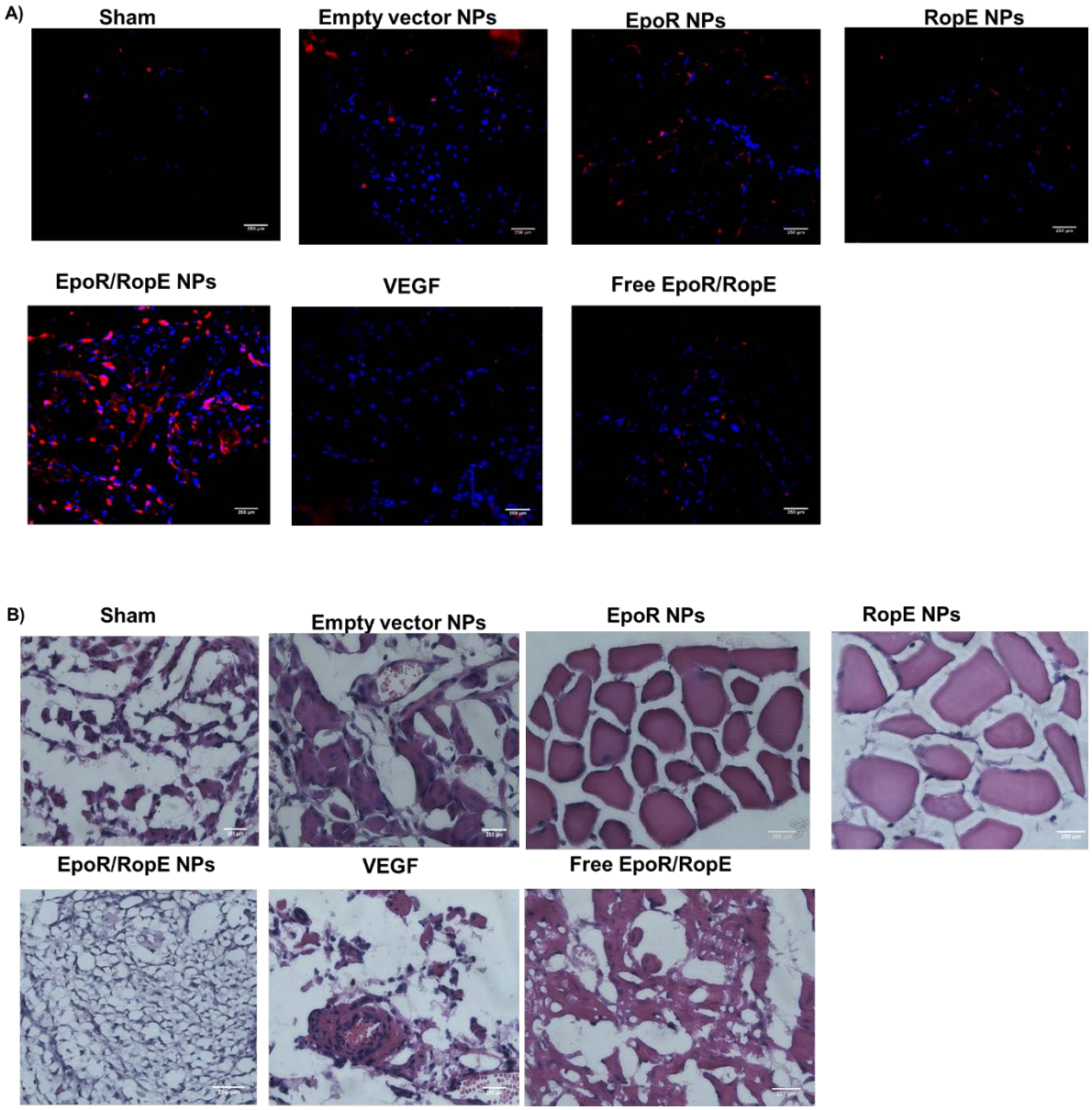

Figure 3. 5. Histological analysis of hindlimb treated with NPs. Representative images of cross section (5µm) of hindlimb ischemia with **A**) double immunohistochemistry staining using CD-31 (red) and DAPI (blue) and **B**) Hematoxylin and eosin stains to observe therapeutic angiogenesis and immune responses**.**

3.3.6. Western blot analysis.

The reperfusion of blood flow to an ischemic tissue is vastly due to the influences of angiogenic growth factors and cytokines. We, therefore, tested the effects EpoR related reagents have on the expression of EpoR, pSTAT-3 and NG2 (**Figure 3.6**). At 14 days post treatment, pSTAT-3 expression was upregulated in the gastrocnemius muscle after ischemia in

all groups except for muscles from sham and empty vector NP groups. Treatment of free EpoR/RopE and VEGF showed lower expression of pSTAT-3 when compared to that of EpoR NPs, RopE NPs, and EpoR/RopE NPs. NG2 is cytokine involved in key signalling pathways of angiogenesis and as a marker presented on blood vessels confirming blood vessel maturation. We asssessed its expression following ischemic treatment and observed that its expression was highest in EpoR/RopE NPs-treated muscles. Lastly, EpoR expression was upregulated in msucles injected with EpoR NPs.

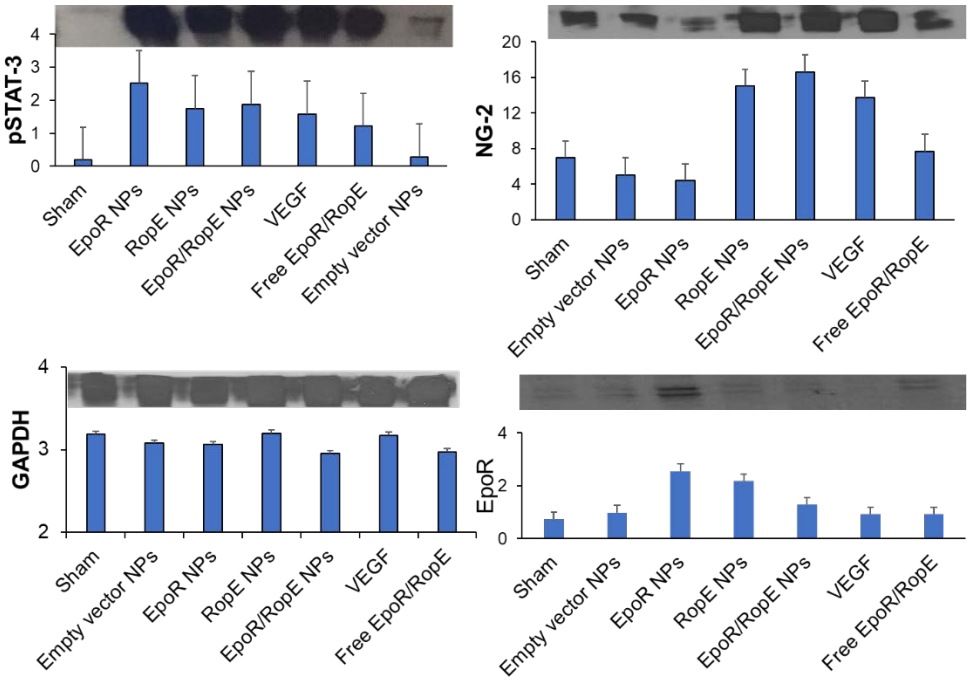

Figure 3. 6. The effect of EpoR related reagents on angiogenesis -regulatory gene expression in the ischemic gastrocnemius muscle. Gene expression of pSTAT-3, NG-2, EpoR and GAPDH (control).

3.3.7. *In vivo* and *ex vivo* tracking of post intramuscular injection in hindlimb muscle.

Noninvasive *in vivo* and and invasive *ex vivo* fluorescence imaging were taken 30 mins and 24 hours post intramuscular injection of dyes-loaded NPs (**Figure 3.7A-B**). Images confirmed that NPs remained in ischemic muscles 24 hrs post injection with no detection of dyes, DiD, in other organs such as heart, lungs, liver, spleen, kidneys, and non-ischemic limb. However, parallel testing of free DiD injection in ischemic muscle

confirmed distribution to the tail as early as 30 mins and by 24 hours, some traces of DiD were detected in organs such as spleen and kidneys (data not shown). This confirms that by applying nanoparticles, therapeutic reagents are protected and made available to tissues to produce therapeutic changes.

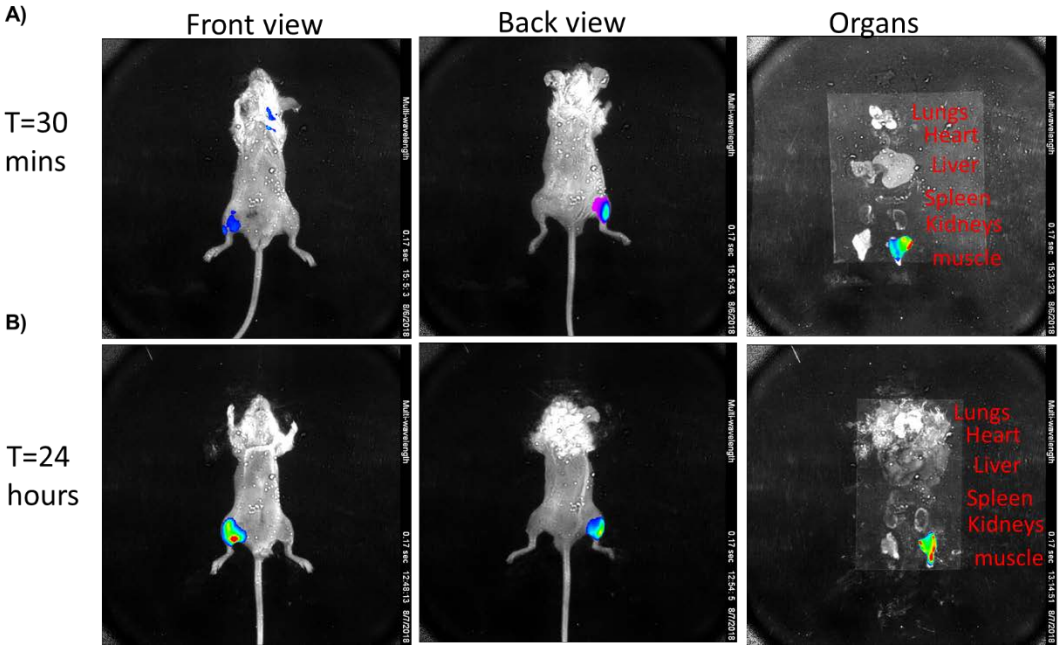

Figure 3. 7 Biodistribution of NPs in ischemic mice. DiD-PLGA NPs were injected in the ischemic muscle. Biodistribution baseline was set at T=30mins. No dye DiD was traced in other organs 24 hours after injection. This confirms that intramuscular injection using nanoparticles is an improved method of treatment administration.

3.4. Discussion

In this work, we have reported for the first time, the applications of nanoparticles for delivering a sense and anti-sense cDNA of the same gene for therapeutic angiogenesis to treat PAD. The present work showed the therapeutic effectiveness of EpoR NPs, RopE NPs, and EpoR/RopE NPs in inducing angiogenesis *in vitro* and its significant reduction in lower leg ischemia post 2 weeks of treatment in hindlimb mice, implying a novel noninvasive therapeutic approach in treating PAD. There are quite a few reports on the gene therapy towards angiogenesis; however, their performance has come short in clinical trials. We demonstrated that 1) PLGA NPs loaded with cDNA plasmids (EpoR, RopE, EpoR/RopE) are stable, hemo-

compatible, biocompatible, good transfection vehicles with biphasic sustained release properties. 2) The released EpoR and RopE plasmids from nanoparticles and their expressed proteins remain functional in endothelial cells where they were involved in facilitating cell proliferation, enhancing cell protection in stressed environment, stimulating EC migration, and facilitating EC tube formation. 3) EpoR NPs, RopE NPs, and EpoR/RopE NPs have proven to effectively stimulate angiogenesis in ischemic mice hindlimb.

Gene therapy via PEI and various cDNA plasmids is being investigated as a potential approach for therapeutic angiogenesis where by endogenous tissues are regenerate and blood flow reperfused. Despite its commonness, these nucleic acid molecules are often delivered naked (free solution) or using viral vectors; hence limiting their performance due to their inability to penetrate through the cell membrane, enzymatic degradation, immunogenicity concerns, and their low performance in reducing amputation rates in CLI patients.[300, 301] To overcome the challenges, we apply nanoparticles as carriers of EpoR, Rope and EpoR/Rope cDNA for delivery to treat PAD. EpoR is a hypoxia induce gene with paracrine/autocrine functions of protecting cells in depleted oxygen environment, facilitating angiogenesis, and preventing apoptosis amongst many;[302] therefore, a clinical therapeutic approach targeting the stimulation of pro-angiogenic proteins could be especially efficient in treating PAD. To preserve the bioactivity and nature of these cDNA, we initially load the cDNA unto PEI polymer via electrostatic bonding. PEI is a prominent organic cationic polymer, highly exploited for its *in-vitro* and *in vivo* transfection efficacy. As a non-viral vector, it is exploited for nucleic acids (pDNA, siRNA, mRNA) transfer into cells[303, 304] with efficiency and toxicity depended on polymer molecular weight.[233] In this study, we used branched, low molecular weight (1.2kDa) PEI with primary, secondary and tertiary amine groups, which serve as functionalizing regions to load more nucleic acid molecules. PEI's cationic nature permits its forming of spherical complexes with cDNA molecules via electrostatic bonding,

leading to more cDNA loading and membrane permeability. This creates a “proton sponge” effect by escaping lysosomal degradation and improve cDNA translocation to the nucleus.[234]

PLGA NPs have been developed and commonly used for gene therapy to treat PAD. The formed cDNA-PEI complex was eventually used in the double emulsion PLGA NP fabrication process. PLGA, a well-known, FDA approved, biodegradable polymer possesses good encapsulation and degradation properties.[203] Through hydrolysis, this polymer decomposes into metabolite monomers (lactic acid and glycolic acid) that are produced during cellular metabolism. PLGA NPs’ biocompatibility characteristics are demonstrated with more than 80% HUVECs viability even with concentrations as high as 2mg/mL. Furthermore, PLGA NPs have higher cDNA plasmid loading efficiency with the use of PEI with 77% (EpoR NP), 83% (RopE NP) and 81% (EpoR/RopE NP) encapsulation, average size ~200nm, this corresponds to previous loading[305] and diameter size of PLGA NPs.[306] The release rate of EpoR NPs (77%), RopE NPs (72%) and EpoR/RopE NPs (100 %) over 21 days supports the minimum time needed for stimulating angiogenesis.[307] Moreover, EpoR NPs, ROPE NPs and EpoR/RopE NPs have proven to be hemo-compatible with <1% RBC lysis when compared to that of control groups. Following transfection, EpoR/RopE NPs treated cells expressed 2.5 ng DNA, whereas EpoR NPs expressed 1.5 ng DNA and ROPE NPs showed around 0.5 ng DNA to that of control. This confirms that EpoR/RopE has synergistic properties despite being complementary strands to one another.

To achieve efficient angiogenesis, single or co-transfection of therapeutic genes have been examined. We have achieved significant higher levels of cell proliferation from EpoR NPs, RopE NPs, and EpoR/RopE NPs when incubated at normal oxygen levels. However, we saw even higher cell proliferation when transfected HUVECs are exposed to reduced oxygen levels. This is because EpoR, just like HIF is a hypoxia inducible gene[308] whose activation/expression modifies the biological cell and/or tissue behavior (e.g. proliferation)

in hypoxic conditions. Although VEGF is well known for its mitogenic potential, stimulate angiogenesis and inhibit apoptosis,[309, 310] low endogenous VEGF levels in injured vasculature can't accomplish the task of angiogenesis, leading to report of poor clinical outcomes with very little reduction in patients' amputation rate. Therefore, via nanoparticles, gene delivery via EpoR, and RopE has been sustained and shown encouraging results. Yang et al.[274] transfected EPCs with plasmid VEGF NPs and 40 times higher protein expression was observed when compared to that of control groups. Furthermore, due to splicing, the various isoforms of VEGF provide mitogenic effects on ECs.[311] EpoR a hematopoietic receptor protein, has been discovered to be endogenously expressed in endothelial cells.[261] Its expression leads to the secretion of Epo protein and the latter has been reported to have synergistic role with VEGF.[312] Even though there is no literature stating the biological function of RopE, as per the present study, we can confirm that EpoR NPs, RopE NPs and EpoR/RopE NPs facilitate endothelial cell proliferation.

We demonstrated that EpoR/RopE NPs, EpoR NPs, and RopE NPs lead to endothelial cell protection in the presence of H_2O_2 up to 3 days exposure. EpoR/RopE NPs, EpoR NPs and RopE NPs had >100% cell protection by day 1. By day 3, EpoR/RopE NPs and RopE NPs maintained a viability above 100% while cell viability in the group exposed to EpoR NPs decreased but remained > 80%. Free EpoR/RopE group-maintained cell viability up to ~ 40% compared to that (20%) of cells exposed to nothing (non-treatment). The EC protection of EpoR and Rope in the presence of ROS might be involved with the following mechanisms: the inactivation of pro-inflammatory cytokines (e.g TNF)[313] and inflammatory pathways (e.g. p38 MAPK).[314] Besides, small molecules such as nitric oxide donor and anti-oxidants also provide cell protection under stress conditions as reiterated by another study in our lab where PLGA-SA-2 NPs were used to produce NO, to provide cell protection, and to stimulate angiogenesis of HUVECs in an oxidatively stressed environment.[294] This NO signaling

pathway might also be involved in the cell protection effects of EpoR and RopE under stress conditions.

Although much on the complex nature of angiogenesis is yet to be fully revealed, cell migration remains an important component to the process. The EpoR/Epo pathway is involved in the mobilization of endogenous progenitor cells in angiogenesis.[315] It is well documented that there exists a lien between the EpoR/Epo pathway and VEGF expression.[242] As a hypoxia dependent growth factor, HIF has been reported for its wound healing and angiogenic potential.[316] In the current work, we observe the synergistic cell migration boost role of EpoR/RopE NPs in HUVECs as it demonstrated a performance outstanding compared to that of a positive control group (VEGF protein). RopE NP-transfected cells showed the second highest cell migrating distance while EpoR NP-transfected cells had the lowest migrating distance of all 3 groups. The boost in EC migration performance was significantly higher than groups of NT or empty vector NPs. Epo has been reported to have some stimulatory influence by increasing in VEGF expression and promote cell migration in diabetic injured mice.[243] Applying exogenous cDNA transcripts of EpoR and RopE via NPs, a healing boost is definite. Other methods have been exploited in plasmid delivery for cell migration. Electroporation of hCAP-18/LL-37 plasmid in hindlimb ischemic mice model resulted in an upregulation of VEGF.[317, 318]

When endothelial cells are exposed to hypoxia, upregulation of various angiogenic proteins is eminent causing an increase in the number of tubes formed.[319] With hypoxia being a stimulator of angiogenesis, neo-vessel formation in ECs is inevitable. This is because activation of regulatory growth factors such as VEGF results in the inhibition of pro-apoptotic signals within that cell and its surrounding tissues. 28 days post administration of VEGF plasmid NPs in mice, higher micro-vessel density was observed than groups of saline or naked VEGF plasmids.[320] In addition, VEGF is a dependent growth factor that requires the input of

other proteins or nucleic acids to achieve significant angiogenesis.[321] EpoR expression is said to influence endogenous VEGF levels.[322] Increase in tube formation by EpoR and Rope cDNA plasmids could be explained by the augmented bioavailability of EpoR and RopE to cells causing higher positive feedback mechanism in the EpoR pathway, which in turns results in more VEGF production observed in our study.[292] More recently, VEGF plasmid/apelin NPs resulted in higher and more compacted tube formation than that of VEGF plasmid alone,[277] while co-delivery of bFGF and VEGF nanogels to EPC-formed tubes whereas alone of without either one did not lead to any observed tube formation.[278] This confirms that despite being a major player in angiogenesis, VEGF and FGF levels are dependent on other factors. In our study, animals treated with EpoR/RopE NPs improved hindlimb ischemia, demonstrating a novel therapy for CLI. Similar to our results, FGF plasmid delivery via magnesium-PLGA NPs have also been reported for therapeutic angiogenesis;[255] 4 weeks sustained release of FGF led to blood flow reperfusion and post ischemic angiogenesis in rat hindlimb. Moreover, other nucleic acids such as RNA transcripts have been exploited in effecting angiogenesis in ischemic tissues.[323] Aside from plasmid cDNA, mRNA molecules have also been applied in gene therapy. miR-126-PLGA NPs was recently reported to increase capillary and arteriolar density whereas miR-126-PLGA NPs demonstrated significantly higher than that of sham and free miR-126.[324]

3.5. Limitation

In the present work, we did not observe consistent synergistic effects in the co-delivery of EpoR and RopE cDNA. Synergism of EpoR/Rope NPs was observed in the total DNA expression levels and cell migration studies. Even though there was no significant difference observed in cell proliferation, cell protection, and tube formation, of all 3 NP groups, EpoR/RopE NPs produced better outcomes when compared to that of EpoR NPs and RopE

NPs. Also, even though we used a low molecular weight PEI, in our cDNA plasmid-loaded PLGA NPs, we observe higher chances of toxicity following cell exposure. This is because PEI is not a biodegradable polymer, so it remains in the cell causing stress within that cell.[325] However, this can be modified by either ester conjugation or by addition of disulfide linkage such as dithiobis (succinimidylpropionate) or dimethyl-3, 3′-dithiobispropionimidate,[326] making them biodegradable.

3.6. Conclusion and future work

Thus far, a biodegradable nanoparticle for sense and antisense DNA of EpoR transcript delivery was synthesized for therapeutic angiogenesis. The nanoparticle demonstrated to have a biphasic release with a controlled rease of both DNA transcripts over time. When compared to single DNA delivery or free DNA, the combination DNA transcript showed higher efficacy, however, even though significance wasn't observed, we are hypothesizing that maybe in longer time points the synergistic effect of the combination DNA nanoparticles vs single DNA nanoparticles might be observed. All DNA groups have demonstrated to be involved in cell proliferation, protection and angiogenic tube formation. This gives us hope for further assessment of the therapeutic role of these transcripts in effecting therapeutic angiogenesis with minimum undesirable effects.

CHAPTER 4

CONCLUSION AND FUTURE DIRECTION

To summarize, we have discused how nanoparticles can be applied towards PAD. In the first chapter, we elaborated the different methods that nanoparticles could be applied for detection, treatment and theranostics of PAD. We progressed with the next chapters in assessing the therapeutic superiority of single versus combinations of recombinant protein ligand (Epo) and its receptor (EpoR) in stimulating angiogenesis. Lastly, we applied nanoparticles towards gene therapy in ischemic muscles using sense and anti-sense cDNA plasmids and assessed their interactions in inducing angiogenesis both *in vitro* and *in vivo*.

With nanoparticles for protein delivery and gene therapy, we formulated similar NP sizes across all groups, and from *in vitro* analysis, we confirmed that Epo NPs, EpoR NPs and EpoR/Epo NPs showed promising efficacy towards vascular reconstruction. *In vitro* analysis for therapeutic properties were similar across the board for all 3 NPs. Despite similar performance by Epo NPs, EpoR NPs, and EpoR/Epo NPs, we chose to further our research by applying gene therapy. We selected gene-gene therapy over gene-protein delivery because no synergisms was observed in the group of EpoR/Epo NPs.

In applying NPs for gene therapy, more proteins are expressed by cells, which would enhance the proangiogenic growth factors needed to restore vascular functions. When tested in small animal models, these plasmid loaded nanoparticles started restoring tissues as early as 5 days following NP administration. We also observed that these EpoR/RopE NPs could produce higher capillary density in ischemic tissues than the single EpoR NPs or RopE NPs. We can state that these combination plasmid cDNA NPs (EpoR/RopE NPs) can be used as an alternative non-invasive PAD treatment. The EpoR and RopE NPs sucessfully demonstrated

to enhance cell proliferation, sustain cell viability in oxidative stressed conditions, boost cellular migration and increase blood reperfusion in ischemic mice limbs. These results support our hypothesis that EpoR/RopE NPs will induce angiogenesis *in vitro* and *in vivo*.

With the above stated oustanding properties, this work still faces some limitations. First, the nanoparticle are designed solely to suit intramuscular injection. The lack of targeting for specificity by the nanoparticle makes it limited for other administration routes. However, this can be corrected by targeting using antibodies such as HIF-1α and EpoR to bind mainly to ischemic tissues through intravenous injection. Based on the encouraging results from this work, future studies will concentrate on the administration of the NPs in larger animal PAD models.

REFERENCES

1. P. Abdulhannan, D. A. Russell, S. Homer-Vanniasinkam, *British Medical Bulletin* **2012,** *104* 1.
2. F. G. Welt, C. Rogers, *Arteriosclerosis, thrombosis, and vascular biology* **2002,** *22* 11.
3. A. T. Hirsch, M. H. Criqui, D. Treat-Jacobson, J. G. Regensteiner, M. A. Creager, J. W. Olin, S. H. Krook, D. B. Hunninghake, A. J. Comerota, M. E. Walsh, M. M. McDermott, W. R. Hiatt, *JAMA: the journal of the American Medical Association* **2001,** *286* 11.
4. K. I. Paraskevas, D. Mukherjee, T. F. Whayne, Jr., *Angiology* **2013,** *64* 8.
5. C. Høyer, J. Sandermann, L. J. Petersen, *Journal of Vascular Surgery* **2013,** *58* 1.
6. A. Bajwa, R. Wesolowski, A. Patel, P. Saha, F. Ludwinski, A. Smith, E. Nagel, B. Modarai, *Circ Cardiovasc Imaging* **2014,** *7* 5.
7. S. K. Harris, M. G. Roos, G. J. Landry, *Journal of Vascular Surgery* **2016,** *64* 6.
8. D. H. Walter, H. Krankenberg, J. O. Balzer, C. Kalka, I. Baumgartner, M. Schluter, T. Tonn, F. Seeger, S. Dimmeler, E. Lindhoff-Last, A. M. Zeiher, P. Investigators, *Circulation: Cardiovascular interventions* **2011,** *4* 1.
9. E. Benoit, T. F. O'Donnell, Jr., M. D. Iafrati, E. Asher, D. F. Bandyk, J. W. Hallett, A. B. Lumsden, G. J. Pearl, S. P. Roddy, K. Vijayaraghavan, A. N. Patel, *Journal of translational medicine* **2011,** *9*.
10. D. W. Losordo, M. R. Kibbe, F. Mendelsohn, W. Marston, V. R. Driver, M. Sharafuddin, V. Teodorescu, B. N. Wiechmann, C. Thompson, L. Kraiss, T. Carman, S. Dohad, P. Huang, C. E. Junge, K. Story, T. Weistroffer, T. M. Thorne, M. Millay, J. P. Runyon, R. Schainfeld, C. D. C. T. f. C. L. I. I. Autologous, *Circulation: Cardiovascular interventions* **2012,** *5* 6.
11. P. V. Kathryn Vowden, *Huntleigh Healthcare Limited* **2004,** *109*.
12. E. F. Bernstein, A. Fronek, *Surg Clin North Am* **1982,** *62* 3.
13. R. Topakian, S. Nanz, B. Rohrbacher, R. Koppensteiner, F. T. Aichner, O. S. Group, *Cerebrovasc Dis* **2010,** *29* 3.
14. D. Ratanakorn, J. Keandoungchun, C. H. Tegeler, *J Stroke Cerebrovasc Dis* **2012,** *21* 6.
15. M. Shanmugasundaram, V. K. Ram, U. C. Luft, M. Szerlip, J. S. Alpert, *Clin Cardiol* **2011,** *34* 8.
16. D. W. Armstrong, C. Tobin, M. F. Matangi, *Can J Cardiol* **2010,** *26* 10.
17. J. R. Jago, A. Murray, *Clinical Physics and Physiological Measurement* **1988,** *9* 4.
18. H. Y. Wang, P. Han, W. H. Zhang, B. Liu, H. L. Li, H. J. Wang, R. P. Huang, *Angiology* **2012,** *63* 4.
19. J. Fan, H. Jouni, M. Khaleghi, K. R. Bailey, I. J. Kullo, *Angiology* **2012,** *63* 6.
20. N. Khandanpour, B. Jennings, M. P. Armon, A. Wright, G. Willis, A. Clark, F. J. Meyer, *Angiology* **2011,** *62* 2.
21. J. C. Deddens, J. M. Colijn, M. I. Oerlemans, G. Pasterkamp, S. A. Chamuleau, P. A. Doevendans, J. P. Sluijter, *J Cardiovasc Transl Res* **2013,** *6* 6.
22. C. J. White, W. A. Gray, *Circulation* **2007,** *116* 19.
23. D. Dumont, J. Dahl, E. Miller, J. Allen, B. Fahey, G. Trahey, *IEEE Trans Ultrason Ferroelectr Freq Control* **2009,** *56* 5.
24. H. Chen, T. Wu, W. S. Kerwin, C. Yuan, *Quant Imaging Med Surg* **2013,** *3* 6.
25. J. T. Lu, M. A. Creager, *Rev Cardiovasc Med* **2004,** *5* 4.
26. S. E. Gollust, S. A. Schroeder, K. E. Warner, *The Milbank Quarterly* **2008,** *86* 4.
27. N. M. Hamburg, G. J. Balady, *Circulation* **2011,** *123* 1.
28. K. Morisaki, T. Yamaoka, K. Iwasa, *Vascular* **2017**.

29. A. Markel, *Int Angiol* **2015,** *34* 5.
30. J. J. Belch, E. J. Topol, G. Agnelli, M. Bertrand, R. M. Califf, D. L. Clement, M. A. Creager, J. D. Easton, J. R. Gavin, 3rd, P. Greenland, G. Hankey, P. Hanrath, A. T. Hirsch, J. Meyer, S. C. Smith, F. Sullivan, M. A. Weber, N. Prevention of Atherothrombotic Disease, *Arch Intern Med* **2003,** *163* 8.
31. D. R. J. Singer, A. Kite, *European Journal of Vascular and Endovascular Surgery 35* 6.
32. D. A. Lane, G. Y. Lip, *Cochrane Database Syst Rev* **2013,** 12.
33. H. Lawall, P. Bramlage, B. Amann, *Journal of Vascular Surgery* **2011,** *53* 2.
34. E. Tateishi-Yuyama, H. Matsubara, T. Murohara, U. Ikeda, S. Shintani, H. Masaki, K. Amano, Y. Kishimoto, K. Yoshimoto, H. Akashi, K. Shimada, T. Iwasaka, T. Imaizumi, I. Therapeutic Angiogenesis using Cell Transplantation Study, *Lancet* **2002,** *360* 9331.
35. C. J. Zhu, J. X. Dong, J. Li, M. J. Zhang, L. P. Wang, L. Luo, *J Tradit Chin Med* **2011,** *31* 3.
36. S. Guiducci, F. Porta, R. Saccardi, S. Guidi, L. Ibba-Manneschi, M. Manetti, B. Mazzanti, S. Dal Pozzo, A. F. Milia, S. Bellando-Randone, I. Miniati, G. Fiori, R. Fontana, L. Amanzi, F. Braschi, A. Bosi, M. Matucci-Cerinic, *Ann Intern Med* **2010,** *153* 10.
37. M. F. Pittenger, A. M. Mackay, S. C. Beck, R. K. Jaiswal, R. Douglas, J. D. Mosca, M. A. Moorman, D. W. Simonetti, S. Craig, D. R. Marshak, *Science* **1999,** *284* 5411.
38. A. W. Gardner, *Vasa* **2015,** *44* 6.
39. M. M. Payne, *Tex Heart Inst J* **2001,** *28* 1.
40. S. B. King, 3rd, B. Meier, *Circulation* **2000,** *102* 20 Suppl 4.
41. N. W. e. a. Shammas, *Cardiovasc Revasc Med.* **2012,** *13*.
42. B. O'Brien, W. Carroll, *Acta Biomater* **2009,** *5* 4.
43. C. H. Chang, J. W. Lin, J. Hsu, L. C. Wu, M. S. Lai, *Sci Rep* **2016,** *6*.
44. A. Gruntzig, H. J. Schneider, *Schweizerische Medizinische Wochenschrift* **1977,** *107* 44.
45. S. Adlakha, M. Sheikh, J. Wu, M. W. Burket, U. Pandya, W. Colyer, E. Eltahawy, C. J. Cooper, *J Interv Cardiol* **2010,** *23* 4.
46. J. A. Beckman, *Circulation* **2007,** *115* 5.
47. K. Dys, J. Drelichowska-Durawa, B. Dolega-Kozierowski, M. Lis, K. Sokratous, W. Iwanowski, S. Drelichowski, W. Witkiewicz, *Pol J Radiol* **2013,** *78* 3.
48. S. A. Brenner, M. Pautler, *Journal of Nanotechnology in Engineering and Medicine* **2010,** *1* 4.
49. T. F. Massoud, S. S. Gambhir, *Genes & Development* **2003,** *17* 5.
50. B. R. Smith, S. S. Gambhir, *Chem Rev* **2017,** *117* 3.
51. J. R. McCarthy, *Current cardiovascular imaging reports* **2010,** *3* 1.
52. W. Cai, X. Chen, *Small* **2007,** *3* 11.
53. D. P. Cormode, T. Skajaa, Z. A. Fayad, W. J. Mulder, *Arteriosclerosis, thrombosis, and vascular biology* **2009,** *29* 7.
54. J. P. Cooke, A. M. Wilson, *Journal of the American College of Cardiology* **2010,** *55* 19.
55. C. Yuan, W. S. Kerwin, M. S. Ferguson, N. Polissar, S. Zhang, J. Cai, T. S. Hatsukami, *Journal of magnetic resonance imaging* **2002,** *15* 1.
56. M. A. Horton, *International journal of biochemistry & cell biology* **1997,** *29* 5.
57. D. A. Sipkins, D. A. Cheresh, M. R. Kazemi, L. M. Nevin, M. D. Bednarski, K. C. Li, *Nature Medicine* **1998,** *4* 5.

58. P. M. Winter, A. M. Neubauer, S. D. Caruthers, T. D. Harris, J. D. Robertson, T. A. Williams, A. H. Schmieder, G. Hu, J. S. Allen, E. K. Lacy, H. Zhang, S. A. Wickline, G. M. Lanza, *Arteriosclerosis, thrombosis, and vascular biology* **2006,** *26* 9.
59. N. MacRitchie, G. Grassia, J. Noonan, P. Garside, D. Graham, P. Maffia, *Heart* **2017**.
60. A. M. Morawski, P. M. Winter, K. C. Crowder, S. D. Caruthers, R. W. Fuhrhop, M. J. Scott, J. D. Robertson, D. R. Abendschein, G. M. Lanza, S. A. Wickline, *Magnetic resonance in medicine* **2004,** *51* 3.
61. T. H. Shin, Y. Choi, S. Kim, J. Cheon, *Chem Soc Rev* **2015,** *44* 14.
62. S. Tong, E. J. Fine, Y. Lin, T. J. Cradick, G. Bao, *Annals of Biomedical Engineering* **2014,** *42* 2.
63. M. J. Lipinski, J. C. Frias, V. Amirbekian, K. C. Briley-Saebo, V. Mani, D. Samber, A. Abbate, J. G. Aguinaldo, D. Massey, V. Fuster, G. W. Vetrovec, Z. A. Fayad, *JACC: Cardiovascular Imaging* **2009,** *2* 5.
64. V. Amirbekian, M. J. Lipinski, K. C. Briley-Saebo, S. Amirbekian, J. G. Aguinaldo, D. B. Weinreb, E. Vucic, J. C. Frias, F. Hyafil, V. Mani, E. A. Fisher, Z. A. Fayad, *Proceedings of the National Academy of Sciences of the United States of America* **2007,** *104* 3.
65. S. H. Lee, B. H. Kim, H. B. Na, T. Hyeon, *Wiley Interdiscip Rev Nanomed Nanobiotechnol* **2014,** *6* 2.
66. A. Elias, A. Tsourkas, *Hematology Am Soc Hematol Educ Program* **2009**.
67. X. X. Li, K. A. Li, J. B. Qin, K. C. Ye, X. R. Yang, W. M. Li, Q. S. Xie, M. E. Jiang, G. X. Zhang, X. W. Lu, *Int J Nanomedicine* **2013,** *8*.
68. K. Morishige, D. F. Kacher, P. Libby, L. Josephson, P. Ganz, R. Weissleder, M. Aikawa, *Circulation* **2010,** *122* 17.
69. K. Briley-Saebo, C. Yeang, J. L. Witztum, S. Tsimikas, *J Cardiovasc Transl Res* **2014,** *7* 8.
70. K. C. Briley-Saebo, Y. S. Cho, P. X. Shaw, S. K. Ryu, V. Mani, S. Dickson, E. Izadmehr, S. Green, Z. A. Fayad, S. Tsimikas, *Journal of the American College of Cardiology* **2011,** *57* 3.
71. Y. Zheng, J. Qin, X. Wang, Z. Peng, P. Hou, X. Lu, *Int J Nanomedicine* **2017,** *12*.
72. X. Feng, Q. Xia, L. Yuan, X. Yang, K. Wang, *Neurotoxicology* **2010,** *31* 4.
73. D. J. Todd, J. Kay, *Curr Rheumatol Rep* **2008,** *10* 3.
74. C. Amene, L. A. Yeh-Nayre, C. E. Dory, J. R. Crawford, *Case Rep Neurol* **2012,** *4* 1.
75. J. Xiao, X. M. Tian, C. Yang, P. Liu, N. Q. Luo, Y. Liang, H. B. Li, D. H. Chen, C. X. Wang, L. Li, G. W. Yang, *Sci Rep* **2013,** *3*.
76. D. Stanicki, L. V. Elst, R. N. Muller, S. Laurent, *Current Opinion in Chemical Engineering* **2015,** *8*.
77. X. Chen, Y. Liu, D. Tu, *Springer Science & Business Media: Berlin, Germany* **2013,** *4*.
78. S. Schrepfer, T. Deuse, H. Reichenspurner, M. P. Fischbein, R. C. Robbins, M. P. Pelletier, *Transplantation Proceedings* **2007,** *39* 2.
79. C. Tu, X. Ma, A. House, S. M. Kauzlarich, A. Y. Louie, *ACS Med Chem Lett* **2011,** *2* 4.
80. S. J. Son, X. Bai, S. B. Lee, *Drug Discovery Today* **2007,** *12* 15-16.
81. R. Ankri, D. Leshem-Lev, D. Fixler, R. Popovtzer, M. Motiei, R. Kornowski, E. Hochhauser, E. I. Lev, *Nano Lett* **2014,** *14* 5.
82. R. Ankri, S. Melzer, A. Tarnok, D. Fixler, *Int J Nanomedicine* **2015,** *10*.
83. D. P. Cormode, E. Roessl, A. Thran, T. Skajaa, R. E. Gordon, J. P. Schlomka, V. Fuster, E. A. Fisher, W. J. Mulder, R. Proksa, Z. A. Fayad, *Radiology* **2010,** *256* 3.

84. M. J. Jacobin-Valat, J. Laroche-Traineau, M. Lariviere, S. Mornet, S. Sanchez, M. Biran, C. Lebaron, J. Boudon, S. Lacomme, M. Cerutti, G. Clofent-Sanchez, *Nanomedicine* **2015,** *11* 4.
85. D. P. Cormode, P. C. Naha, Z. A. Fayad, *Contrast Media Mol Imaging* **2014,** *9* 1.
86. R. Grombe, L. Kirsten, M. Mehner, T. P. Linsinger, H. Emons, E. Koch, *Food Chem* **2014,** *153*.
87. J. M. Schmitt, G. Kumar, *Appl Opt* **1998,** *37* 13.
88. C. Zou, B. Wu, Y. Dong, Z. Song, Y. Zhao, X. Ni, Y. Yang, Z. Liu, *Int J Nanomedicine* **2017,** *12*.
89. M. Habara, M. Terashima, T. Suzuki, *Journal of Invasive Cardiology* **2009,** *21* 10.
90. M. F. Brancati, F. Burzotta, C. Trani, O. Leonzi, C. Cuccia, F. Crea, *Pragmatic and Observational Research* **2017,** *8*.
91. I. Ben-Dor, M. Mahmoudi, A. D. Pichard, L. F. Satler, R. Waksman, *Journal of interventional cardiology* **2011,** *24* 2.
92. Y. Ozaki, M. Okumura, T. F. Ismail, H. Naruse, K. Hattori, S. Kan, M. Ishikawa, T. Kawai, Y. Takagi, J. Ishii, F. Prati, P. W. Serruys, *European Heart Journal* **2010,** *31* 12.
93. A. de la Zerda, S. Prabhulkar, V. L. Perez, M. Ruggeri, A. S. Paranjape, F. Habte, S. S. Gambhir, R. M. Awdeh, *Clinical and Experimental Ophthalmology* **2015,** *43* 4.
94. J. Yguerabide, E. E. Yguerabide, *J Cell Biochem Suppl* **2001,** *Suppl 37*.
95. M. C. Skala, M. J. Crow, A. Wax, J. A. Izatt, *Nano Lett* **2008,** *8* 10.
96. A. M. Gobin, M. H. Lee, N. J. Halas, W. D. James, R. A. Drezek, J. L. West, *Nano Lett* **2007,** *7* 7.
97. T. Kume, H. Okura, T. Kawamoto, T. Akasaka, E. Toyota, N. Watanabe, Y. Neishi, Y. Sadahira, K. Yoshida, *Circulation* **2008,** *118* 4.
98. J. Kim, P. Herrero, T. Sharp, R. Laforest, D. J. Rowland, Y. C. Tai, J. S. Lewis, M. J. Welch, *J Nucl Med* **2006,** *47* 2.
99. L. W. Dobrucki, A. J. Sinusas, *Nature Reviews: Cardiology* **2010,** *7* 1.
100. H. P. Luehmann, E. D. Pressly, L. Detering, C. Wang, R. Pierce, P. K. Woodard, R. J. Gropler, C. J. Hawker, Y. Liu, *Journal of nuclear medicine* **2014,** *55* 4.
101. Y. J. Liu, E. D. Pressly, D. R. Abendschein, C. J. Hawker, G. E. Woodard, P. K. Woodard, M. J. Welch, *Journal of Nuclear Medicine* **2011,** *52* 12.
102. H. Orbay, Y. Zhang, H. Hong, T. A. Hacker, H. F. Valdovinos, J. A. Zagzebski, C. P. Theuer, T. E. Barnhart, W. Cai, *Mol Pharm* **2013,** *10* 7.
103. H. P. Luehmann, L. Detering, B. P. Fors, E. D. Pressly, P. K. Woodard, G. J. Randolph, R. J. Gropler, C. Hawker, Y. Liu, *Journal of nuclear medicine* **2016,** *57* 7.
104. S. J. Lee, J. C. Paeng, *Korean J Radiol* **2015,** *16* 5.
105. G. Hendrikx, S. Voo, M. Bauwens, M. J. Post, F. M. Mottaghy, *Eur J Nucl Med Mol Imaging* **2016,** *43* 13.
106. B. L. van der Hoeven, M. J. Schalij, V. Delgado, *Nature Reviews: Cardiology* **2012,** *9* 6.
107. A. J. Sinusas, *Quarterly journal of nuclear medicine and molecular imaging* **2010,** *54* 2.
108. C. Wu, F. Li, G. Niu, X. Chen, *Theranostics* **2013,** *3* 7.
109. C. G. England, H. J. Im, L. Z. Feng, F. Chen, S. A. Graves, R. Hernandez, H. Orbay, C. Xu, S. Y. Cho, R. J. Nickles, Z. Liu, D. S. Lee, W. B. Cai, *Biomaterials* **2016,** *100*.
110. H. J. Im, C. G. England, L. Z. Feng, S. A. Graves, R. Hernandez, R. J. Nickles, Z. Liu, D. S. Lee, S. Y. Cho, W. B. Cai, *Acs Applied Materials & Interfaces* **2016,** *8* 28.
111. M. Nahrendorf, H. Zhang, S. Hembrador, P. Panizzi, D. E. Sosnovik, E. Aikawa, P. Libby, F. K. Swirski, R. Weissleder, *Circulation* **2008,** *117* 3.

112. S. Goel, F. Chen, E. B. Ehlerding, W. Cai, *Small* **2014,** *10* 19.
113. A. M. Smith, X. Gao, S. Nie, *Photochemistry and Photobiology* **2004,** *80* 3.
114. V. Brunetti, H. Chibli, R. Fiammengo, A. Galeone, M. A. Malvindi, G. Vecchio, R. Cingolani, J. L. Nadeau, P. P. Pompa, *Nanoscale* **2013,** *5* 1.
115. E. C. Ximendes, U. Rocha, B. del Rosal, A. Vaquero, F. Sanz-Rodriguez, L. Monge, F. Q. Ren, F. Vetrone, D. L. Ma, J. Garcia-Sole, C. Jacinto, D. Jaque, N. Fernandez, *Advanced Healthcare Materials* **2017,** *6* 4.
116. A. M. Smith, H. Duan, M. N. Rhyner, G. Ruan, S. Nie, *Physical Chemistry Chemical Physics* **2006,** *8* 33.
117. Y. Xing, Q. Chaudry, C. Shen, K. Y. Kong, H. E. Zhau, L. W. Chung, J. A. Petros, R. M. O'Regan, M. V. Yezhelyev, J. W. Simons, M. D. Wang, S. Nie, *Nature Protocols* **2007,** *2* 5.
118. H. N. Yang, J. S. Park, D. G. Woo, S. Y. Jeon, K. H. Park, *Biomaterials* **2012,** *33* 33.
119. F. Q. Chen, D. Gerion, *Nano Letters* **2004,** *4* 10.
120. K. Douma, R. T. Megens, M. A. van Zandvoort, *Wiley Interdisciplinary Reviews. Nanomedicine and Nanobiotechnology* **2011,** *3* 4.
121. N. Dan, *Langmuir* **2014,** *30* 46.
122. Y. Zhang, Q. Li, W. J. Welsh, P. V. Moghe, K. E. Uhrich, *Biomaterials* **2016,** *84*.
123. A. Faig, L. K. Petersen, P. V. Moghe, K. E. Uhrich, *Biomacromolecules* **2014,** *15* 9.
124. D. S. Abdelhamid, Y. Zhang, D. R. Lewis, P. V. Moghe, W. J. Welsh, K. E. Uhrich, *Biomaterials* **2015,** *53*.
125. D. Peters, M. Kastantin, V. R. Kotamraju, P. P. Karmali, K. Gujraty, M. Tirrell, E. Ruoslahti, *Proceedings of the National Academy of Sciences of the United States of America* **2009,** *106* 24.
126. E. J. Chung, L. B. Mlinar, K. Nord, M. J. Sugimoto, E. Wonder, F. J. Alenghat, Y. Fang, M. Tirrell, *Adv Healthc Mater* **2015,** *4* 3.
127. J. D. Ransohoff, J. C. Wu, *Current Vascular Pharmacology* **2012,** *10* 3.
128. A. S. Gupta, *Nanomedicine* **2011,** *7* 6.
129. M. P. Turunen, M. O. Hiltunen, M. Ruponen, L. Virkamaki, F. C. Szoka, Jr., A. Urtti, S. Yla-Herttuala, *Gene Ther* **1999,** *6* 1.
130. R. Srinivasan, R. E. Marchant, A. S. Gupta, *J Biomed Mater Res A* **2010,** *93* 3.
131. G. F. Huang, Z. M. Zhou, R. Srinivasan, M. S. Penn, K. Kottke-Marchant, R. E. Marchant, A. S. Gupta, *Biomaterials* **2008,** *29* 11.
132. C. L. Modery, M. Ravikumar, T. L. Wong, M. J. Dzuricky, N. Durongkaveroj, A. Sen Gupta, *Biomaterials* **2011,** *32* 35.
133. H. Hwang, H. S. Kim, H. S. Jeong, B. T. Rajasaheb, M. Kim, P. S. Oh, S. T. Lim, M. H. Sohn, H. J. Jeong, *Drug Delivery* **2016,** *23* 9.
134. V. Gorenoi, M. U. Brehm, A. Koch, A. Hagen, *Cochrane Database Syst Rev* **2017,** *6*.
135. S. He, T. C. Zhao, H. Guo, Y. Z. Meng, G. J. Qin, D. A. Goukassian, J. H. Han, X. M. Gao, Y. Zhu, *Plos One* **2016,** *11* 12.
136. J. S. Golub, Y. T. Kim, C. L. Duvall, R. V. Bellamkonda, D. Gupta, A. S. Lin, D. Weiss, W. R. Taylor, R. E. Guldberg, *American Journal of Physiology-Heart and Circulatory Physiology* **2010,** *298* 6.
137. H. Jiang, T. Zhang, X. Sun, *J Surg Res* **2005,** *126* 1.
138. K. Albrecht-Schgoer, J. Barthelmes, W. Schgoer, M. Theurl, I. Nardin, D. Lener, C. Gutmann, S. Dunnhaupt, A. Bernkop-Schnurch, R. Kirchmair, *Journal of controlled release* **2017,** *250*.
139. S. Das, G. Singh, A. B. Baker, *Biomaterials* **2014,** *35* 1.
140. P. Baluk, C. G. Lee, H. Link, E. Ator, A. Haskell, J. A. Elias, D. M. McDonald, *American Journal of Pathology* **2004,** *165* 4.

141. E. Chung, L. M. Ricles, R. S. Stowers, S. Y. Nam, S. Y. Emelianov, L. J. Suggs, *Nano Today* **2012,** *7* 6.
142. H. K. Makadia, S. J. Siegel, *Polymers* **2011,** *3* 3.
143. B. D. Klugherz, N. Meneveau, W. Chen, F. Wade-Whittaker, G. Papandreou, R. Levy, R. L. Wilensky, *Journal of cardiovascular pharmacology and therapeutics* **1999,** *4* 3.
144. L. S. Lian, F. Tang, J. Yang, C. W. Liu, Y. J. Li, *Journal of Nanomaterials* **2012**.
145. R. Nagahama, T. Matoba, K. Nakano, S. Kim-Mitsuyama, K. Sunagawa, K. Egashira, *Arteriosclerosis, Thrombosis, and Vascular Biology* **2012,** *32* 10.
146. I. Osman, L. Segar, *Biochemical Pharmacology* **2016,** *101*.
147. B. Kwon, C. Kang, J. Kim, D. Yoo, B. R. Cho, P. M. Kang, D. Lee, *International Journal of Pharmaceutics* **2016,** *511* 2.
148. F. Felice, Y. Zambito, E. Belardinelli, C. D'Onofrio, A. Fabiano, A. Balbarini, R. Di Stefano, *Eur J Pharm Sci* **2013,** *50* 3-4.
149. B. R. Cho, D. R. Ryu, K. S. Lee, D. K. Lee, S. Bae, D. G. Kang, Q. G. Ke, S. S. Singh, K. S. Ha, Y. G. Kwon, D. Lee, P. M. Kang, Y. M. Kim, *Biomaterials* **2015,** *53*.
150. T. A. Johnson, N. A. Stasko, J. L. Matthews, W. E. Cascio, E. L. Holmuhamedov, C. B. Johnson, M. H. Schoenfisch, *Nitric Oxide-Biology and Chemistry* **2010,** *22* 1.
151. A. Jeremias, A. Kirtane, *Annals of internal medicine* **2008,** *148* 3.
152. M. Chorny, I. Fishbein, B. B. Yellen, I. S. Alferiev, M. Bakay, S. Ganta, R. Adamo, M. Amiji, G. Friedman, R. J. Levy, *Proceedings of the National Academy of Sciences of the United States of America* **2010,** *107* 18.
153. B. Johnson, B. Toland, R. Chokshi, V. Mochalin, S. Koutzaki, B. Polyak, *Curr Drug Deliv* **2010,** *7* 4.
154. H. D. Danenberg, G. Golomb, A. Groothuis, J. Gao, H. Epstein, R. V. Swaminathan, P. Seifert, E. R. Edelman, *Circulation* **2003,** *108* 22.
155. F. D. Kolodgie, M. John, C. Khurana, A. Farb, P. S. Wilson, E. Acampado, N. Desai, P. Soon-Shiong, R. Virmani, *Circulation* **2002,** *106* 10.
156. N. Tsukie, K. Nakano, T. Matoba, S. Masuda, E. Iwata, M. Miyagawa, G. Zhao, W. Meng, J. Kishimoto, K. Sunagawa, K. Egashira, *Journal of atherosclerosis and thrombosis* **2013,** *20* 1.
157. M. Joner, K. Morimoto, H. Kasukawa, K. Steigerwald, S. Merl, G. Nakazawa, M. C. John, A. V. Finn, E. Acampado, F. D. Kolodgie, H. K. Gold, R. Virmani, *Arterioscler Thromb Vasc Biol* **2008,** *28* 11.
158. T. Liu, Z. Zeng, Y. Liu, J. Wang, M. F. Maitz, Y. Wang, S. Liu, J. Chen, N. Huang, *ACS Appl Mater Interfaces* **2014,** *6* 11.
159. P. A. Lemos, V. Farooq, C. K. Takimura, P. S. Gutierrez, R. Virmani, F. Kolodgie, U. Christians, A. Kharlamov, M. Doshi, P. Sojitra, H. M. van Beusekom, P. W. Serruys, *EuroIntervention* **2013,** *9* 1.
160. P. Zilla, D. Bezuidenhout, P. Human, *Biomaterials* **2007,** *28* 34.
161. B. C. Evans, K. M. Hocking, M. J. Osgood, I. Voskresensky, J. Dmowska, K. V. Kilchrist, C. M. Brophy, C. L. Duvall, *Sci Transl Med* **2015,** *7* 291.
162. D. Fayol, C. Le Visage, J. Ino, F. Gazeau, D. Letourneur, C. Wilhelm, *Cell Transplantation* **2013,** *22* 11.
163. I. M. Kennedy, D. Wilson, A. I. Barakat, H. E. I. H. R. Committee, *Res Rep Health Eff Inst* **2009,** 136.
164. A. A. Shvedova, A. Pietroiusti, B. Fadeel, V. E. Kagan, *Toxicology and Applied Pharmacology* **2012,** *261* 2.
165. M. Ishii, R. Shibata, Y. Numaguchi, T. Kito, H. Suzuki, K. Shimizu, A. Ito, H. Honda, T. Murohara, *Arteriosclerosis, Thrombosis, and Vascular Biology* **2011,** *31* 10.

166. T. Kito, R. Shibata, M. Ishii, H. Suzuki, T. Himeno, Y. Kataoka, Y. Yamamura, T. Yamamoto, N. Nishio, S. Ito, Y. Numaguchi, T. Tanigawa, J. K. Yamashita, N. Ouchi, H. Honda, K. Isobe, T. Murohara, *Sci Rep* **2013,** *3*.
167. M. Kim, D. L. Kim, E. K. Kim, C. W. Kim, *Cell Transplantation* **2017,** *26* 2.
168. S. Uchida, K. Itaka, T. Nomoto, T. Endo, Y. Matsumoto, T. Ishii, K. Kataoka, *Biomaterials* **2014,** *35* 8.
169. S. Kishimoto, K. Inoue, S. Nakamura, H. Hattori, M. Ishihara, M. Sakuma, S. Toyoda, H. Iwaguro, I. Taguchi, T. Inoue, K. Yoshida, *Atherosclerosis* **2016,** *249*.
170. J. H. Lee, Y. S. Han, S. H. Lee, *Biomol Ther (Seoul)* **2016,** *24* 3.
171. B. M. Mattix, T. R. Olsen, M. Casco, L. Reese, J. T. Poole, J. Zhang, R. P. Visconti, A. Simionescu, D. T. Simionescu, F. Alexis, *Biomaterials* **2014,** *35* 3.
172. G. Mehta, A. Y. Hsiao, M. Ingram, G. D. Luker, S. Takayama, *Journal of Controlled Release* **2012,** *164* 2.
173. J. Feng, K. Mineda, S. H. Wu, T. Mashiko, K. Doi, S. Kuno, K. Kinoshita, K. Kanayama, R. Asahi, A. Sunaga, K. Yoshimura, *Sci Rep* **2017,** *7* 1.
174. D. Surder, M. Radrizzani, L. Turchetto, V. Lo Cicero, S. Soncin, S. Muzzarelli, A. Auricchio, T. Moccetti, *Clinical Cardiology* **2013,** *36* 8.
175. Y. Mima, S. Fukumoto, H. Koyama, M. Okada, S. Tanaka, T. Shoji, M. Emoto, T. Furuzono, Y. Nishizawa, M. Inaba, *PLoS One* **2012,** *7* 4.
176. S. Vosen, S. Rieck, A. Heidsieck, O. Mykhaylyk, K. Zimmermann, W. Bloch, D. Eberbeck, C. Plank, B. Gleich, A. Pfeifer, B. K. Fleischmann, D. Wenzel, *Acs Nano* **2016,** *10* 1.
177. D. Deshpande, S. Kethireddy, D. R. Janero, M. M. Amiji, *PLoS One* **2016,** *11* 2.
178. J. Lee, I. Jun, H. J. Park, T. J. Kang, H. Shin, S. W. Cho, *Biomacromolecules* **2014,** *15* 1.
179. C. A. Herberts, M. S. Kwa, H. P. Hermsen, *Journal of translational medicine* **2011,** *9*.
180. J. Tang, M. E. Lobatto, J. C. Read, A. J. Mieszawska, Z. A. Fayad, W. J. Mulder, *Current Cardiovascular Imaging Reports* **2012,** *5* 1.
181. G. M. Lanza, X. Yu, P. M. Winter, D. R. Abendschein, K. K. Karukstis, M. J. Scott, L. K. Chinen, R. W. Fuhrhop, D. E. Scherrer, S. A. Wickline, *Circulation* **2002,** *106* 22.
182. P. M. Winter, S. D. Caruthers, H. Zhang, T. A. Williams, S. A. Wickline, G. M. Lanza, *JACC Cardiovasc Imaging* **2008,** *1* 5.
183. J. Kim, L. Cao, D. Shvartsman, E. A. Silva, D. J. Mooney, *Nano Lett* **2011,** *11* 2.
184. L. Deveza, J. Choi, J. Lee, N. Huang, J. Cooke, F. Yang, *Theranostics* **2016,** *6* 8.
185. Y. Heun, S. Hildebrand, A. Heidsieck, B. Gleich, M. Anton, J. Pircher, A. Ribeiro, O. Mykhaylyk, D. Eberbeck, D. Wenzel, A. Pfeifer, M. Woernle, F. Krotz, U. Pohl, H. Mannell, *Theranostics* **2017,** *7* 2.
186. M. E. Lobatto, Z. A. Fayad, S. Silvera, E. Vucic, C. Calcagno, V. Mani, S. D. Dickson, K. Nicolay, M. Banciu, R. M. Schiffelers, J. M. Metselaar, L. van Bloois, H. S. Wu, J. T. Fallon, J. H. Rudd, V. Fuster, E. A. Fisher, G. Storm, W. J. Mulder, *Mol Pharm* **2010,** *7* 6.
187. A. Fernandez-Fernandez, R. Manchanda, A. J. McGoron, *Appl Biochem Biotechnol* **2011,** *165* 7-8.
188. S. M. Janib, A. S. Moses, J. A. MacKay, *Adv Drug Deliv Rev* **2010,** *62* 11.
189. J. Xie, S. Lee, X. Chen, *Adv Drug Deliv Rev* **2010,** *62* 11.
190. T. Tanaka, L. S. Mangala, P. E. Vivas-Mejia, R. Nieves-Alicea, A. P. Mann, E. Mora, H.-D. Han, M. M. K. Shahzad, X. Liu, R. Bhavane, J. Gu, J. R. Fakhoury, C. Chiappini, C. Lu, K. Matsuo, B. Godin, R. L. Stone, A. M. Nick, G. Lopez-Berestein, A. K. Sood, M. Ferrari, *Cancer Research* **2010,** *70* 9.

191. B. Kwon, C. Kang, J. Kim, D. Yoo, B. R. Cho, P. M. Kang, D. Lee, *International journal of pharmaceutics* **2016,** *511* 2.
192. E. A. Osborn, F. A. Jaffer, *Curr Atheroscler Rep* **2013,** *15* 10.
193. H. Leong-Poi, *Cardiovasc Res* **2009,** *84* 2.
194. M. H. Criqui, M. J. Alberts, F. G. Fowkes, A. T. Hirsch, P. T. O'Gara, J. W. Olin, G. American Heart Association Writing, *Circulation* **2008,** *118* 25.
195. H. Aronow, *Am J Cardiovasc Drugs* **2008,** *8* 6.
196. E. Minar, *Hamostaseologie* **2009,** *29* 1.
197. S. S. Said, J. G. Pickering, K. Mequanint, *J Vasc Res* **2013,** *50* 1.
198. M. Sugano, K. Tsuchida, N. Makino, *Circulation* **2004,** *109* 6.
199. M. Lee, M. Aoki, T. Kondo, K. Kobayashi, K. Okumura, K. Komori, T. Murohara, *Arterioscler Thromb Vasc Biol* **2005,** *25* 12.
200. T. Kofidis, D. Nolte, A. R. Simon, A. Metzakis, L. Balsam, R. Robbins, A. Haverich, *Angiogenesis* **2002,** *5* 1-2.
201. S. Takeshita, L. P. Zheng, E. Brogi, M. Kearney, L. Q. Pu, S. Bunting, N. Ferrara, J. F. Symes, J. M. Isner, *J Clin Invest* **1994,** *93* 2.
202. M. Zhang, L. S. Qiu, Y. Y. Zhang, D. S. Xu, J. L. C. Zheng, L. Jiang, *Scientific Reports* **2017,** *7*.
203. F. Danhier, E. Ansorena, J. M. Silva, R. Coco, A. Le Breton, V. Preat, *J Control Release* **2012,** *161* 2.
204. J. C. Vogel, *Hum Gene Ther* **2000,** *11* 16.
205. E. Gammella, C. Leuenberger, M. Gassmann, L. Ostergaard, *Am J Physiol Lung Cell Mol Physiol* **2013,** *304* 4.
206. Y. Li, G. Takemura, H. Okada, S. Miyata, R. Maruyama, L. Li, M. Higuchi, S. Minatoguchi, T. Fujiwara, H. Fujiwara, *Cardiovasc Res* **2006,** *71* 4.
207. L. Wang, Z. Zhang, Y. Wang, R. Zhang, M. Chopp, *Stroke* **2004,** *35* 7.
208. G. Lindgren, L. Ekblad, J. Vallon-Christersson, E. Kjellen, M. Gebre-Medhin, J. Wennerberg, *BMC Cancer* **2014,** *14*.
209. B. B. Beleslin-Cokic, V. P. Cokic, X. Yu, B. B. Weksler, A. N. Schechter, C. T. Noguchi, *Blood* **2004,** *104* 7.
210. M. L. Trincavelli, E. Da Pozzo, O. Ciampi, S. Cuboni, S. Daniele, M. P. Abbracchio, C. Martini, *Int J Mol Sci* **2013,** *14* 2.
211. P. Kimakova, P. Solar, Z. Solarova, R. Komel, N. Debeljak, *Int J Mol Sci* **2017,** *18* 7.
212. M. C. Hu, M. J. Shi, H. J. Cho, J. N. Zhang, A. Pavlenco, S. Z. Liu, S. Sidhu, L. J. S. Huang, O. W. Moe, *Kidney International* **2013,** *84* 3.
213. P. Ravikumar, J. U. Menon, P. Punnakitikashem, D. Gyawali, O. Togao, M. Takahashi, J. Zhang, J. Ye, O. W. Moe, K. T. Nguyen, C. C. W. Hsia, *Nanomedicine* **2016,** *12* 3.
214. J. U. Menon, P. Ravikumar, A. Pise, D. Gyawali, C. C. W. Hsia, K. T. Nguyen, *Acta Biomaterialia* **2014,** *10* 6.
215. J. U. Menon, V. Tumati, J. T. Hsieh, K. T. Nguyen, D. Saha, *Journal of Biomedical Materials Research Part A* **2015,** *103* 5.
216. N. Pandey, A. Hakamivala, C. C. Xu, P. Hariharan, B. Radionov, Z. Huang, J. Liao, L. P. Tang, P. Zimmern, K. T. Nguyen, Y. Hong, *Advanced Healthcare Materials* **2018,** *7* 7.
217. S. Kona, J. F. Dong, Y. L. Liu, J. F. Tan, K. T. Nguyen, *International Journal of Pharmaceutics* **2012,** *423* 2.
218. G. F. Liang, Y. L. Zhu, B. Sun, F. H. Hu, T. Tian, S. C. Li, Z. D. Xiao, *Nanoscale Research Letters* **2011,** *6*.
219. Y. Choi, J. E. Lee, J. H. Lee, J. H. Jeong, J. Kim, *Langmuir* **2015,** *31* 23.
220. J. L. Wu, P. Ravikumar, K. T. Nguyen, C. C. W. Hsia, Y. Hong, *Plos One* **2017,** *12* 2.

221. J. U. Menon, A. Kuriakose, R. Iyer, E. Hernandez, L. Gandee, S. R. Zhang, M. Takahashi, Z. Zhang, D. Saha, K. T. Nguyen, *Scientific Reports* **2017,** *7*.
222. S. Kona, J. F. Dong, Y. Liu, J. Tan, K. T. Nguyen, *Int J Pharm* **2012,** *423* 2.
223. J. U. Menon, P. Ravikumar, A. Pise, D. Gyawali, C. C. Hsia, K. T. Nguyen, *Acta Biomater* **2014,** *10* 6.
224. P. Madeddu, *Exp Physiol* **2005,** *90* 3.
225. D. Q. Le, A. E. Kuriakose, D. X. Nguyen, K. T. Nguyen, S. Acharya, *Scientific Reports* **2017,** *7*.
226. R. Sui, X. Liao, X. Zhou, Q. Tan, *Stem Cell Rev* **2011,** *7* 1.
227. J. Tongers, D. W. Losordo, U. Landmesser, *Eur Heart J* **2011,** *32* 10.
228. T. Dvir, A. Kedem, E. Ruvinov, O. Levy, I. Freeman, N. Landa, R. Holbova, M. S. Feinberg, S. Dror, Y. Etzion, J. Leor, S. Cohen, *Proc Natl Acad Sci U S A* **2009,** *106* 35.
229. P. Punnakitikashem. *Nanostructured biomaterials for tissue regeneration and repair*. **2016**.
230. Z. He, Z. Shi, W. Sun, J. Ma, J. Xia, X. Zhang, W. Chen, J. Huang, *Tumour Biol* **2016,** *37* 6.
231. M. Bokharaei, A. Margaritis, A. Xenocostas, D. J. Freeman, *Curr Drug Deliv* **2011,** *8* 2.
232. A. Kumari, S. K. Yadav, S. C. Yadav, *Colloids Surf B Biointerfaces* **2010,** *75* 1.
233. L. H. Peng, W. Wei, Y. H. Shan, T. Y. Zhang, C. Z. Zhang, J. H. Wu, L. Yu, J. Lin, W. Q. Liang, G. Khang, J. Q. Gao, *J Biomed Nanotechnol* **2015,** *11* 4.
234. X. Z. Zhang, X. Zeng, Y. X. Sun, R. X. Zhuo, 8 - Bioactive materials in gene therapy. In *Bioactive Materials in Medicine*, Woodhead Publishing: 2011; pp 179-219.
235. M. Bivas-Benita, S. Romeijn, H. E. Junginger, G. Borchard, *Eur J Pharm Biopharm* **2004,** *58* 1.
236. R. B. Shmueli, J. C. Sunshine, Z. Xu, E. J. Duh, J. J. Green, *Nanomedicine* **2012,** *8* 7.
237. R. N. Gacche, R. J. Meshram, *Biochimica Et Biophysica Acta-Reviews on Cancer* **2014,** *1846* 1.
238. H. Sorg, C. Krueger, T. Schulz, M. D. Menger, F. Schmitz, B. Vollmar, *Faseb Journal* **2009,** *23* 9.
239. H. S. Peng, X. H. Xu, R. Zhang, X. Y. He, X. X. Wang, W. H. Wang, T. Y. Xu, X. R. Xiao, *Surgery Today* **2014,** *44* 6.
240. L. Li, H. Okada, G. Takemura, M. Esaki, H. Kobayashi, H. Kanamori, I. Kawamura, R. Maruyama, T. Fujiwara, H. Fujiwara, Y. Tabata, S. Minatoguchi, *J Am Coll Cardiol* **2009,** *53* 25.
241. T. Simon-Yarza, E. Tamayo, C. Benavides, H. Lana, F. R. Formiga, C. N. Grama, C. Ortiz-de-Solorzano, M. N. Kumar, F. Prosper, M. J. Blanco-Prieto, *Int J Pharm* **2013,** *454* 2.
242. D. Altavilla, A. Saitta, D. Cucinotta, M. Galeano, B. Deodato, M. Colonna, V. Torre, G. Russo, A. Sardella, G. Urna, G. M. Campo, V. Cavallari, G. Squadrito, F. Squadrito, *Diabetes* **2001,** *50* 3.
243. M. Galeano, D. Altavilla, D. Cucinotta, G. T. Russo, M. Calo, A. Bitto, H. Marini, R. Marini, E. B. Adamo, P. Seminara, L. Minutoli, V. Torre, F. Squadrito, *Diabetes* **2004,** *53* 9.
244. K. K. Chereddy, C. H. Her, M. Comune, C. Moia, A. Lopes, P. E. Porporato, J. Vanacker, M. C. Lam, L. Steinstraesser, P. Sonveaux, H. J. Zhu, L. S. Ferreira, G. Vandermeulen, V. Preat, *Journal of Controlled Release* **2014,** *194*.
245. A. E. Krausz, B. L. Adler, V. Cabral, M. Navati, J. Doerner, R. A. Charafeddine, D. Chandra, H. Y. Liang, L. Gunther, A. Clendaniel, S. Harper, J. M. Friedman, J. D.

Nosanchuk, A. J. Friedman, *Nanomedicine-Nanotechnology Biology and Medicine* **2015,** *11* 1.
246. A. J. Monteforte, B. Lam, S. Das, S. Mukhopadhyay, C. S. Wright, P. E. Martin, A. K. Dunn, A. B. Baker, *Biomaterials* **2016,** *94*.
247. J. Slezak, N. Tribulova, J. Pristacova, B. Uhrik, T. Thomas, N. Khaper, N. Kaul, P. K. Singal, *Am J Pathol* **1995,** *147* 3.
248. R. Breton-Romero, S. Lamas, *Redox Biol* **2014,** *2*.
249. F. Rezaeian, R. Wettstein, J. F. Egger, F. Sandmann, M. Rucker, M. Tobalem, B. Vollmar, M. D. Menger, Y. Harder, *Lab Invest* **2010,** *90* 1.
250. X. Chen, B. T. Andresen, M. Hill, J. Zhang, F. Booth, C. Zhang, *Curr Hypertens Rev* **2008,** *4* 4.
251. M. Chorny, E. Hood, R. J. Levy, V. R. Muzykantov, *J Control Release* **2010,** *146* 1.
252. A. Mohandas, B. S. Anisha, K. P. Chennazhi, R. Jayakumar, *Colloids Surf B Biointerfaces* **2015,** *127*.
253. X. Jiang, Q. Xiong, G. Xu, H. Lin, X. Fang, D. Cui, M. Xu, F. Chen, H. Geng, *Ann Biomed Eng* **2015,** *43* 10.
254. S. Nakamura, M. Ishihara, M. Takikawa, S. Kishimoto, S. Isoda, M. Fujita, M. Sato, T. Maehara, *Tissue Eng Part A* **2012,** *18* 21-22.
255. H. Bao, F. Lv, T. Liu, *Acta Biomater* **2017,** *64*.
256. R. A. Ashley, S. H. Dubuque, B. Dvorak, S. S. Woodward, S. K. Williams, P. J. Kling, *Pediatr Res* **2002,** *51* 4.
257. Y. B. Yu, K. H. Su, Y. R. Kou, B. C. Guo, K. I. Lee, J. Wei, T. S. Lee, *Acta Physiol (Oxf)* **2017,** *219* 2.
258. S. W. Kang, H. W. Lim, S. W. Seo, O. Jeon, M. Lee, B. S. Kim, *Biomaterials* **2008,** *29* 8.
259. J. H. Lim, H. J. Shin, K. S. Park, C. H. Lee, C. R. Jung, D. S. Im, *Mol Ther* **2012,** *20* 4.
260. G. O. Ouma, E. Rodriguez, K. Muthumani, D. B. Weiner, R. L. Wilensky, E. R. Mohler, 3rd, *J Vasc Surg* **2014,** *59* 3.
261. M. V. Alvarez Arroyo, M. A. Castilla, F. R. Gonzalez Pacheco, D. Tan, A. Riesco, S. Casado, C. Caramelo, *J Am Soc Nephrol* **1998,** *9* 11.
262. A. Paul, A. Hasan, H. A. Kindi, A. K. Gaharwar, V. T. Rao, M. Nikkhah, S. R. Shin, D. Krafft, M. R. Dokmeci, D. Shum-Tim, A. Khademhosseini, *ACS Nano* **2014,** *8* 8.
263. P. Wu, N. Zhang, X. Wang, C. Zhang, T. Li, X. Ning, K. Gong, *PLoS One* **2012,** *7* 9.
264. F. He, L. Zuo, *Int J Mol Sci* **2015,** *16* 11.
265. Y. Zhao, H. Li, L. L. Men, R. C. Huang, H. C. Zhou, Q. Xing, J. J. Yao, C. H. Shi, J. L. Du, *J Transl Med* **2013,** *11*.
266. R. K. Mistry, A. C. Brewer, *Free Radic Biol Med* **2017,** *108*.
267. Y. Higashi, K. Nishioka, T. Umemura, K. Chayama, M. Yoshizumi, *Curr Pharm Biotechnol* **2006,** *7* 2.
268. Y. Y. Xu, Y. J. Li, H. Guan, C. W. Liu, Y. H. Zheng, B. Liu, J. Yang, C. X. Song, *Zhonghua Wai Ke Za Zhi* **2004,** *42* 1.
269. L. Zhang, M. Zhou, G. Qin, N. L. Weintraub, Y. Tang, *Biochem Biophys Res Commun* **2014,** *446* 4.
270. W. J. Cao, J. D. Rosenblat, N. C. Roth, M. A. Kuliszewski, P. N. Matkar, D. Rudenko, C. Liao, P. J. Lee, H. Leong-Poi, *Arterioscler Thromb Vasc Biol* **2015,** *35* 11.
271. Y. Endo-Takahashi, Y. Negishi, A. Nakamura, S. Ukai, K. Ooaku, Y. Oda, K. Sugimoto, F. Moriyasu, N. Takagi, R. Suzuki, K. Maruyama, Y. Aramaki, *Sci Rep* **2014,** *4*.
272. I. H. Ng, D. C. Ng, D. A. Jans, M. A. Bogoyevitch, *Biochem J* **2012,** *447* 1.

273. S. H. Chen, D. A. Murphy, W. Lassoued, G. Thurston, M. D. Feldman, W. M. Lee, *Cancer Biol Ther* **2008,** *7* 12.
274. H. N. Yang, J. S. Park, D. G. Woo, S. Y. Jeon, K.-H. Park, *Biomaterials* **2012,** *33* 33.
275. A. A. Khan, A. Paul, S. Abbasi, S. Prakash, *Int J Nanomedicine* **2011,** *6*.
276. M. C. Arokiaraj, *BMC Cardiovasc Disord* **2017,** *17* 1.
277. J. S. Park, H. N. Yang, S. W. Yi, J. H. Kim, K. H. Park, *Biomaterials* **2016,** *76*.
278. H. N. Yang, J. H. Choi, J. S. Park, S. Y. Jeon, K. D. Park, K.-H. Park, *Biomaterials* **2014,** *35* 16.
279. M. Takikawa, S. Nakamura, M. Ishihara, Y. Takabayashi, M. Fujita, H. Hattori, T. Kushibiki, M. Ishihara, *J Surg Res* **2015,** *196* 2.
280. P. E. Norman, J. W. Eikelboom, G. J. Hankey, *Med J Aust* **2004,** *181* 3.
281. J. M. Peacock, H. H. Keo, S. Duval, I. Baumgartner, N. C. Oldenburg, M. R. Jaff, T. D. Henry, X. Yu, A. T. Hirsch, *Prev Chronic Dis* **2011,** *8* 6.
282. C. E. Thomas, A. Ehrhardt, M. A. Kay, *Nat Rev Genet* **2003,** *4* 5.
283. J. W. Yockman, A. Kastenmeier, H. M. Erickson, J. G. Brumbach, M. G. Whitten, A. Albanil, D. Y. Li, S. W. Kim, D. A. Bull, *J Control Release* **2008,** *132* 3.
284. D. W. Pack, A. S. Hoffman, S. Pun, P. S. Stayton, *Nat Rev Drug Discov* **2005,** *4* 7.
285. K. Kunath, A. von Harpe, D. Fischer, H. Petersen, U. Bickel, K. Voigt, T. Kissel, *J Control Release* **2003,** *89* 1.
286. S. M. Moghimi, P. Symonds, J. C. Murray, A. C. Hunter, G. Debska, A. Szewczyk, *Mol Ther* **2005,** *11* 6.
287. I. Baumgartner, A. Pieczek, O. Manor, R. Blair, M. Kearney, K. Walsh, J. M. Isner, *Circulation* **1998,** *97* 12.
288. S. Rajagopalan, E. R. Mohler, 3rd, R. J. Lederman, F. O. Mendelsohn, J. F. Saucedo, C. K. Goldman, J. Blebea, J. Macko, P. D. Kessler, H. S. Rasmussen, B. H. Annex, *Circulation* **2003,** *108* 16.
289. A. Beenken, M. Mohammadi, *Nat Rev Drug Discov* **2009,** *8* 3.
290. S. Nikol, I. Baumgartner, E. Van Belle, C. Diehm, A. Visona, M. C. Capogrossi, N. Ferreira-Maldent, A. Gallino, M. Graham Wyatt, L. Dinesh Wijesinghe, M. Fusari, D. Stephan, J. Emmerich, G. Pompilio, F. Vermassen, E. Pham, V. Grek, M. Coleman, F. Meyer, *Mol Ther* **2008,** *16* 5.
291. H. Makino, M. Aoki, N. Hashiya, K. Yamasaki, J. Azuma, Y. Sawa, Y. Kaneda, T. Ogihara, R. Morishita, *Arterioscler Thromb Vasc Biol* **2012,** *32* 10.
292. Q. Zhang, J. Zhang, O. W. Moe, C. C. Hsia, *Proc Natl Acad Sci U S A* **2008,** *105* 21.
293. K. C.-F. Leung, C.-P. Chak, S.-F. Lee, J. M. Y. Lai, X.-M. Zhu, Y.-X. J. Wang, K. W. Y. Sham, C. H. K. Cheng, *Chemical communications (Cambridge, England)* **2013,** *49* 6.
294. D. Q. Le, A. E. Kuriakose, D. X. Nguyen, K. T. Nguyen, S. Acharya, *Sci Rep* **2017,** *7* 1.
295. H. Niiyama, N. F. Huang, M. D. Rollins, J. P. Cooke, *J Vis Exp* **2009,** 23.
296. R. Nagahama, T. Matoba, K. Nakano, S. Kim-Mitsuyama, K. Sunagawa, K. Egashira, *Arterioscler Thromb Vasc Biol* **2012,** *32* 10.
297. M. Heil, T. Ziegelhoeffer, S. Wagner, B. Fernandez, A. Helisch, S. Martin, S. Tribulova, W. A. Kuziel, G. Bachmann, W. Schaper, *Circ Res* **2004,** *94* 5.
298. V. A. Kumar, Q. Liu, N. C. Wickremasinghe, S. Shi, T. T. Cornwright, Y. Deng, A. Azares, A. N. Moore, A. M. Acevedo-Jake, N. R. Agudo, S. Pan, D. G. Woodside, P. Vanderslice, J. T. Willerson, R. A. Dixon, J. D. Hartgerink, *Biomaterials* **2016,** *98*.
299. G. H. Su, Y. F. Sun, Y. X. Lu, X. X. Shuai, Y. H. Liao, Q. Y. Liu, J. Han, P. Luo, *J Huazhong Univ Sci Technolog Med Sci* **2013,** *33* 4.

300. A. Liew, V. Bhattacharya, J. Shaw, G. Stansby, *Cochrane Database of Systematic Reviews* **2016,** 1.
301. M. Shimamura, H. Nakagami, Y. Taniyama, R. Morishita, *Expert Opin Biol Ther* **2014,** *14* 8.
302. X. Yu, C. S. Lin, F. Costantini, C. T. Noguchi, *Blood* **2001,** *98* 2.
303. J. Song, Y. Chen, S. Jiang, K. Yang, X. Li, X. Zhao, Y. Ouyang, C. Fan, W. Yuan, *Front Immunol* **2016,** *7*.
304. J. Song, X. Li, Y. Li, J. Che, X. Li, X. Zhao, Y. Chen, X. Zheng, W. Yuan, *Int J Nanomedicine* **2017,** *12*.
305. K. K. Chereddy, A. Lopes, S. Koussoroplis, V. Payen, C. Moia, H. Zhu, P. Sonveaux, P. Carmeliet, A. des Rieux, G. Vandermeulen, V. Preat, *Nanomedicine* **2015,** *11* 8.
306. C. Gutiérrez-Valenzuela, P. Guerrero-Germán, A. Tejeda-Mansir, R. Esquivel, R. Guzmán-Z, A. Lucero-Acuña, *Applied Sciences* **2016,** *6* 12.
307. Q. Tan, H. Tang, J. Hu, Y. Hu, X. Zhou, Y. Tao, Z. Wu, *Int J Nanomedicine* **2011,** *6*.
308. X. D. Zhang, Q. Wu, S. H. Yang, *Pak J Med Sci* **2017,** *33* 2.
309. A. W. Griffioen, G. Molema, *Pharmacol Rev* **2000,** *52* 2.
310. N. Ferrara, H. P. Gerber, J. LeCouter, *Nat Med* **2003,** *9* 6.
311. B. Witzenbichler, T. Asahara, T. Murohara, M. Silver, I. Spyridopoulos, M. Magner, N. Principe, M. Kearney, J. S. Hu, J. M. Isner, *Am J Pathol* **1998,** *153* 2.
312. M. Nakano, K. Satoh, Y. Fukumoto, Y. Ito, Y. Kagaya, N. Ishii, K. Sugamura, H. Shimokawa, *Circ Res* **2007,** *100* 5.
313. D. Joshi, D. Abraham, S. W. Xu, D. Baker, J. Tsui, *Journal of Vascular Surgery* **2014,** *60* 1.
314. J. E. Baker, D. Kozik, A. K. Hsu, X. P. Fu, J. S. Tweddell, G. J. Gross, *Journal of Cardiovascular Pharmacology* **2007,** *49* 6.
315. A. Cubranic, A. Redzovic, R. Dobrila-Dintinjana, J. Vukelic, M. Dintinjana, *Hepatogastroenterology* **2015,** *62* 139.
316. Y. Heun, K. Pogoda, M. Anton, J. Pircher, A. Pfeifer, M. Woernle, A. Ribeiro, P. Kameritsch, O. Mykhaylyk, C. Plank, F. Kroetz, U. Pohl, H. Mannell, *Molecular Therapy 25* 7.
317. L. Steinstraesser, M. C. Lam, F. Jacobsen, P. E. Porporato, K. K. Chereddy, M. Becerikli, I. Stricker, R. E. Hancock, M. Lehnhardt, P. Sonveaux, V. Preat, G. Vandermeulen, *Mol Ther* **2014,** *22* 4.
318. S. Kos, K. Vanvarenberg, T. Dolinsek, M. Cemazar, J. Jelenc, V. Preat, G. Sersa, G. Vandermeulen, *Bioelectrochemistry* **2017,** *114*.
319. F. Felice, A. M. Piras, S. Rocchiccioli, M. C. Barsotti, T. Santoni, A. Pucci, S. Burchielli, F. Chiellini, N. Ucciferri, R. Solaro, A. Altomare, A. Cecchettini, R. Di Stefano, *Int J Pharm* **2018,** *542* 1-2.
320. G. Liu, Z. Fang, M. Yuan, W. Li, Y. Yang, M. Jiang, Y. Ouyang, W. Yuan, *Front Pharmacol* **2017,** *8*.
321. G. Odent Grigorescu, A. M. Rosca, M. B. Preda, R. Tutuianu, M. Simionescu, A. Burlacu, *J Tissue Eng Regen Med* **2017,** *11* 11.
322. T. Asahara, H. Masuda, T. Takahashi, C. Kalka, C. Pastore, M. Silver, M. Kearne, M. Magner, J. M. Isner, *Circ Res* **1999,** *85* 3.
323. S. Mulik, J. Xu, P. B. Reddy, N. K. Rajasagi, F. Gimenez, S. Sharma, P. Y. Lu, B. T. Rouse, *Am J Pathol* **2012,** *181* 2.
324. S. Tsumaru, H. Masumoto, K. Minakata, M. Izuhara, K. Yamazaki, T. Ikeda, K. Ono, R. Sakata, K. Minatoya, *Journal of Vascular Surgery* **2017**.
325. S. A. Chew, M. C. Hacker, A. Saraf, R. M. Raphael, F. K. Kasper, A. G. Mikos, *Biomacromolecules* **2009,** *10* 9.

326. K. C. Remant Bahadur, H. Uludag, *J Biomater Sci Polym Ed* **2011,** *22* 7.

BIOGRAPHICAL INFORMATION

Linda Noukeu was born and spent the first 18 years of her life in west Africa. Upon completing her high school education, she gained admission at Texas Southern University (TSU) in Houston, Texas in 2006 where she earned B.Sc in Biology and chemistry (2010) and an M.Sc. in Biology in (2013). Following completion of her Master degree, she decided to further her studies by applying to the Bioengineering doctoral program at the University of Texas at Arlington, Arlington, Texas (2013). When admitted, she immediately joined the nanomedicine and drug delivery lab group under the supervision of Dr. Kytai Nguyen. As a doctoral student, she focused on the applications of various nanoparticles for protein delivery and gene therapy in cardiovascular diseases. Linda has also been the recipient of awards such as the Franklyn Alexander Biomedical scholarship, the Bioengineering GAANN scholarship, and the Bioengineering STEM doctoral fellowship. Over the course of her research career, Linda has been actively represented at various local and national conferences. She also published a very detailed review paper in the Small Journal in 2018, and a book chapter. Currently, she has manuscripts in preparation for submission to the Circulation Research journal. Following her graduation, Linda will be moving to the industry section where she plans on effecting positive outcomes in the healthcare system.